


บทบาทของไอน้ำต่อปฏิกิริยาออกซิเดชันแบบเลือกเกิดของแอลกอฮอล์

บนตัวเร่งปฏิกิริยา V-Mg-O/TiO₂



นางสาวใจชนก ปัญญาวงศ์

วิทยานิพนธ์นี้เป็นส่วนหนึ่งของการศึกษาตามหลักสูตรปริญญาวิศวกรรมศาสตรมหาบัณฑิต

สาขาวิชาวิศวกรรมเคมี ภาควิชาวิศวกรรมเคมี

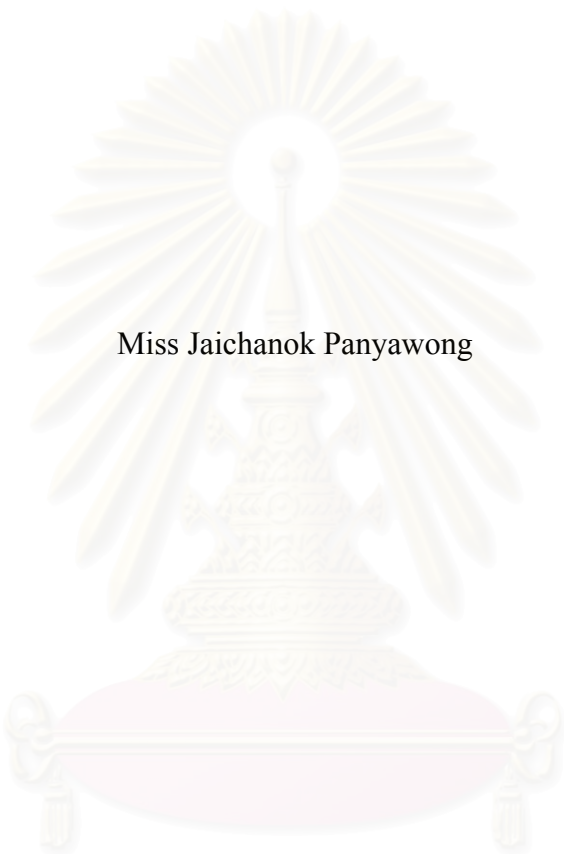
คณะวิศวกรรมศาสตร์ จุฬาลงกรณ์มหาวิทยาลัย

ปีการศึกษา 2543

ISBN 974-13-0908-2

ลิขสิทธิ์ของ จุฬาลงกรณ์มหาวิทยาลัย

THE ROLE OF WATER VAPOR ON THE SELECTIVE OXIDATION
OF ALCOHOLS OVER V-Mg-O/TiO₂ CATALYST



Miss Jaichanok Panyawong

สถาบันวิทยบริการ
จุฬาลงกรณ์มหาวิทยาลัย

A Thesis Submitted in Partial Fulfillment of the Requirements
for the Degree of Master of Engineering in Chemical Engineering
Department of Chemical Engineering


Faculty of Engineering
Chulalongkorn University

Academic year 2000

ISBN 974-13-0908-2

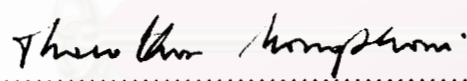
Thesis Title The role of water vapor on the selective oxidation of alcohols
 over V-Mg-O/TiO₂ catalyst
By Miss Jaichanok Panyawong
Field of Study Chemical Engineering
Thesis Advisor Assistant Professor Tharathon Mongkhonsi, Ph.D.
Thesis Co-advisor Professor Piyasan Prasertthdam, Dr.Ing.

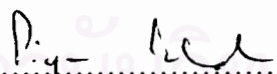
Accepted by Faculty of Engineering, Chulalongkorn University in Partial
Fulfillment of the Requirements for the Master's Degree



.....Dean of Faculty of Engineering
(Professor Somsak Panyakeow, Dr.Eng.)

Thesis Committee


.....Chairman
(Associate Professor Ura Pancharoen, D.Eng.Sc)


.....Thesis advisor
(Assistant Professor Tharathon Mongkhonsi, Ph.D.)


.....Thesis Co-Advisor
(Professor Piyasan Prasertthdam, Dr.Ing.)


.....Member
(Assistant Professor Prasert Pavasant, Ph.D.)

โจชนก ปัญญาวงศ์ : บทบาทของไอน้ำต่อปฏิกิริยาออกซิเดชันแบบเลือกเกิดของ แอลกอฮอล์บนตัวเร่งปฏิกิริยา V-Mg-O/TiO₂ (THE ROLE OF WATER VAPOR ON THE SELECTIVE OXIDATION OF ALCOHOL OVER V-Mg-O/TiO₂ CATALYST)

อ. ที่ปรึกษา : ผศ.ดร. ธราธร มงคลศรี, อ. ที่ปรึกษาร่วม : ศ.ดร. ปิยะสาร ประเสริฐธรรม, 105 หน้า.

บทบาทของไอน้ำต่อปฏิกิริยาออกซิเดชันแบบเลือกเกิดของเมทานอล, เอทานอล, 1-โพรพานอล และ 2-โพรพานอล บนตัวเร่งปฏิกิริยา V-Mg-O/TiO₂ งานวิจัยนี้ทำการศึกษารอบบาทของไอน้ำที่ความเข้มข้นต่าง ๆ (0-40% โดยปริมาตร) สำหรับแต่ละปฏิกิริยา ผลิตภัณฑ์หลักที่ได้จากปฏิกิริยาออกซิเดชันของเอทานอลและ 1-โพรพานอล คือ อะเซทาลดีไฮด์และโพรพิโอนาลดีไฮด์ตามลำดับ และคาร์บอนไดออกไซด์ การเพิ่มไอน้ำไม่มีผลที่เด่นชัดต่อปฏิกิริยาออกซิเดชันของเอทานอล ที่อุณหภูมิสูงผลได้ของอะเซทาลดีไฮด์ลดลงเพียงเล็กน้อย สำหรับปฏิกิริยาออกซิเดชันของ 1-โพรพานอลพบว่าผลได้ของโพรพิโอนาลดีไฮด์เพิ่มขึ้นเล็กน้อย แต่ไอน้ำกลับลดค่าการเปลี่ยนของเมทานอลในช่วงอุณหภูมิระหว่าง 200-400 องศาเซลเซียส ในกรณีของปฏิกิริยาออกซิเดชันของ 2-โพรพานอล ค่าการเปลี่ยนเพิ่มตามความเข้มข้นของไอน้ำ นอกจากนี้ ไอน้ำยังส่งเสริมการเกิดผลิตภัณฑ์จากปฏิกิริยาคีไฮเดรชันคือแอลคีนในปฏิกิริยาออกซิเดชันของเอทานอล, 1-โพรพานอล และ 2-โพรพานอล

ภาควิชา.....วิศวกรรมเคมี.....
สาขาวิชา.....วิศวกรรมเคมี.....
ปีการศึกษา.....2543.....

ลายมือชื่อนิสิต.....
ลายมือชื่ออาจารย์ที่ปรึกษา.....
ลายมือชื่ออาจารย์ที่ปรึกษาร่วม.....

#4270260621: MAJOR CHEMICAL ENGINEERING

KEY WORD: WATER VAPOR / SELECTIVE OXIDATION / METHANOL / ETHANOL / 1-PROPANOL / 2-PROPANOL / V-Mg-O/TiO₂ CATALYST

JAICHANOK PANYAWONG : THE ROLE OF WATER VAPOR ON THE SELECTIVE OXIDATION OF ALCOHOLS OVER V-Mg-O/TiO₂ CATALYST. THESIS ADVISOR: ASSIST.PROF. THARATHON MONGKHONSI, Ph.D. THESIS CO-ADVISOR : PROF. PIYASAN PRASERTHDAM, Dr.Ing. 105 pp.

The role of water vapor on the selective oxidation of methanol, ethanol, 1-propanol over V-Mg-O/TiO₂ catalyst is investigated. In this research, the various concentrations of water vapor (0-40 %vol) have been performed to determine the role of water vapor for each reaction. The main products from ethanol and 1-propanol oxidation are acetaldehyde and propionaldehyde, respectively and CO₂. The addition of water vapor has no strong effect in ethanol oxidation. At high temperature, yield to acetaldehyde slightly decreases. For 1-propanol oxidation, yield to propionaldehyde slightly increases. But water vapor depresses methanol conversion in the range of reaction temperature between 200-400°C. In the case of 2-propanol oxidation, conversion increases with the concentration of water vapor like. In addition, water vapor also promotes the formation of dehydration products, alkenes, in ethanol, 1-propanol and 2-propanol oxidation.

สถาบันวิทยบริการ
จุฬาลงกรณ์มหาวิทยาลัย

Department.....Chemical Engineering.....	Student's signature.....
Field of study..Chemical Engineering.....	Advisor's signature.....
Academic year.....2000.....	Co-advisor's signature.....

ACKNOWLEDGEMENT

I would like to express my greatest gratitude to Assistant Professor Tharathon Mongkhonsi, my advisor for his invaluable guidance and supervision during my study. I am grateful to Professor Dr. Piyasan Prasertthdam for his guidance and encouragement.

Furthermore, I am also grateful to Associate Professor Ura Pancharoen and Assistant Professor Prasert Pavasant for serving as chairman and member of the thesis evaluating committee, respectively, whose comments have been especially helpful. I would like to thank Assistant Professor Suttichai Assabumrungrat, Dr. Suphot Phatanasri for their suggestions.

My sincere thanks are due to Mr. Viboon Kerdpokasub, Mr. Manop T. and Mr. Maetee and Mr. Wanadara at Scientific and Technological Research Equipment Center, department of Chemical Engineering, Chulalongkorn University.

I also would like to thank Miss Nungruetai Chaiyasit and Mr. Solos Chuwet for their valuable suggestions and useful help and many best friends in the Petrochemical Research Laboratory at the Department of Chemical Engineering who have provided encouragement and cooperation throughout this study.

Thanks for the financial support are to Thailand Research Fund (TRF).

Finally, I would like to express my highest gratitude to my parents for their inspiration and valuable support throughout this study.

CONTENTS

	PAGE
ABSTRACT (IN THAI).....	iv
ABSTRACT (IN ENGLISH).....	v
ACKNOWLEDGEMENTS.....	vi
LIST OF TABLES.....	ix
LIST OF FIGURES.....	x
NOMENCLATURE.....	xi
CHAPTER	
I INTRODUCTION.....	1
II LITERATURE REVIEWS.....	4
2.1 Reviewed literature.....	4
2.2 Comment on previous works.....	17
III THEORY.....	18
3.1 Nature of supported oxides.....	20
3.2 Activation of the hydrocarbon and selectivity.....	21
3.3 Partial oxidation to oxygenates.....	21
3.4 The role of water.....	25
IV EXPERIMENT.....	26
4.1 Preparation of catalyst.....	27
4.2 The catalyst characterization.....	28
4.3 Catalytic reaction.....	29
V RESULTS AND DISCUSSION.....	33
5.1 Catalyst characterization.....	33
5.2 Catalytic reaction.....	38
5.3 Proposed reaction pathway.....	64
VI CONCLUSIONS AND RECOMMENDATIONS.....	65
6.1 Conclusions.....	65
6.2 Recommendations.....	66
REFERENCES.....	67
APPENDICES.....	71
APPENDIX A. CALCULATION OF CATALYST PREPARATION.....	72

	PAGE
APPENDIX B. CALCULATION OF DIFFUSIONAL LIMITATION EFFECT.....	73
APPENDIX C. GAS CHROMATOGRAPH.....	89
APPENDIX D. DATA OF EXPERIMENT.....	97
APPENDIX E. X-RAY DIFFRACTION (XRD).....	103
APPENDIX F. FOURIER TRANSFORM INFRARED SPECTROSCOPY (FTIR).....	104
VITA.....	105



สถาบันวิทยบริการ
จุฬาลงกรณ์มหาวิทยาลัย

LIST OF TABLES

TABLE	PAGE
4.1 The chemicals used in this research.....	27
5.1 The compositions of catalyst and BET surface area.....	33



สถาบันวิทยบริการ
จุฬาลงกรณ์มหาวิทยาลัย

LIST OF FIGURES

FIGURE	PAGE
4.1 Flow diagram of the oxidation reaction system.....	30
5.1 Electron Micrograph of 10V2MgTi catalyst.....	34
5.2 X-ray diffraction of TiO ₂	35
5.3 X-ray diffraction of 10V2MgTi catalyst.....	35
5.4 IR spectrum of TiO ₂	37
5.5 IR spectrum of 10V2MgTi catalyst.....	37
5.6 TGA result of 10V2MgTi catalyst.....	38
5.7 The result of ethanol oxidation (no water added).....	41
5.8 The result of ethanol oxidation in the presence of 7% water vapor.....	42
5.9 The result of ethanol oxidation in the presence of 20% water vapor.....	43
5.10 The result of ethanol oxidation in the presence of 40% water vapor.....	44
5.11 %yield C ₂ H ₄ O.....	45
5.12 The result of 1-propanol oxidation (no water added).....	47
5.13 The result of 1-propanol oxidation in the presence of 7% water vapor....	48
5.14 The result of 1-propanol oxidation in the presence of 20% water vapor...	49
5.15 The result of 1-propanol oxidation in the presence of 40% water vapor...	50
5.16 %yield C ₃ H ₆ O.....	51
5.17 The result of methanol oxidation (no water added).....	53
5.18 The result of methanol oxidation in the presence of 7% water vapor.....	54
5.19 The result of methanol oxidation in the presence of 20% water vapor.....	55
5.20 The result of methanol oxidation in the presence of 40% water vapor.....	56
5.21 %methanol conversion.....	57
5.22 The result of 2-propanol oxidation (no water added).....	59
5.23 The result of 2-propanol oxidation in the presence of 7% water vapor.....	60
5.24 The result of 2-propanol oxidation in the presence of 20% water vapor.....	61
5.25 The result of 2-propanol oxidation in the presence of 40% water vapor.....	62
5.26 %2-propanol conversion.....	63

Nomenclature

AAS	atomic absorption spectroscopy
BET	Brunauer, Emmett, and Teller
EXAFS	extended X-ray absorption fine structure
FID	flame ionization detector
FTIR	fourier transform infrared
GC	gas chromatograph
HREM	high resolution electron microscopy
SCR	selective catalytic reduction
SEM	scanning electron microscopy
TAP	temporal analysis of products
TCD	thermal conductivity detector
TEM	transmission electron microscopy
TGA	thermal gravimetric analysis
TPR	temperature-programmed reduction
UV-vis	UV-visible reflectance spectroscopy
XRD	X-ray diffraction

สถาบันวิทยบริการ
จุฬาลงกรณ์มหาวิทยาลัย

CHAPTER I

INTRODUCTION

The first studies on the effect of water on the selective oxidation reaction appeared in 1962. Studies made since that time examined whether water takes part in the reaction. The presence of water vapor in the reaction mixture during the selective oxidation of propene is known to improve the selectivity and depress the formation of carbon oxides. Thus, water vapor is added to the feed for the industrial production of acrolein and acrylic acid by the catalytic oxidation of propene. In some cases, the feed mixture may contain between 40 and 60 %vol water. It also appears to influence the chemistry.

The role of water in the oxidative dehydrogenation of light alkanes has not been elucidated yet. Most researchers agree that the addition of steam to the reacting mixture has a negative effect on the conversion, while concerning the selectivity, the beneficial or not effect of steam depends on the catalyst and process variables.

Catalytic oxidation continues to be a very important technology in modern chemical industry. Over the past 15 years many examples of catalysts active in the selective oxidation and dehydrogenation of paraffins have been reported in patents and in scientific publications. Supported vanadium oxides which form a group of industrially important catalysts are extensively employed for many selective oxidations of hydrocarbons. They are active and selective in the production of anhydrides and acids. The superior performance of vanadium oxide based system arises from its specific activity in the C-H bond activation in paraffins, and in some cases from its specificity in oxygen insertion onto the activated molecule.

Supported vanadium oxide catalysts are generally more selective and active for the partial oxidation of hydrocarbons than bulk V_2O_5 . The supports which are currently used are TiO_2 , Al_2O_3 , SiO_2 , and ZrO_2 . The V_2O_5/TiO_2 is used in practice as one of the best catalysts for the medium temperature range SCR of NO_x with NH_3 and

for selective oxidation of various hydrocarbons. In both cases, TiO_2 in the form of anatase is used as the support. This is primarily because of the remarkable fit of the crystal planes in contact with the vanadia-titania interface, which is assumed to give rise to the epitaxial growth of the vanadia (010) plane at the monolayer level. In spite of this advantage, titania as a support suffers from limited surface area, lack of abrasion resistance, poor mechanical strength, and high price. In addition, the anatase phase of titania has a poor thermal stability at high temperatures. Temperature stability in catalysis is of vital importance, since in high temperature oxidations or SCR, long-term thermal stability dictates the catalyst life.

The magnesia supported vanadia system does not form the monolayer structure like the titania supported vanadia system because of the acid-base reaction between the acidic vanadium oxide and basic magnesia. The strong interaction between vanadia and magnesia results in the formation of a mixed metal oxide compound, V-Mg-O, rather than a stable surface vanadia over layer on the magnesia support. V-Mg-O catalysts have exhibited a promising yield for the production of propene and butenes from the corresponding alkanes via oxidative dehydrogenation, as well as promoted V-Mg-O catalyst systems. They have also been successfully tested in other reactants: ethylbenzene, 2-methylpropane, cyclohexane. However, a poor selectivity was found for V-Mg-O catalysts in the oxidative dehydrogenation of ethane.

The V_2O_5 and V-Mg-O systems are the effective catalysts for many selective oxidations. Thus, the combination of V-Mg-O and $\text{V}_2\text{O}_5/\text{TiO}_2$ system was established to apply this catalysts system, V-Mg-O/ TiO_2 , on the selective oxidation of alcohols i.e. methanol, ethanol, 1-propanol, and 2-propanol in the presence of water vapor (0, 7, 20 and 40 % vol). Hence, this work was set up to investigate the effect of the content of water vapor in the selective oxidation of each reactant.

The present work is arranged as follows:

Chapter II presents literature reviews of investigation related to supported vanadia systems on the selective oxidation and the role of water vapor in the selective oxidation.

The theory of this work, studies about the reactivity of vanadium oxide species on oxide support especially TiO_2 and MgO and the role of water are described in chapter III

The experimental systems and the operational procedure are presented in chapter IV.

The experimental results of the characterization of catalyst and the methanol, ethanol, 1-propanol and 2-propanol oxidation reactions over V-Mg-O/TiO_2 in the presence of steam are shown in chapter V.

In the last chapter, the overall conclusion emerged from this work is presented.

Finally, the sample of calculation of catalyst preparation, diffusion limitation effect, the details of gas chromatograph including the operation conditions, the calibration curves and data of experiments which has emerged from this study are included in appendices at the end of this thesis.

สถาบันวิทยบริการ
จุฬาลงกรณ์มหาวิทยาลัย

CHAPTER II

LITERATURE REVIEW

Selective oxidation is at present the main method of synthesis of a series of important chemical products such as aldehydes, acids, nitriles, etc. A large body of patent literature is concerned with the development of catalysis for this reaction. Supported vanadium oxide catalysts have been reported to be effective in many selective oxidations of hydrocarbons. They can exhibit interesting catalytic properties depending on the composition of the catalysts and on the nature of support. Many recent studies have shown that supported V_2O_5/TiO_2 is a superior catalyst to unsupported crystalline V_2O_5 for the selective oxidation of hydrocarbon, especially for the partial oxidation of o-xylene to phthalic anhydride. A number of observations on V-Mg-O system have also been made. It has been proposed that the V-Mg-O system was efficient for the oxidative dehydrogenation of butane and propane. In addition to the V_2O_5/TiO_2 and the V-Mg-O system, the other V-containing systems have been investigated too.

2.1 Reviewed literature

Matralis *et al.* (1995) investigated the influence of vanadium loading and molybdenum presence on the catalytic performance of vanadia-titania (anatase) catalysts for the selective oxidation of toluene. Two series of V_2O_5/TiO_2 and $V_2O_5-MoO_3/TiO_2$ catalysts were prepared. In the first series the loading of vanadium varied from 0 to 8 %mol, whereas in the second the atomic ratio $V/(V+Mo)$ varied from 0 to 1 while the total loading of active elements (V+Mo) was kept constant and equal to 8 %mol. The samples were characterized by XPS, TPR, XRD and BET measurements. It was found that the activity for the oxidation of toluene and the selectivity for side chain partial oxidation products (benzaldehyde and benzoic acid) exhibited by V_2O_5/TiO_2 catalysts increased with the vanadium loading up to monolayer coverage. This increase was attributed to the parallel increase of the surface concentration of easily reducible isolated vanadium species interacting with the anatase surface. When the vanadium content increased above monolayer coverage both activity and

selectivity decreased. V_2O_5 - MoO_3 / TiO_2 catalysts were found to be less active and selective than the corresponding V_2O_5 / TiO_2 ones. Molybdenum species supported on anatase were less active for this reaction than vanadium and, in addition, the presence of molybdenum inhibited the interaction between vanadium and anatase leading to a poor vanadium dispersion.

Elguezabal and Corberan (1996) studied the effect of the modification of vanadia catalysts supported on TiO_2/SiO_2 by the oxides of Al, Mg and Te, and K_2SO_4 on the selective oxidation of toluene in the vapor phase. The catalysts were prepared by successive impregnation and characterized by BET surface measurements, XRD, XPS, and TPR. Addition of the second component decreased specific activity in all cases, except Al, mainly due to the decrease of surface area. Intrinsic activity was increased with addition of Te and Al, and decreased by that of Mg, while K_2SO_4 , had little effect. These differences could be explained by the observed changes in either vanadium surface dispersion or reducibility. Selectivity to benzaldehyde increased markedly with addition of Te or K_2SO_4 , that caused the formation of new oxide phases, $V_3Ti_6O_{17}$ and TiV_2O_6 , in which vanadium is in a partially reduced state.

Pantazidis *et al.* (1996) studied the oxidative dehydrogenation of propane over VMgO catalysts in a wide range of V contents (5-45wt%). The highest propene yields were observed for samples with low-to-medium V content. Electrical conductivity measurements demonstrated the presence of anionic vacancies, which participated to the redox catalytic cycle. The reoxidation step was shown to be rate limiting. Microcalorimetry measurements and DRIFT spectroscopy showed that an acid/base balance was equally required. Thus, the highest propene yields corresponded to adjusted redox potential combined with a strong Lewis acidity and a mild basicity. These observations, completed by the structural properties of the VMgO solids, led to the description of the active sites for the oxidative dehydrogenation reaction.

Saleh-Alhamed *et al.* (1996) studied the role of water on the partial oxidation of propene over antimony-tin vanadium oxide (Sb/Sn/V oxide) catalyst at 1 atm pressure and 340°C using a microcatalytic packed bed reactor. Steady-state, transient kinetics, TPD, and isotopic transient experiments were performed. Water suppressed the formation of CO₂ by blocking the most active sites which are responsible for CO₂ formation but water also enhanced the rate of the catalytic oxidation by keeping the catalyst surface at a high oxidation state and preventing the formation of strongly bonded oxygenates. Isotopic transient experiments with labeled O₂ in the presence of water indicated a strong interaction between water and the catalyst surface. Water exchanged oxygen slowly with the surface of the catalyst.

Quaranta *et al.* (1997) studied the effect of coating the SiO₂ support of a V₂O₅ oxidation catalyst with different amounts of TiO₂. X-ray photoelectron spectroscopy of the resulting V₂O₅/TiO₂/SiO₂ showed that the highest dispersion was reached for the low TiO₂ coverages. The catalysts were prepared by depositing vanadia in a quantity equivalent to one monolayer onto SiO₂, TiO₂, or TiO₂-coated SiO₂ samples, by impregnation with a vanadyl acetylacetonate solution in ethanol, drying at 75 °C, and calcining at 500 °C in air. This procedure decreased the surface area by up to 30%. TPR profiles of binary and ternary samples were similar, showing only a single peak, suggesting the presence of just one vanadium species. Electron spin resonance spectra of partially reduced TiO₂-coated silica carriers showed that, at very low titania content, titanium ions were present in the silica surface in small clusters. In the high content sample, TiO₂ covered the silica surface, as in a crystalline TiO₂ phase. The characteristics of supported vanadium oxide were affected by the TiO₂ distribution. These V/xTiSi catalysts were found to be active for the selective oxidation of ethanol. The titania coating of the support increased the activity of the supported vanadia as compared to that of the oxide supported on silica, but maintained a similar product distribution. This increase of activity depended on the number of titania monolayers (x), being maximum for x greater than or equal to 1. The selectivity to acetaldehyde also increased with x, being maximum for the same composition. The combination of the two factors allowed the attainment of acetaldehyde yields of 74% per pass at temperatures as low as 200 °C. The modifications in the catalytic behavior

were discussed in terms of the changes of the support surface and its interaction with the supported vanadia caused by the presence of the titania coating.

Sun *et al.* (1997) found that vanadia was well dispersed and presented as a two-dimensional overlayer when supported on SiO₂, TiO₂, SnO₂, 3 wt% TiO₂/SiO₂, 3 wt% MoO₃/SiO₂, and 3 wt% SnO₂/SiO₂. Partial oxidation of methane by oxygen formed formaldehyde most selectively over the V₂O₅/SiO₂ catalyst, but catalytic performance was strongly dependent on vanadia coverage and autocatalytic behavior was observed. At very low conversions, the formaldehyde activity increased linearly with vanadia coverage, indicating that isolated V⁵⁺ species were responsible for the active sites. No significant structural changes were revealed by in situ Raman spectroscopy for the V₂O₅/SiO₂ catalyst, which indicated that the fully oxidized surface sites were related to the high formaldehyde selectivity. This selectivity exhibited a maximum at 1 wt% V₂O₅ content, and the lower selectivities at higher loadings appeared to be due to the increasing Lewis acidity of the catalysts. Space-time yields of 0.1-1.4 kg CH₂O/kg cat/hr and selectivities of 2-78% were reported herein for the V₂O₅/SiO₂ catalysts. Deep oxidation products, CO and CO₂, were principally produced over the V₂O₅/TiO₂ and V₂O₅/SnO₂ catalysts. For the first time, in situ Raman analysis clearly showed that for these latter catalysts the surface vanadium(V) oxide species were partially reduced under the steady-state reaction conditions. The performance of the V₂O₅/TiO₂/SiO₂ catalyst was similar to that of the V₂O₅/TiO₂ catalyst, consistent with the earlier observation that vanadia was largely bound to the titania overlayer. It appeared that formaldehyde selectivity decreased with increasing catalyst reducibility, but no direct correlation of catalyst activity with reducibility was observed.

Dunn *et al.* (1998) prepared a series of supported vanadia catalysts on various metal-oxide supports: ceria, zirconia, titania, alumina and silica. Raman spectroscopy was used to determine the coordination of surface species. At low vanadia loadings, vanadia preferentially existed on oxide support surfaces as isolated tetrahedrally coordinated (M-O)₃V⁺⁵=O species. At higher vanadia loadings, the isolated

$(M-O)_3V^{+5}=O$ species polymerize on the oxide support surface breaking two V–O–M bonds and forming two V–O–V bridging bonds. The turnover frequency for sulfur dioxide oxidation was very low, 10^{-4} to 10^{-6} s⁻¹ at 400°C, and was independent of vanadia coverage suggesting that only one vanadia site is required for the oxidation reaction. As the support was varied, sulfur dioxide oxidation activity of the supported vanadia catalysts varied by one order of magnitude (Ce>Zr, Ti>Al>Si). The basicity of the bridging V–O–M oxygen appeared to be responsible for influencing the adsorption and subsequent oxidation of the acidic sulfur dioxide molecule. Over the range of conditions studied, the rate of sulfur dioxide oxidation is zero-order in oxygen, first-order in sulfur dioxide and inhibited by sulfur trioxide. The turnover frequency for sulfur dioxide oxidation over WO₃/TiO₂ was an order of magnitude lower than that found for V₂O₅/TiO₂, and no redox synergism between the surface vanadia and tungsten oxide species was evident for a ternary V₂O₅/WO₃/TiO₂ catalyst. This suggested that WO₃ promoted catalysts may be suitable for low-temperature SCR where minimal sulfur dioxide oxidation activity is required.

Leklertsunthorn (1998) investigated the oxidation property of a series of V-Mg-O/TiO₂ catalyst in the oxidation reaction of propane, propene, 1-propanol and carbon monoxide. It had been found that the catalytic behavior of the catalyst depended on the reactants. Propene and CO₂ were the major products in the propane oxidation reaction. The vanadium and magnesium contents affected the catalytic property of the V-Mg-O/TiO₂ catalyst in the reaction. The sequence of magnesium loading also affected the structure and catalytic performance of this catalyst. In addition, this catalyst was inactive for propene oxidation, from which it could be indicated that propene formed in propane oxidation reaction was not further oxidized to CO₂. According to 1-propanol oxidation, propanal was the main observable product at low reaction temperatures, and it was oxidized rapidly to CO₂ when the reaction temperature was increased. Moreover, the dehydration of 1-propanol became significant at high temperatures. It was found that the sequence of magnesium loading and magnesium content had no effect on the catalytic performance of the catalyst. On the other hand, increasing vanadium content improved the propene

selectivity and decreased the CO₂ selectivity. Finally, in CO oxidation, this catalyst was rather inactive. Since CO was an unobservable product in propane, propene and 1-propanol reactions, on the V-Mg-O/TiO₂ catalysts, CO was not produced in these three reactions.

Lemonidou *et al.* (1998) investigated the oxidative dehydrogenation of *n*-butane over VMgO mixed oxide and pure magnesium ortho- and pyrovanadate catalysts. The formulation containing 30 wt% V₂O₅ and consisting of the Mg₃(VO₄)₂ and MgO crystal phases is more selective than the pure Mg₃(VO₄)₂, while the Mg₂V₂O₇ phase is the least selective. The selectivity to butenes and butadiene increases with the reaction temperature and the feed molar ratio of butane/oxygen. Addition of water tended to decrease the conversion of butane and enhanced the oxydehydrogenation product selectivity. The relative importance of the primary and secondary paths of the reaction network was analyzed by the method of addition of intermediate products.

Lemonidou and Stambouli (1998) investigated the thermal pyrolysis and the catalytic and non-catalytic oxydehydrogenation of *n*-butane. It was found that, under optimum conditions, the non-catalyzed reaction can be very efficient and selective. The effect of temperature, butane/oxygen ratio and residence time was studied and it was concluded that high selectivity in butenes can be achieved at relatively low temperatures and low butane/oxygen ratios. Conversion of *n*-butane up to 90%, at 580°C, and 1.8 s residence time with an overall alkenes C₂–C₄ selectivity exceeding 55% were observed. Based on experimental results, it is suggested that oxygen participates in the reaction mechanism of butane decomposition not only in the initiation steps but in the propagation steps as well. Oxidative dehydrogenation was also examined in the presence of mixed oxide catalyst comprising 30 wt% V₂O₅ and 70 wt% MgO. It was observed that the catalyst is very active and quite selective in desirable products at reaction temperatures (540–580°C), similar to those applied in non-catalytic experiments. Very promising results were obtained when *n*-butane and oxygen were fed over a catalytic bed (VMgO catalyst) combined in series with a void volume (post-catalytic). High conversion of *n*-butane was achieved with high C₂–C₄ selectivity and relatively low CO_x selectivity.

Liu *et al.* (1998) prepared two series of catalysts, V_2O_5/TiO_2 and modified V_2O_5/TiO_2 with a conventional impregnation method. They were tested in the selective oxidation of toluene to benzoic acid under microwave irradiation. The reaction conditions were optimized over V_2O_5/TiO_2 . It was found that in the microwave catalytic process the optimum reactor bed temperature of the titled reaction decreased to 227 °C (327 °C in the conventional process). The modification of V_2O_5/TiO_2 with MoO_3 , WO_3 , Nb_2O_5 or Ta_2O_5 , which has no negative influence on the reaction in the conventional catalytic process, could greatly promote the catalytic activities in the microwave process, leading to a high yield of benzoic acid (~41%).

Nieto *et al.* (1998) have prepared, characterized and tested vanadium–magnesium oxide (VMgO) catalysts in the oxidative dehydrogenation of *n*-butane. The catalysts were prepared by two variations of the wet-impregnation method using aqueous ammonium metavanadate or organically-based methanolic vanadyl acetylacetonate solutions. The catalyst surface area depends on the vanadium content and the preparation method. Catalyst characterization (i.e. XRD, ^{51}V NMR, FTIR, LRS) results indicated the presence of poor crystalline Mg-orthovanadate ($Mg_3V_2O_8$), while the presence of other Mg-vanadates was not clear. Oxygen isotopic-exchange experiments on VMgO catalysts indicate an R_2 process: $[^{18}O_2 + 2^{16}O^{2-}_{(s)} \longrightarrow (^{18}O^{18}O^{16}O^{16}O)^{4-}_{(s)} \longrightarrow 2^{18}O^{2-}_{(s)} + ^{16}O_{2(g)}]$ at temperatures higher than 750 °C, while an R_0 -type $[^{18}O_{2(g)} + ^{16}O_{2(g)} \longrightarrow 2^{16}O^{18}O_{(g)}]$ is observed at 550 °C, as a consequence of a small activity for homophase isotopic. Both the catalytic activity and the selectivity to oxydehydrogenation products depend on the vanadium content but is independent on the catalyst preparation method. This behavior is observed in the oxidative dehydrogenation of *n*-butane with both O_2 and N_2O . However, while conversion of *n*-butane was higher when using O_2 as oxidant, the selectivity to C_4 -olefins was higher with N_2O as oxidant. Pulse experiments show that prerduced surfaces are not effective in producing olefins while selective catalysts were achieved with preoxidized surface.

Pantazidis *et al.* (1998a) studied the oxidative dehydrogenation of propane over an optimised V–Mg–O catalyst at 500°C using the vacuum transient kinetic technique in the temporal-analysis-of-products (TAP) reactor. The only products detected were C₃H₆ and CO_x. The experiments reveal that both, propene and carbon oxides are primary reaction products and that CO_x is also produced by secondary oxidation of propene. Partial and deep oxidation of propane occur at the same surface site but involve different forms of reactive oxygen, associated to different site arrangements: nucleophilic lattice oxygen takes part in the propane partial oxidation to propene, while adsorbed electrophilic oxygen adspecies, originating from the gas-phase oxygen, are involved in the direct deep oxidation process of propane. The secondary oxidation of propene could involve both types of oxygen species. In the absence of gas-phase oxygen, the oxidation state of the catalyst determined the importance of the consecutive propene total oxidation.

Pantazidis *et al.* (1998b) investigated an optimised VMgO catalyst (14 wt% V) for the oxidative dehydrogenation of propane, carried out in order to elucidate the nature and behaviour of the active surface. The catalyst morphology and the surface composition were studied by means of HREM, XPS, UV-vis, XRD, and *in-situ* electrical conductivity techniques, as a function of the gaseous environments of the catalyst. The active surface is shown to be essentially a monolayer of amorphous VO₄³⁻ units scattered over the magnesia as isolated and polymeric species. These surface vanadia units are found to stabilise an unusual polar (111) orientation of MgO up to temperatures of 800°C. A direct and outstanding evidence of a totally reversible phenomenon of order/disorder restructuring of this V overlayer was provided in conjunction with the redox state of the surface depending on the properties of the surrounding atmosphere (reductive or oxidative). These fast surface phenomena were assumed to determine the elementary steps of propane activation within the overall oxidative dehydrogenation process.

Burrows *et al.* (1999) examined a VMgO catalyst (containing 14 wt% vanadium) that is used in the oxidative dehydrogenation of propane in detail by in situ EXAFS, in situ XRD and HREM. These characterisation techniques have revealed that, as prepared, the catalyst was in effect a three-component system comprising discrete magnesium orthovanadate ($\text{Mg}_3\text{V}_2\text{O}_8$) particles, magnesium oxide and a disordered vanadium-containing overlayer supported on the MgO. When the catalyst was exposed to typical oxidative dehydrogenation reaction conditions at 500 °C the in situ EXAFS indicates a change in vanadium oxidation state from 5+ to 3+. Under the same conditions, in situ XRD suggests that $\text{Mg}_3\text{V}_2\text{O}_8$ transforms to a cubic spinel type structure with a lattice parameter of 8.42 Å. These changes are reversible on exposure to air at 500 °C. HREM shows that the overlayer on MgO changes from a disordered state to a weakly ordered structure after exposure to normal reaction conditions whilst pure propane (strongly reducing conditions) induced pronounced structural ordering of the overlayer. Image simulations had led to the conclusion that the ordered layer comprised a cubic spinel (MgV_2O_4) phase in parallel epitaxy with the MgO support. The surface regions of the bulk $\text{Mg}_3\text{V}_2\text{O}_8$ particles were also found to undergo structural modification under typical reaction conditions decomposing to a mixture of MgO crystallites and MgV_2O_4 ; strong reduction causes a complete conversion to MgV_2O_4 .

del Val *et al.* (1999) studied the oxidation of toluene and o-xylene on alpha-Ti (HPO_4)₂·H₂O-supported vanadium oxide catalysts. Vanadium was incorporated at different loadings by VOCl_3 grafting and by vanadyl oxalate wet impregnation. Their catalytic properties and the results of the physico-chemical characterisation (Laser Raman, XRD, SEM, Na adsorption, XPS, and thermal analysis) were compared with those of a conventional $\text{V}_2\text{O}_5/\text{TiO}_2$ catalyst (with an 8 V_2O_5 wt% loading). It was shown that toluene oxidation was as selective in Ti phosphate-based catalysts as in the conventional system, whereas o-xylene oxidation was less selective: a much lower phthalic anhydride yield was obtained. Vanadium uptake on Ti phosphate reached a limit value when the grafting method was used: V_2O_5 loadings higher than 5 wt% could not be surpassed. A vanadium oxide-Ti phosphate support interaction exists at V loadings lower than 5 V_2O_5 wt% as suggested by the fact that the same VOPO_4 -like environment is detected irrespective of the method used to incorporate V. Higher

vanadium loadings by using wet impregnation result in the formation of larger V_2O_5 crystallites than in the case of the conventional V_2O_5/TiO_2 catalyst. The lack of interaction at high V loadings leaves the support uncovered. The poorly covered Ti phosphate surface exposing acid surface sites must account for the lower o-xylene oxidation to phthalic anhydride.

Doornkamp *et al.* (1999) studied the reactivity of lattice oxygen of vanadium oxide catalysts with the oxygen isotopic exchange reaction. The reactivity of pure V_2O_5 was compared with the reactivity of $Li_{0.33}V_2O_5$, V_2O_5/TiO_2 , V_2O_5/Al_2O_3 , V_2O_5/SiO_2 , δ -VOPO₄, and $(VO)_2P_2O_7$. According to their behaviour in the oxygen exchange reaction, two types of vanadium oxide catalysts could be distinguished. The first type of catalysts only showed exchange activity in the R-2 exchange mechanism and the second type showed activity in both the R-1 and R-2 exchange mechanisms. The catalysts which belong to the first group were bulk V_2O_5 and δ -VOPO₄ and the catalysts which belong to the second group are $Li_{0.33}V_2O_5$, V_2O_5/TiO_2 , V_2O_5/Al_2O_3 , V_2O_5/SiO_2 , and $(VO)_2P_2O_7$. If only the R-2 mechanism was observed then diffusion of lattice oxygen was probably faster than when both the R-1 and R-2 mechanisms were observed. The activity of the supported vanadium oxide catalysts in the oxygen exchange reaction was dependent on the support. The reactivity order is $V_2O_5/TiO_2 > V_2O_5/Al_2O_3$ similar to V_2O_5/SiO_2 .

Dunn *et al.* (1999) investigated in the catalytic oxidation of sulfur dioxide to sulfur trioxide over several binary (M_xO_y/TiO_2) and ternary ($V_2O_5/M_xO_y/TiO_2$) supported metal oxide catalysts. The supported metal oxide components were essentially 100% dispersed as surface metal oxide species, as confirmed by Raman spectroscopy characterization. The sulfur dioxide oxidation turnover frequencies of the binary catalysts were all within an order of magnitude ($V_2O_5/TiO_2 > Fe_2O_3/TiO_2 > Re_2O_7/TiO_2 \sim CrO_3/TiO_2 \sim Nb_2O_5/TiO_2 > MoO_3/TiO_2 \sim WO_3/TiO_2$). An exception was the K_2O/TiO_2 catalysts, which was essentially inactive for sulfur dioxide oxidation. With the exception of K_2O , all of the surface metal oxide species present in the ternary catalysts (i.e., oxides of V, Fe, Re, Cr, Nb, Mo and W) could undergo

redox cycles and oxidize SO_2 to SO_3 . The turnover frequency for sulfur dioxide oxidation over all of these catalysts is approximately the same at both low and high surface coverages. This indicates that the mechanism of sulfur dioxide oxidation is not sensitive to the coordination of the surface metal oxide species. A comparison of the activities of the ternary catalysts with the corresponding binary catalysts suggests that the surface vanadium oxide and the additive surface metal oxide redox sites act independently without synergistic interactions. The $\text{V}_2\text{O}_5/\text{K}_2\text{O}/\text{TiO}_2$ catalyst showed a dramatic reduction in the catalytic activity in comparison to the unpromoted $\text{V}_2\text{O}_5/\text{TiO}_2$ catalyst. The ability of K_2O to significantly retard the redox potential of the surface vanadia species is primarily responsible for the lower catalytic activity of the ternary catalytic system.

Pimanmas (1999) investigated the application of V-Mg-O/ TiO_2 catalyst on the selective oxidation of methanol, ethanol, 1-propanol and 2-propanol. In this research, the various conditions had been performed to determine the suitable conversion for each reaction. The amounts of oxygen and alcohols were varied in the range of 5-20% and 4-12%, respectively. The main products from ethanol and 1-propanol oxidation were acetaldehyde and propionaldehyde, respectively and CO_2 . From investigating the effect of amounts of oxygen and alcohols, it was found that the CO_2 selectivity had the lowest value at 5% oxygen and the highest aldehyde yield obtained at 8% alcohols. Thus, it could be concluded that one of the best alcohol/oxygen ratio was to 8/5 gave the best results. Then, the effect of WHSV was studied by changing from 60,000 to 20,000 ml/hr.g of catalyst or increasing the catalyst content from 0.1 to 0.3 g. The results showed that an increase in the amount of catalyst or a decrease in the WHSV values gave the higher aldehyde yield. After that, the methanol oxidation was examined by using the methanol/oxygen ratio equals to 8/5. CO_2 is the main product while CO was detected at high temperature. Due to CO formed, a further experiment was carried out by increasing the oxygen content to 20%, the result showed that no CO was obtained. Therefore, it could be concluded that at 5% oxygen used, the reaction was not complete combustion. For the oxidation of 2-propanol, propene and CO_2 were the major products, which was different from the case of 1-propanol.

Reddy *et al.* (1999) prepared a series of titania based mixed oxides viz., $\text{TiO}_2\text{-SiO}_2$, $\text{TiO}_2\text{-Al}_2\text{O}_3$, $\text{TiO}_2\text{-ZrO}_2$, and $\text{TiO}_2\text{-Ga}_2\text{O}_3$ by a co-precipitation method. These mixed oxides were impregnated with V_2O_5 ranging from 2 to 30 wt% by using ammonium metavanadate as source of vanadium oxide. The mixed oxide supports and the vanadia impregnated catalysts were then subjected to thermal treatments from 500 to 800 °C and were investigated by XRD, FTIR, O_2 uptake and BET surface area methods to establish the effects of vanadia loading and thermal treatments on the surface structure of dispersed vanadia species and thermal stability of the catalysts. Calcination of coprecipitated support hydroxides at 500 °C resulted in the formation of an amorphous phase, and further heating to 800 °C resulted in the formation of titania anatase phase, except with $\text{TiO}_2\text{-ZrO}_2$ support where a ZrTiO_4 compound was observed. All these mixed oxides exhibited a high thermal stability. Oxygen uptake results suggested a high dispersion of vanadia on these mixed oxide supports when calcined at 500 °C. The mixed oxide based V_2O_5 catalysts studied were found to be very active and selective for the synthesis of isobutyraldehyde from methanol and ethanol, and for the selective oxidation of 4-methylanisole to anisaldehyde.

Lemonidou *et al.* (2000) investigated the oxidative dehydrogenation of propane using vanadia type catalysts supported on Al_2O_3 , TiO_2 , ZrO_2 and MgO . The promotion of $\text{V}_2\text{O}_5/\text{Al}_2\text{O}_3$ catalyst with alkali metals (Li, Na, K) was also attempted. Evaluation of temperature programmed reduction patterns showed that the reducibility of V species is affected by the support acid-base character. The catalytic activity is favored by the V reducibility of the catalyst as it was confirmed from runs conducted at 450-550 °C. $\text{V}_2\text{O}_5/\text{TiO}_2$ catalyst exhibits the highest activity in oxydehydrogenation of propane. The support's nature also affects the selectivity to propene. V_2O_5 supported on Al_2O_3 catalyst exhibits the highest selectivity. Reaction studies showed that addition of alkali metals decreases the catalytic activity in the order non-doped > Li > Na > K. Propene selectivity significantly increases in the presence of doped catalysts.

Medeiros *et al.* (2000) studied the role of water in the oxidation of ethanol to acetic acid on Sn–Mo–O catalysts in gas phase by catalytic test and FTIR spectroscopy of adsorbed species. The reaction showed a typical behavior of series reactions involving oxidation of ethanol to acetaldehyde and of the latter to acetic acid and CO₂. Addition of water to the feed gas decreased the oxidation rate and significantly increased the selectivity to acetic acid, strongly contributing to decreasing the number of secondary products. FTIR analyses showed that water promoted desorption of ethanol and carboxylates, present as bridging and monodentate species. Decreasing catalytic rate values and increasing selectivity to acetic acid in the presence of water follow from site blocking by hydroxyl groups.

Mongkhonsi *et al.* (2000) investigated the selective oxidation reaction of ethanol and 1-propanol over V-Mg-O/TiO₂ catalyst. Ethanol and 1-propanol could be selectively oxidized to ethanal and propanal, respectively. Aldehyde yields up to 73% and 66% for ethanal and propanal, respectively, were achieved in the temperature range 200-250°C. The catalyst was rather inactive for the further oxidation of aldehyde products to carboxylic acids.

Tellez *et al.* (2000) characterized a VMgO catalyst using a battery of both *in situ* and *ex situ* techniques in order to gain insight into the relationship between the state of the catalyst surface and the catalytic performance observed during the oxidative dehydrogenation of n-butane. It has been found that treating the catalyst under oxygen-rich or oxygen-lean atmospheres markedly changes the activity, selectivity, and rate of catalyst deactivation. The performance of the catalyst under both types of atmospheres was also notably different. A certain degree of catalyst reduction is desirable for this reaction, because it increased the selectivity to dehydrogenation products by limiting the amount of oxygen available at the catalyst surface. However, the performance of the catalyst under oxygen-depleted reaction atmospheres is not stable, the main cause for catalyst deactivation being the formation of coke.

2.2 Comment on previous works

From the above reviewed literature, several supported vanadium oxide or V-containing systems have been studied in the selective oxidation reactions such as V-Mg-O [Pentazidis *et al.* (1996), Lemonidou *et al.* (1998)], $V_2O_5/TiO_2/SiO_2$ [Quaranta *et al.* (1997)], V_2O_5/TiO_2 [Liu *et al.* (1998)]. It can be seen that supported vanadium oxide catalysts have a good performance in many hydrocarbon oxidation reactions.

For water vapor, it plays some important roles in the selective oxidation reactions [Saleh-Alhamed *et al.* (1996), Medeiros *et al.* (2000)]. Water was formed to be able to suppress the formation of CO_2 and decreases the oxidation rate.

Although many studies have focused on the vanadia-titania and vanadium-magnesium oxide system, there are no informations about the combination of these two systems. Furthermore, there are also no information about the role of water vapor in the reactions over supported vanadium oxide catalysts. In this research, the system consists of oxides of vanadium, titanium and magnesium is investigated to study the catalytic property in the oxidation reaction in the presence of water vapor.

CHAPTER III

THEORY

Of all the reactions used to convert alkenes into more useful and valuable products, none is more widely exploited than selective oxidation. Great effort has been expended on discovering and developing catalysts that can convert alkenes by reaction with air in a single step into partially oxidized products, which in turns can be transformed into useful polymers and other chemicals for which there is a great demand. Aromatic hydrocarbons, and some saturated hydrocarbons, can also be selectively oxidized to more valuable products.

Selective oxidation reactions catalyzed by surfaces of transition-metal oxides are some of the most widely applied processes for converting hydrocarbons into valuable chemical intermediates. A catalyst for a selective oxidation process is designed to provide a limited amount of oxygen to a reactant, allowing formation of the desired product but restricting further oxidation that would give CO and CO₂. The industrial catalysts which are successful in this way are usually complex solid oxides, the surfaces of which donate oxygen to adsorbed hydrocarbon reactants. Catalyst selectivity, measured by the rate of formation of desired products relative to CO, CO₂, and other undesired side products, is often sensitive to reaction conditions, especially temperature; reactor design is difficult since the reactions are strongly exothermic and reactor temperature profiles are difficult to predict.

Reactor operation can be illustrated easily in a qualitative way for a fixed bed. For simplicity, only two reactions are considered, selective oxidation to give the desired product and further oxidation of the desired product to give CO₂. Both reactions are usually highly exothermic, total oxidation being the more so.

From results of kinetics experiments on the oxidation of naphthalene catalyzed by V_2O_5 , Mars and van Krevelen (1954) concluded that the reaction took place in two steps:

1) a reaction between the oxide and the hydrocarbon in which the hydrocarbon is oxidized and the oxide reduced

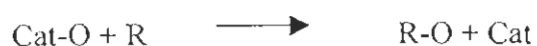
2) a reaction of the reduced oxide with O_2 to give back its initial state

The species directly responsible for the oxidation is generally assumed to be the O^{2-} ion on the surface of the oxide catalyst.

The validity of this pattern has now been established for numerous oxidation reactions and catalysts. The Mars-van Krevelen mechanism prevails with some generality in hydrocarbon oxidation reactions catalyzed by oxide surfaces.

In partial oxidation reactions, it usually necessitates H atom(s) abstraction, and O atom(s) insertion from the surface into the hydrocarbon molecule and several electron transfers. In the Mars-van Krevelen mechanism, lattice oxygen anions are assumed to be inserted in the substrate molecule or to facilitate its dehydrogenation by forming H_2O while the metallic cations inserted the redox mechanism to occur by changing their oxidation state. This was postulated that the catalytic reaction comprises two steps by the followings:

1) Reaction between catalyst in an oxidized form, Cat-O, and the hydrocarbon R, in which the oxide becomes reduced.



2) The reduced catalyst, Cat, becomes oxidized again by oxygen from the gas phase.



3.1 Nature of supported oxides

Supported oxides consist of an oxide deposited on the surface of another oxide (support). The supported oxide (M) binds to the support (S) via bridging M-O-S bonds. For instance, surface vanadia species present a terminal V=O bond. Supported oxide species are present as surface isolated or bidimensional polymeric species, and aggregate as crystals above the monolayer coverage. Silica with a much higher surface area than alumina reaches monolayer coverage at 12% V₂O₅ (ca. 2 V atoms/nm²), whereas a loading of 25% V₂O₅ is required on alumina to reach a monolayer coverage (ca. 13 V atoms/nm²). For most oxides, surface monolayer coverage is 5-10 times higher than for silica [Wachs (1996)]. As the loading increases, the interaction among the supported metal oxide species (M) increases, thus resulting in surface polymeric species, characterized by the formation of M-O-M bonds.

The presence of additives and impurities (Ca, Na, K, etc.) tend to coordinate to acidic supported oxides (V, Mo, W, etc.) by altering the M-O bonds [Deo and Wachs (1994), Ramis *et al.* (1993)]. Acidic additives affect the structure of the supported species since the support sites must be shared with a second component, resulting in an effective increase in surface coverage [Wachs *et al.* (1996)]. The interaction with P, for supported vanadium oxide species may result in VOPO₄ if V is added prior to P; otherwise P coordinates strongly on the support. However, if silica is the support, its weak interaction with any supported species will allow the formation of VOPO₄ and of alkali vanadates irrespective of the preparation procedure [Owens and Kung (1994)], thus removing surface oxide species [Banares *et al.* (1994)].

3.2 Activation of the hydrocarbon and selectivity

The affinity between the hydrocarbon and the surface promotes the activation of the molecules. Selectivity is also determined by the hydrocarbon-catalyst interaction, the reactivity of the catalyst, and the stability of surface hydrocarbon species. A strong acid-base interaction with the support may also promote further degradation of partial oxidation products. Thus, higher hydrocarbons require basic sites to promote selectivity to olefin such as for butane [Madeira *et al.* (1997)]. The appropriate use of alkaline additives increase selectivity at a given conversion. The selectivity to olefins in a series of catalysts depends on their basic character and on the specific hydrocarbon. n-butane increase its selectivity in the order $\text{VO}_x/\text{Al}_2\text{O}_3 < \text{VO}_x/\text{MgO}+\text{Al}_2\text{O}_3 < \text{VO}_x/\text{MgO}$: corresponding to a decrease in relative acidity, as determined by pyridine adsorption. In a different series (alkali-doped $\text{V}_2\text{O}_5/\text{TiO}_2$), the conversion in propane dehydrogenation decreases, but the yield to propene increases, due to a decrease in the heat of adsorption of propane [Grabowski *et al.* (1996)]. The performance of the catalyst is also affected by the acid-base characteristics of the hydrocarbon vs. that of the catalyst. The reactivity of the catalyst is also of great relevance, because it determines how fast the surface intermediates react. By contrast, non-reducible oxides are much less reactive and require high reaction temperatures.

3.3 Partial oxidation to oxygenates

3.3.1 Vanadium oxide-based catalysts

V-containing catalysts have been extensively used in a large number of catalytic processes involving selective oxidation reactions (such as the conversion of butane to maleic anhydride, oxidation of o-xylene, 1,3-butadiene, methanol, CO, ammoxidation of hydrocarbons, selective catalytic reduction of NO, and the partial oxidation of methane).

- On the active oxygen site

Like other reactions, the terminal metal-oxygen double bond has been proposed to be the active site for selective oxidation of hydrocarbons, however, the interaction of a hydrocarbon molecule is most favourable with a bridging oxygen than with a terminal one for vanadium oxide clusters. Furthermore, several experimental evidences support the relevance of bridging oxygens for selective oxidation of hydrocarbons. Initially, studies on molybdenum oxide suggests that the oxygen involved in catalytic selective oxidation is the bridging one. Combined Raman and isotopic labeling on β -VOPO₄ suggests that the V-O-P oxygen is involved in the selective dehydrogenation of C₄ hydrocarbons, while the contribution from the terminal V=O bond to this selective process appears to be very reduced. The terminal oxygen is not critical for the selective oxidation of hydrocarbons. In fact, an in situ isotopic Raman study with ¹⁸O₂ revealed that the terminal V=¹⁸O bond is stable for nearly 20 times the characteristic reaction time. More recently, in different environments, vanadium has the same activity irrespective of the presence of the terminal V=O bond.

- Support effect (V-O support bond)

The oxygen species bridging surface vanadium oxide species to the support may play a significant role in catalyst activity. The change in support alters the turnover frequency number by four orders of magnitude for methanol oxidation and two orders of magnitude for butane oxidation. These results suggest that the bridging V-O-S bond would be directly involved in the reactivity of supported vanadium oxide species. The evaluation of vanadium sites in different environments underlines the relevance of the V-O-S bond for activity vs. the terminal V=O bond. The activity order is close to the reducibility of surface vanadium oxide species on these supports, which correlates with the Sanderson electronegativity of the cation of the oxide support. However, this trend follows as CeO₂ > ZrO₂-TiO₂ > Nb₂O₅ > Al₂O₃ > SiO₂. Ceria and niobia react with the

supported vanadia, forming new compounds that remove surface vanadia species thus decreasing their activity. The presence of an acidic support (alumina) also increases activity but to a lesser extent than a reducible support. The higher reducibility results in a higher turnover frequency number, but oxidation state under reaction conditions does not correspond with the reducibility, as observed by in situ Raman and Vis-UV spectroscopy. The stability of the supported vanadium oxide catalyst is an important factor. Reducibility of V on SnO and CeO₂ is high but the activity is low. When tin oxide is used as a support for vanadium oxide it promotes its integration into the rutile lattice of SnO as V⁴⁺. A similar phenomenon takes place for titania-supported vanadium oxide, which decreases its activity due to integration of V⁴⁺ sites into the rutile phase of titania, along with the utilization of anatase phase. It should be noted that the lower activity of surface vanadium oxide species is not affected by the specific oxide support phase. It has been shown that the structure (according to Raman spectroscopy and ⁵¹V-NMR) and reactivity of surface vanadia species for methanol oxidation is not affected for a series of titania-supported vanadia on a series of titania supports possessing different phases (anatase, rutile, brookite and B). As comment above the low turnover frequency numbers for V₂O₅/Nb₂O₅ and V₂O₅/CeO₂ are due to a solid state reaction with the support.

Unlike the above supported vanadia catalysts, the magnesia supported vanadia catalyst system cannot form a complete close packed surface vanadia monolayer because of acid-base reaction between acidic vanadia and basic magnesia. The strong interaction between vanadia and magnesia results in the formation of a mixed metal oxide compound rather than a stable surface vanadia overlayer on the magnesia support [Deo *et al.* (1992)]. The vanadia coordination in bulk V-Mg-O mixed metal oxide catalysts consist of VO₄, VO₅ and VO₆ units. Thus, the magnesia supported vanadia catalyst system possesses both surface and bulk vanadia species.

- Surface vanadium oxide coverage effect (V-O-V bonds)

Surface coverage alters the population ratio of (V-O-V)/(V-O- support) bonds. This trend is not observed on silica-supported vanadia, where isolated surface vanadium oxide species are dominant up to monolayer coverage.

In methane conversion to oxygenates [Faraldos *et al.* (1996)] with vanadium loading on silica, selectivity is affected by the coordination of vanadium oxide sites since the presence of V-O-V bonds with increasing coverage of vanadium decreases the selectivity to ethylene, it may be due to a larger number of active sites that may attack the hydrocarbon molecule. In fact, the site isolation proves to improve selectivity. In this line, it is interesting to note that the best selectivities are reached on silica-supported oxides. It should be noted that no surface polymeric species are observed in silica-supported vanadia under dehydrated conditions, and only surface isolated vanadium oxide species are present up to monolayer coverage as measured by Raman and ^{51}V -NMR spectroscopy and by ^{51}V -NMR and TPR measurements [Koranne *et al.* (1994)]. At high surface coverage, ethylene is the main oxidation product whereas at low surface coverage CO_2 is the main oxidation product. The formation of selective oxygen-containing products (mainly acetaldehyde) is only observed at high vanadia surface coverage on silica.

3.3.2 Alkaline and metal additives

Alkali doping has afforded positive effects in many catalytic processes, like the synthesis in ammonia, the oxidation of SO_2 to SO_3 or the dehydrogenation of ethylbenzene to styrene. As regards supported metal oxides, alkaline additives tend to coordinate to acidic surface species (V, Mo, etc.), affecting the V-O bonds. The presence of alkaline additives has a beneficial effect for the dehydrogenation of larger

hydrocarbons due to a modification on the acid-base interaction of the hydrocarbon with the catalyst.

The addition of acidic niobia has no effect on the structure of supported vanadium oxide species, it simply increases the surface density of vanadia sites. This increases the amount of surface polymeric species, except for silica, where no surface polymeric species are observed. The addition of niobia to vanadia titania catalysts modified the redox properties and increases the acidic properties of the V_2O_5/TiO_2 catalyst.

3.4 The role of water

The role of water in improving the selectivity in several reactions of selective oxidation is known, but usually water is considered to help only the desorption of the products or to limit the adsorption of reactants due to competitive chemisorption [Saleh-Alhamed *et al.* (1996)]. In the presence of steam, on the contrary, the coordination characteristics of the active centers and the surface acid-base characteristics of the catalyst can also be modified. In the case of Cu-ZrO₂ catalysts [Mortera *et al.* (1998)], water has a much more complex effect. Water in the gas phase (i) influences the degree of hydroxylation of the surface and thus coordination environment of copper sites as well as (ii) acts as a coordination ligand. Both effects were found to determine the coordination and redox activity of copper sites with a consequent effect on the catalytic reactivity of copper sites in N₂O decomposition.

CHAPTER IV

EXPERIMENT

The experiment in this work consists of three parts: (i) the catalyst preparation: (ii) the catalyst characterization: (iii) catalytic reaction of methanol, ethanol, 1-propanol and 2-propanol. The details of the experiments are described as the following:

The reaction conditions are chosen as follows:

Catalyst	: 10 wt% V 2wt%Mg/TiO ₂
Reactant	: methanol
	: ethanol
	: 1-propanol
	: 2-propanol
	: water
	: N ₂
	: air (used as O ₂ source)
Flow rate of reactant	: 100 ml/min
Reaction temperature	: 200-500 °C
Gas hourly space velocity	: 60,000 ml/hr.g

*The wt% of V calculated as V₂O₅

The wt% of Mg calculated as Mg

4.1 Preparation of catalyst

4.1.1 Materials

The detail of chemicals used in this experiment is shown in table 4.1.

Table 4.1 The chemicals used in this research

Chemicals	Grade	Manufacturer
Titanium oxide [TiO ₂]	JRC-TIO1	Dept. of Material Science, Shimane University
Ammonium metavanadate [NH ₄ VO ₃]	Analytical	Carlo Erba, Italy
Magnesium nitrate [Mg(NO ₃) ₂]	Analytical	Fluka, Switzerland

4.1.2 Preparation of V-Mg-O/TiO₂ Catalyst

V-Mg-O/TiO₂ catalyst was prepared by wet impregnation method. First step of the preparation, TiO₂ powder was added to an aqueous solution of ammonium metavanadate (NH₄VO₃) at 70°C. The suspension was dried at 80°C and calcined in air at 550°C for 6 hours. The sample obtained was V₂O₅/TiO₂. Then Mg was introduced into the V₂O₅/TiO₂ by impregnation from magnesium nitrate (Mg(NO₃)₂) solution and the suspension was dried and calcined in the same above condition. The catalyst was denoted as xVyMgTi where x was wt% of V calculated as V₂O₅ and y is wt% of Mg. For this research, 10V2MgTi [Pimanmas (1999)] was used.

4.2 The catalyst characterization

4.2.1 Thermogravimetric Analysis

The thermal stability of catalyst was determined by thermal gravimetric analysis (TGA) in a Shimadzu TA-50 thermal analyzer in the range of reaction temperature (200-500 °C).

4.2.2 Transmission Electron Microscopy (TEM)

This method is used to determine the atomic structure of catalyst.

4.2.3 Determination of composition contents of catalyst

The actual composition contents of the prepared catalyst were determined by atomic absorption spectroscopy (AAS) at the center service of science. The sample of calculation of catalyst preparation is shown in Appendix A.

4.2.4 Surface Area Measurement

The BET surface area of the sample was determined by nitrogen absorption in an automatic apparatus ASAP 2000 constructed by Micromeritics U.S.A. The data obtained were recorded by a microcomputer.

4.2.5 X-ray Diffraction Experiments

The crystal structure of the catalyst was identified by X-ray diffraction (XRD) analysis carried out on a Siemens D500 diffractometer with $\text{CuK}\alpha$ radiation in the 2θ range of 10-80°

4.2.6 Fourier Transform Infrared Spectroscopy (FT-IR)

The sample was mixed with KBr with ratio of sample:KBr equal to 1:100. Then the mixture was grounded into a fine powder and pressed into a thin wafer. Infrared spectra were recorded between 2000 and 400 cm^{-1} with FT-IR spectroscopy, Nicolet Impact 400, Nicolet Instrument Corporation, U.S.A. The spectra were used to study the functional group of surface vanadium oxide species of V-Mg-O/TiO₂ catalyst.

4.3 Catalytic Reaction

Flow diagram of the reaction system is shown in Figure 4.1. The methanol, ethanol, 1-propanol and 2-propanol oxidation system consist of a reactor, an automatic temperature controller, an electrical furnace, a gas controlling system and 2 saturators for evaporating the reactants and water before entering the reactor.

The microreactor is made from a stainless steel tube. Two sampling points are provided above and below the catalyst bed. Catalyst is placed between quartz glass wool layer.

An automatic controller consists of a magnetic contactor, a variable voltage transformer, RKC series RE-96 temperature controller and Eurotherm digital temperature indicator model Telex 87114. Temperature was measured at the bottom of the catalyst bed in the reactor. The temperature control setpoint is adjustable within the range of 0-800°C.

Electrical furnace supplies heat to the reactor for methanol, ethanol, 1-propanol and 2-propanol oxidation. The reactor can be operated from room temperature to 800°C at the maximum voltage of 220 volt.

The gas supplying system consists of cylinders of:

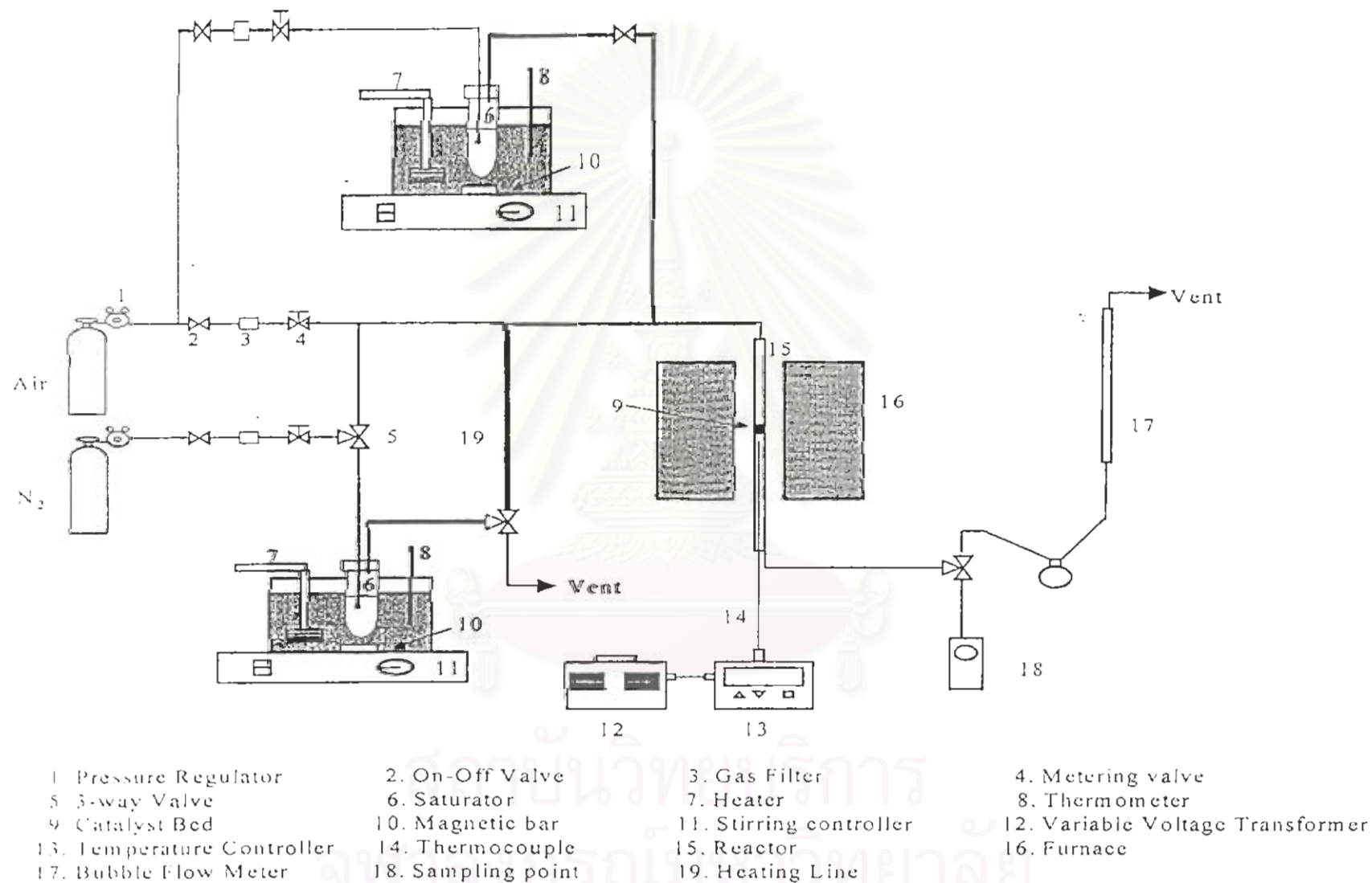


Figure 4.1 Flow diagram of the oxidation reaction system

1. A cylinder of air, equipped with a pressure regulator (0-120 psig), an on-off valve and a fine-metering valve used for adjusting the flow rate of air that passes through the saturator.

2. A cylinder of N₂, equipped with a pressure regulator (0-120 psig), an on-off valve and a fine-metering valve used for adjusting the flow rate of air that passes through the saturator.

The compositions of hydrocarbons in the feed and product streams were analyzed by flame ionization detector gas chromatograph Shimadzu 14B and 14A. The amount of CO₂ formed in the reaction was measured using a gas chromatograph Shimadzu GC-8A equipped with thermal conductivity detector. The operating conditions of GC are described in appendix C.

4.3.2 Procedure

1. 0.1 g of catalyst was packed in the middle of the stainless steel microreactor. Then, the reactor was placed in the electrical furnace.

2. 8 vol% of reactants, 5 vol% O₂, water vapor and balanced N₂ were fed into the reactor. Flow rates of water vapor were adjusted to the required values (0, 7, 20 and 40 vol%).

3. The reaction temperature was between 200-500°C. The reactor was heated up with the heating rate of 10°C/min. Effluent gas was analyzed by the gas chromatograph.

4. The result of catalytic test was calculated in the term of:

$$\%A \text{ conversion} = \frac{\text{mole of A reacted}}{\text{mole of A in feed}} \times 100\%$$

$$\% \text{Selectivity to B} = \frac{\text{mole of A converted to B}}{\text{mole of A reacted}} \times 100\%$$

where A is reactant

B is reaction product



สถาบันวิทยบริการ
จุฬาลงกรณ์มหาวิทยาลัย

CHAPTER V

RESULTS AND DISCUSSION

In this chapter, the results and discussion are categorized into two main parts: (1) The catalyst characterization, (2) The catalytic test by the selective oxidation of methanol, ethanol, 1-propanol and 2-propanol.

5.1 Catalyst Characterization

5.1.1 Determination of composition content of catalyst and surface area

The composition and the BET surface area of 10V2MgTi catalyst, which was determined by AAS and BET surface area measurement, are listed in Table 5.1.

Table 5.1 The composition of catalyst and BET surface area.

Catalyst	%V ^a	%Mg ^b	Surface area (m ² /g)
10 [*] V2MgTi	11.72	1.67	16.57

*The number in the catalyst symbol denotes the approximate weight percentage of V calculated as V₂O₅

^aThe content of vanadium is calculated in terms of %by weight of V₂O₅

^bThe content of magnesium is calculated in terms of %by weight

5.1.2 Transmission Electron Microscopy (TEM)

Transmission electron microscopy showed that crystals have been formed in 10V2MgTi sample, as can be seen in Figure 5.1. A mean value of 200 nm for the crystal size was observed.

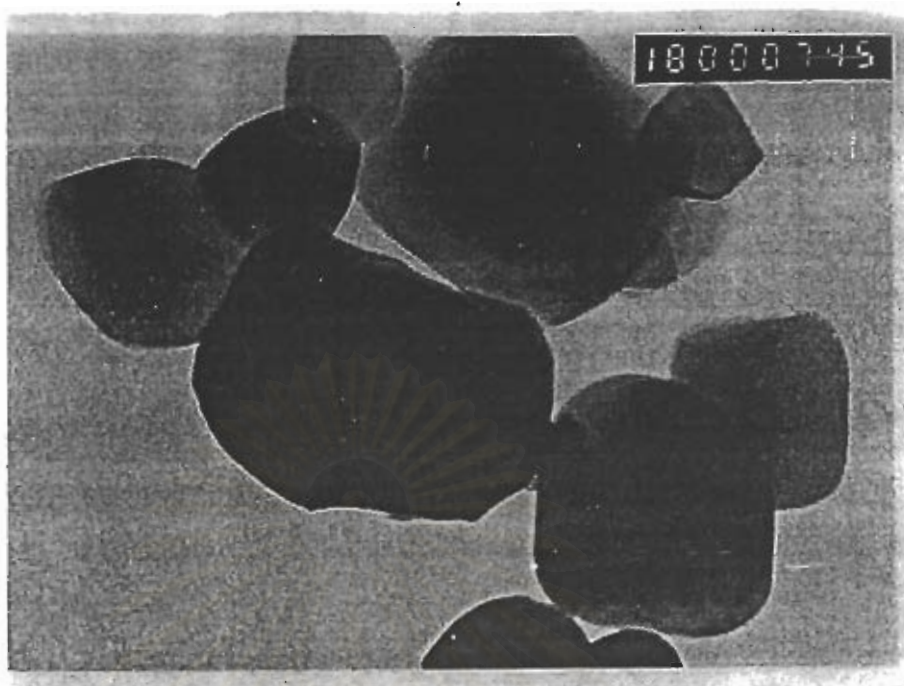


Figure 5.1 Electron micrograph of 10V2MgTi catalyst (1.5 cm = 1 μ m)

5.1.3 X-ray Diffraction

The crystal structure of all samples is characterized by XRD. Figures 5.2 and 5.3 illustrate XRD spectra of TiO₂ and 10V2MgTi, respectively.

From figure 5.3, spectrum of 10V2MgTi shows peaks at the same 2θ values as TiO₂ (figure 5.2). It can be seen that crystalline V₂O₅ peaks can not be detected in this sample. That means the amount of vanadium oxides on 10V2MgTi surface may not enough to be determined by XRD or the vanadium oxide did not form a V₂O₅ crystal structure on the TiO₂ support.

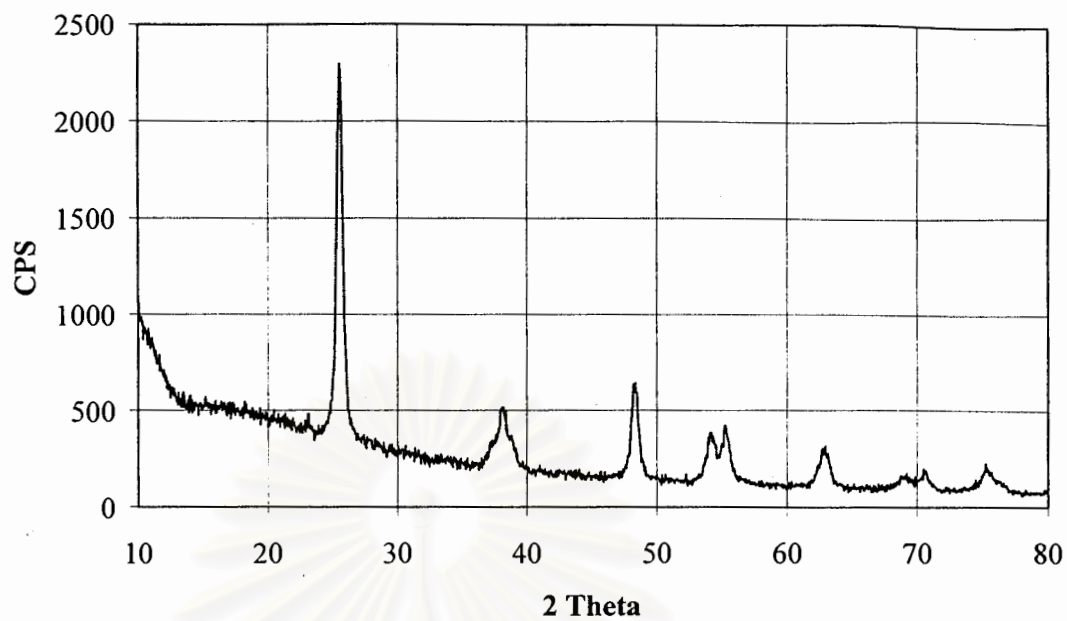


Figure 5.2 X-ray diffraction of TiO₂

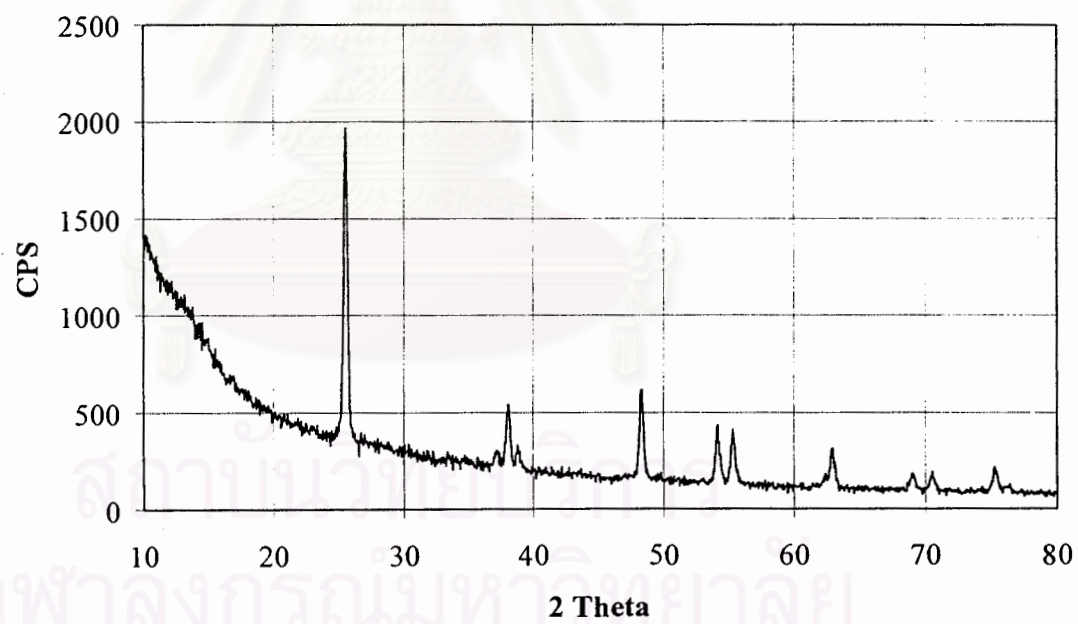


Figure 5.3 X-ray diffraction of 10V₂MgTi catalyst

5.1.4 Fourier Transform Infrared Spetrometer (FT-IR)

The functional group on the surface of 10V2MgTi catalyst can be identified by using infrared radiation in the wavelength of $400\text{-}2000\text{ cm}^{-1}$, which is the proper wavelength for determining the solid surface. Figure 5.4 presents IR spectrum of TiO_2 . Strong absorption bands at 580 and 680 cm^{-1} are observed. As presented in figure 5.5, IR spectrum of 10V2MgTi catalyst exhibits the absorption bands at the same position as TiO_2 . This can be indicated that the amounts of vanadium and magnesium on TiO_2 surface are much less to observe the changes in IR bands.



สถาบันวิทยบริการ
จุฬาลงกรณ์มหาวิทยาลัย

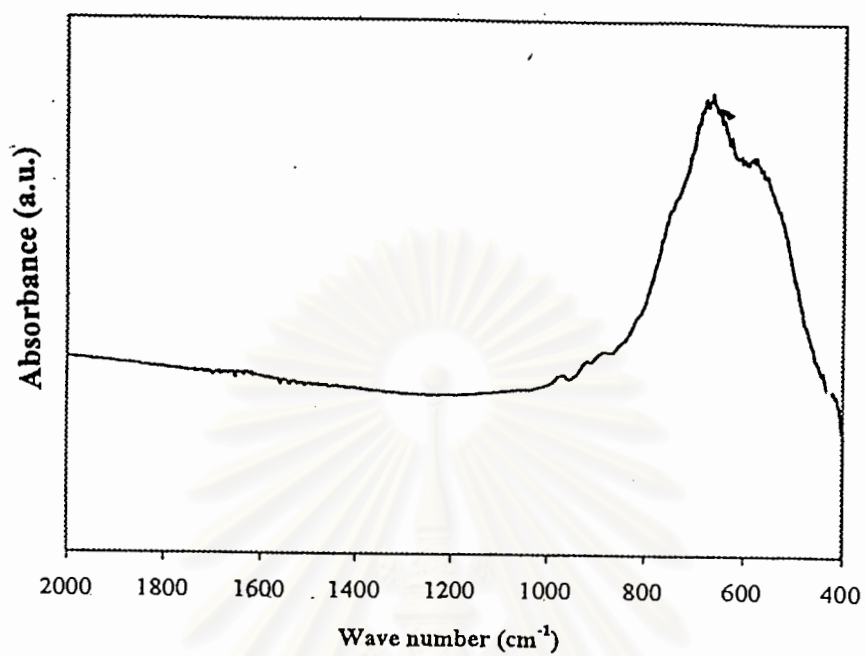


Figure 5.4 IR spectrum of TiO₂

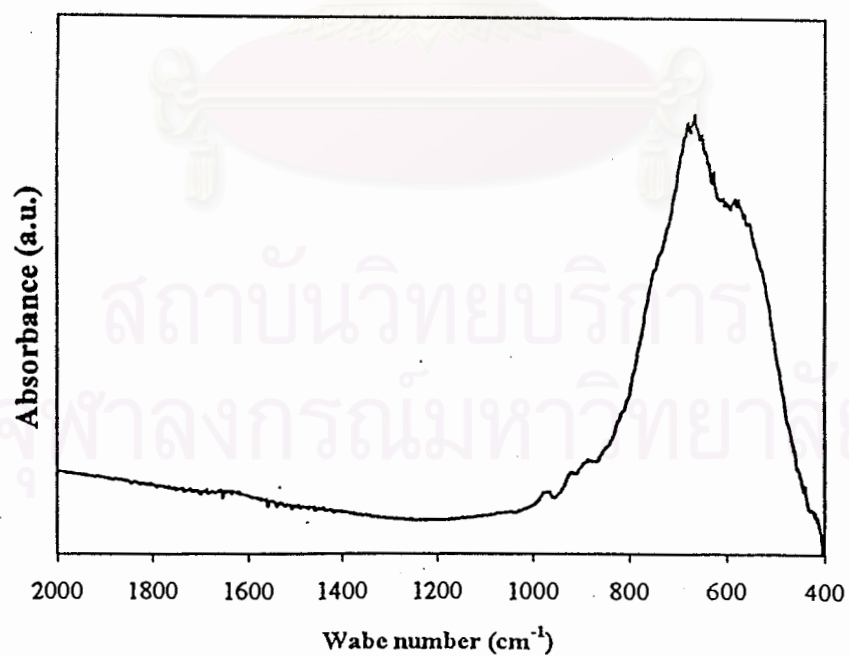


Figure 5.5 IR spectrum of 10V₂MgTi catalyst

5.1.5 Thermogravimetric Analysis (TGA)

The TGA results recorded under reaction temperature (figure 5.6) indicated that 10V2MgTi underwent 2.88 wt% total mass loss after heating to 200°C. This is associated to the release of adsorbed molecular water.

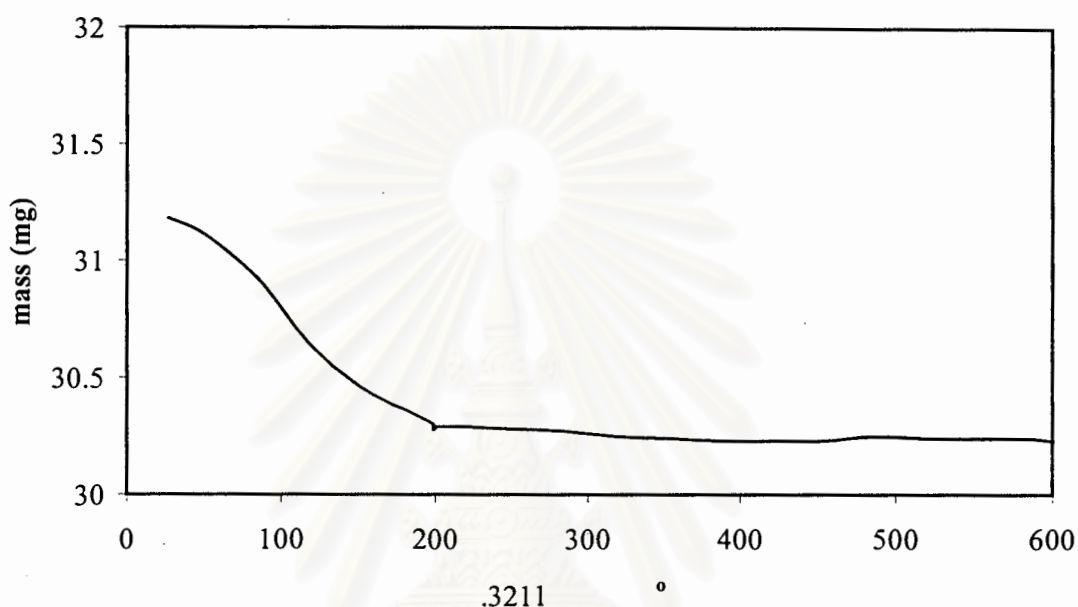


Figure 5.6 TGA result of 10V2MgTi catalyst

5.2 Catalytic reaction

5.2.1 Ethanol oxidation

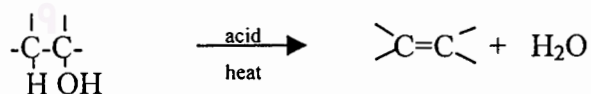
Ethanol is in the class of primary alcohol. Thus, the oxidation of ethanol may give acetaldehyde and acetic acid. The role of water vapor investigated are described in figures 5.7 to 5.10. Figure 5.11 displays yield to acetaldehyde as a function of reaction temperature, in presence of water and without it. The concentration of water used in this reaction are the following: (1) 0 vol%, (2) 7 vol%, (3) 20 vol%, (4) 40 vol%.

For all experiments, the major products obtained are acetaldehyde and CO₂. Small amount of methane, ethane, propene and propane are also detected.

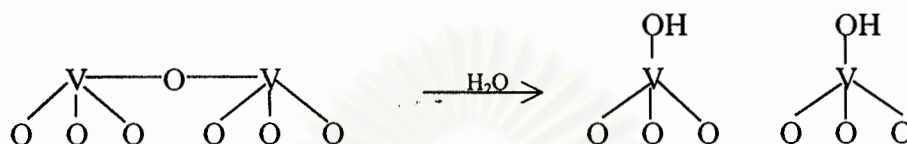
From figures 5.7 to 5.10, the selectivity to acetaldehyde and CO₂ have similar pattern in all cases. The experiment shows that the selectivity to acetaldehyde drops continuously with reaction temperature while the selectivity to CO₂ rises continuously to a high value at 500°C. The conversion of ethanol increases to a maximum value nearly 100% after 350°C. The selectivity to acetaldehyde decreases from nearly 100% at 200°C to nearly 50% at 500°C. In contrast, the selectivity to CO₂ increases from about 0% at 200°C to about 30% at 500°C. The results show that the addition of water to the reaction between 0 to 40 vol% has no strong effect on both conversion and main product selectivity. However, for the case of 20% and 40% water vapor, the selectivity to ethane is higher than obtained from the reactions with 7% and without water vapor.

Since the required product from ethanol oxidation is acetaldehyde. Thus, yields to acetaldehyde from each value of water vapor were plotted in figure 5.11 to determine the effect of the presence of water. It can be seen that the aldehyde yields show the same trends of yield to acetaldehyde for all reaction temperature. For the cases of 0, 7 and 20% water vapor, the best yield to acetaldehyde was obtained between the range of 300-350°C. But the best yield to acetaldehyde in 40% water vapor case is at 250°C. It should be noted that, after 300°C, the results show that addition of water to the reaction slightly decreases yield to acetaldehyde.

Consider the following reaction [Morrison and Boyd (1992)]. An alcohol is converted into alkene by dehydration: elimination of a molecule of water.



The dehydration reaction products of ethanol oxidation consists of ethene and water. But from the results of ethanol oxidation experiments, it can be seen that after the concentration of water increases, the selectivity to ethene is also increases. It is possible that the adsorption of water on the surface of catalyst may form acidic sites, V-OH, which ease the dehydration reaction instead of V=O or V-O-V sites.



So addition of water may promotes dehydration of ethanol.

สถาบันวิทยบริการ
จุฬาลงกรณ์มหาวิทยาลัย

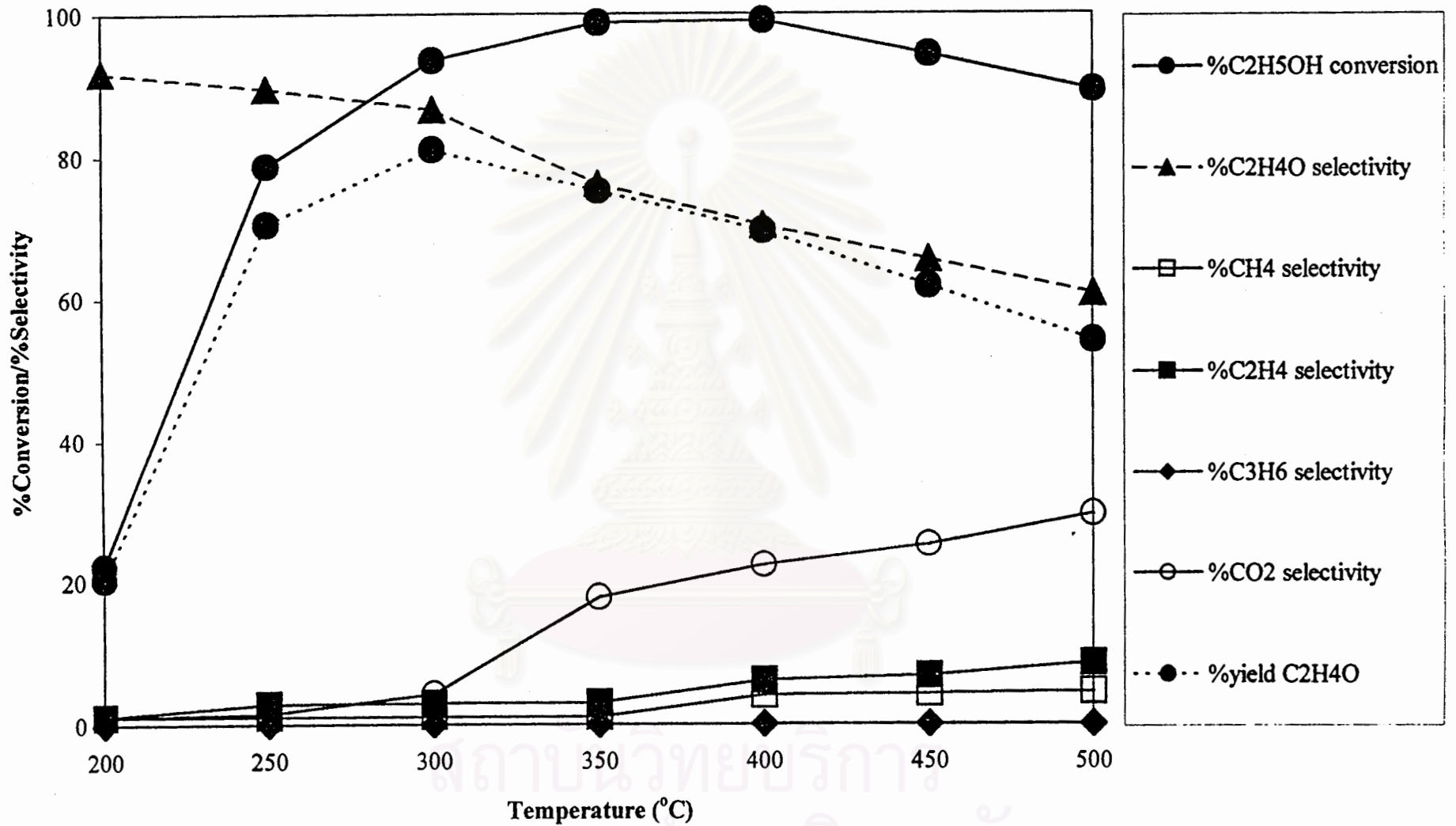


Figure 5.7 The result of ethanol oxidation (no water added)

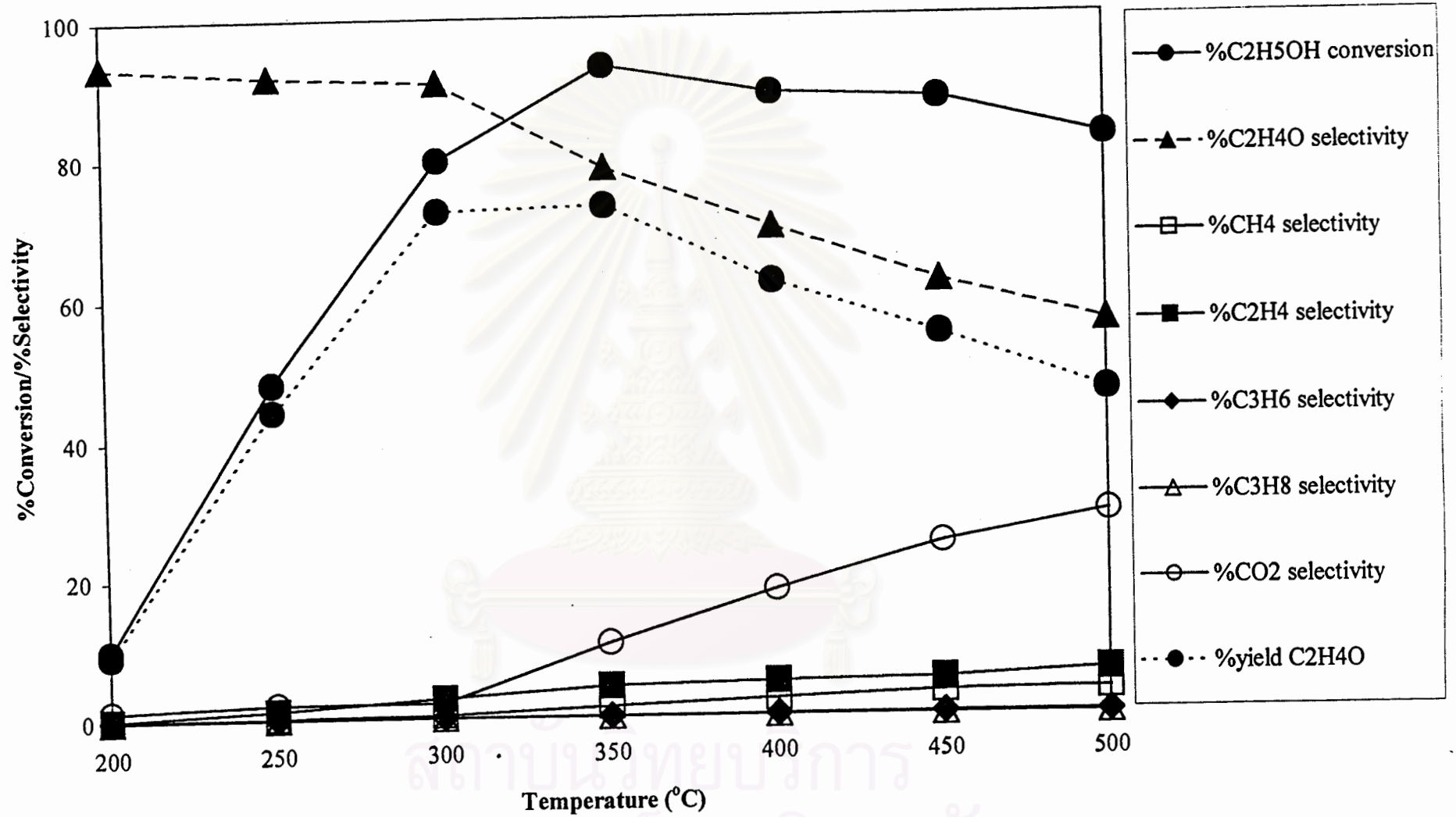


Figure 5.8 The result of ethanol oxidation in the presence of 7% water vapor

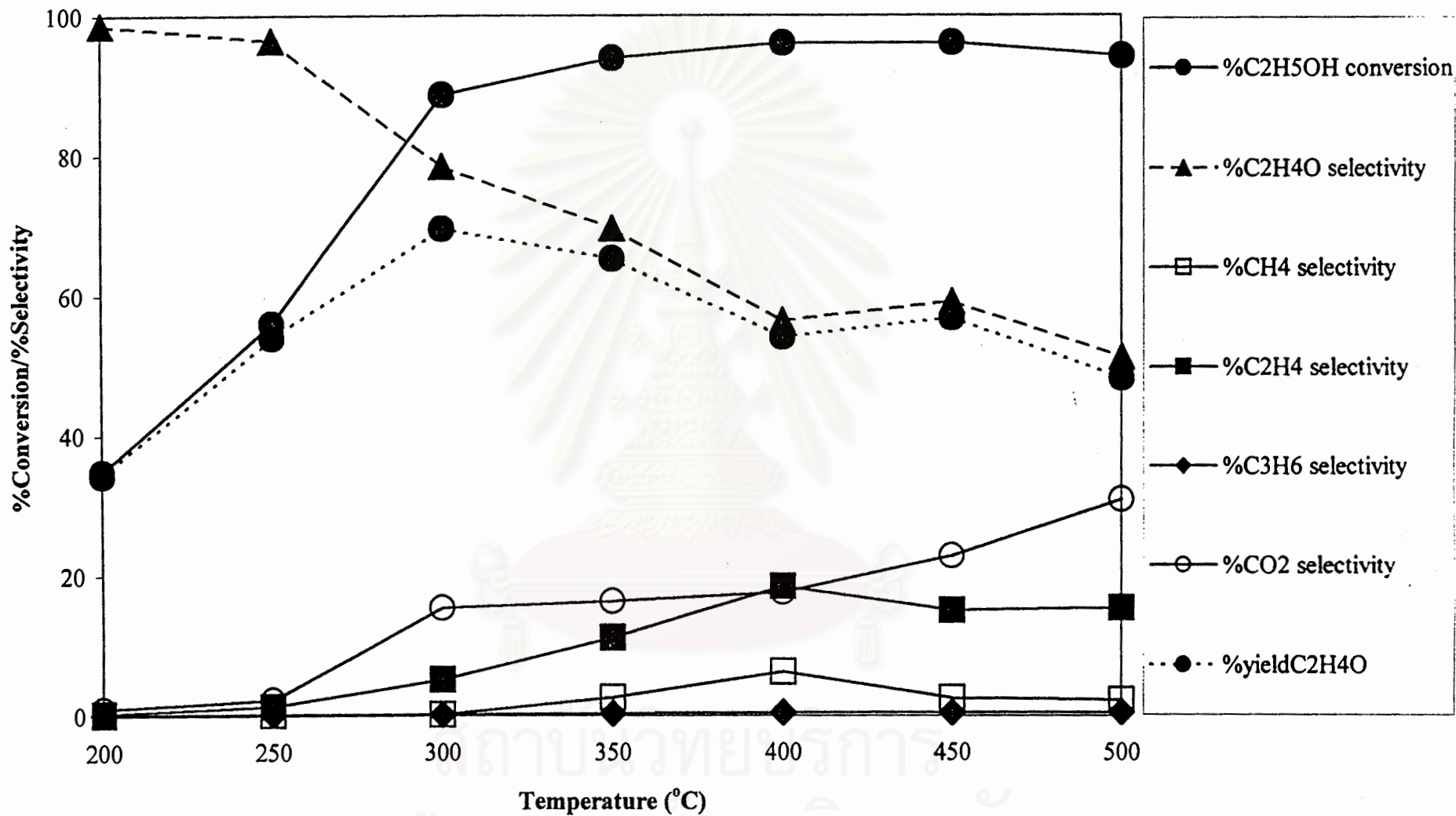


Figure 5.9 The result of ethanol oxidation in the presence of 20% water vapor

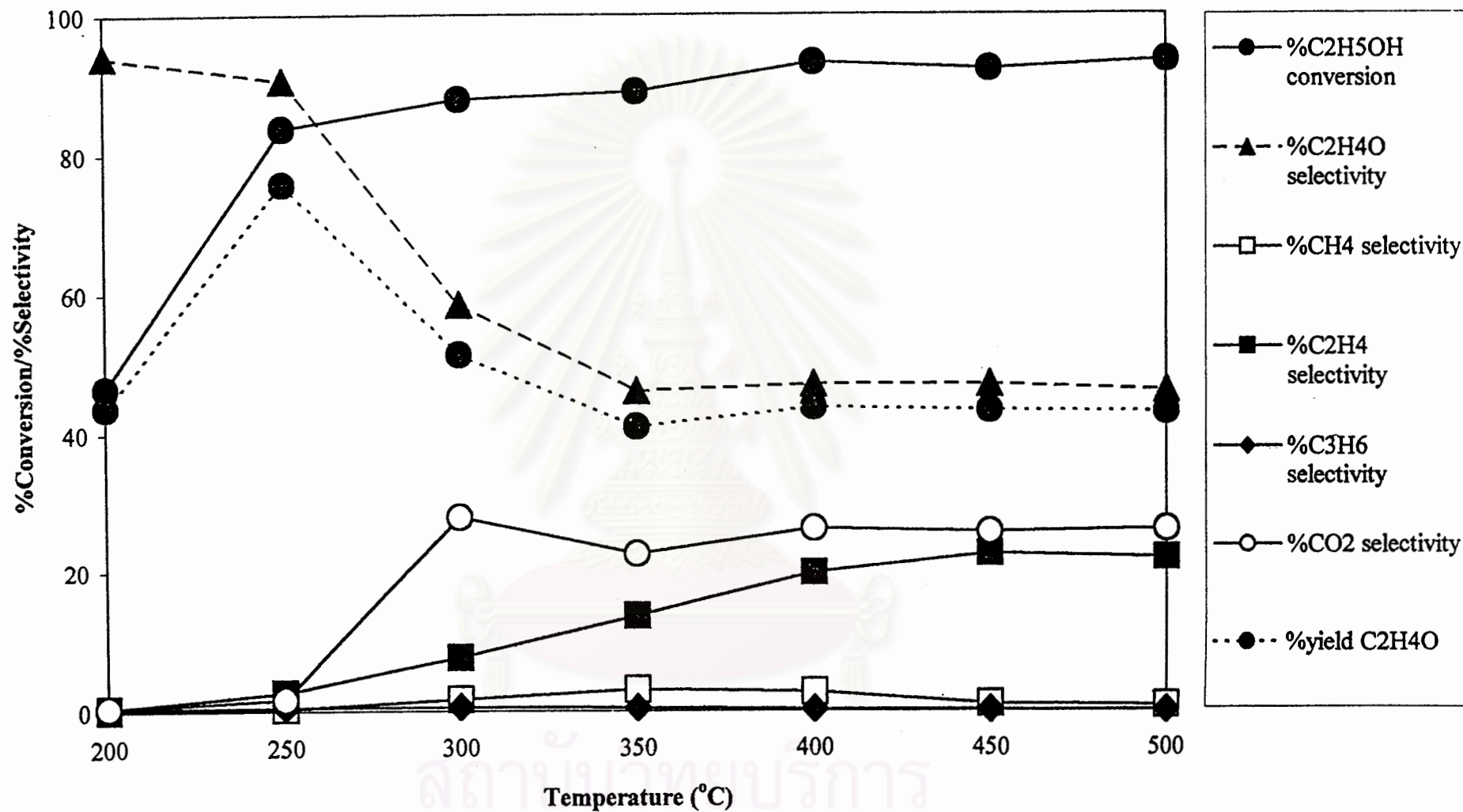


Figure 5.10 The result of ethanol oxidation in the presence of 40% water vapor

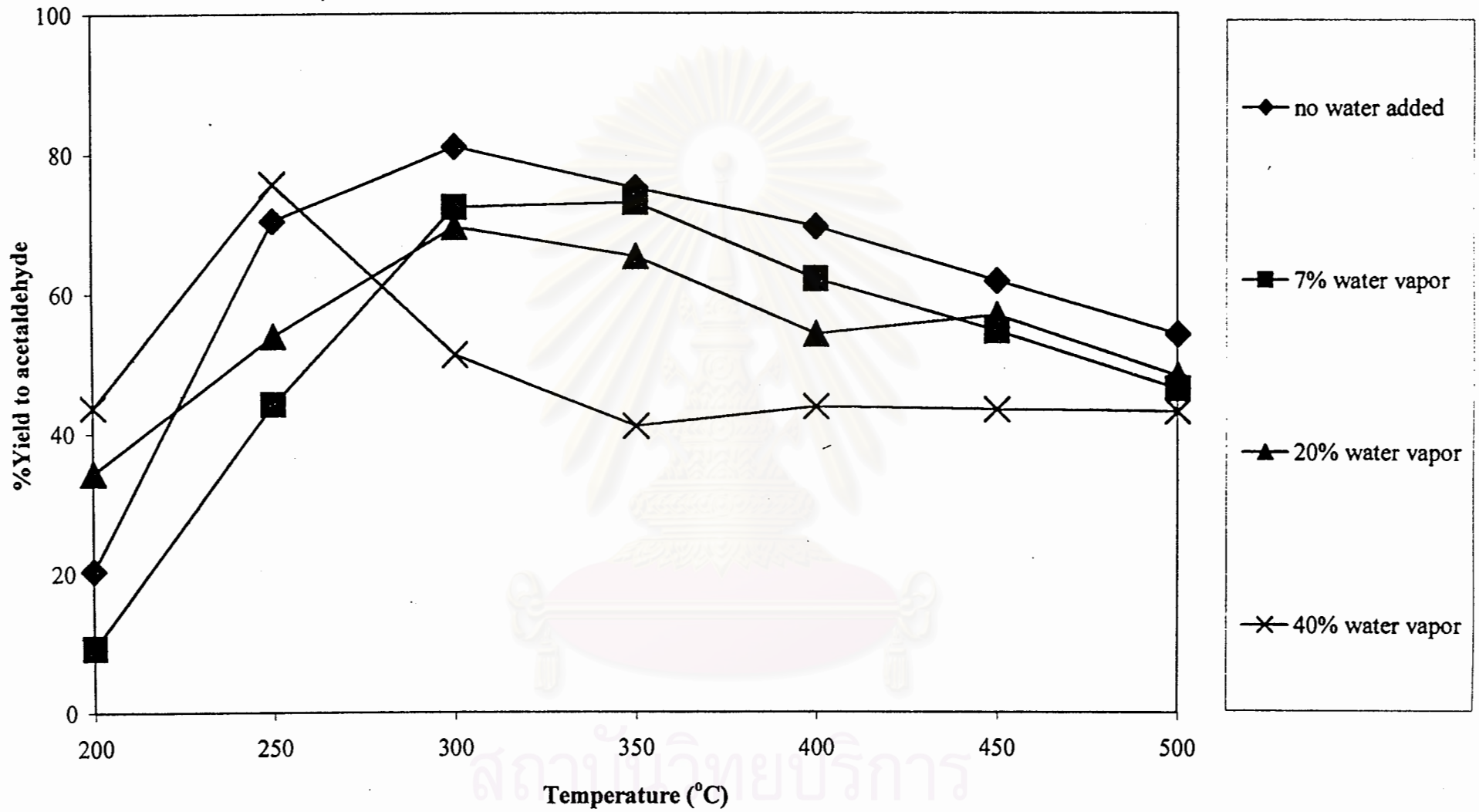


Figure 5.11 %yield C₂H₄O

5.2.2 1-Propanol oxidation

1-propanol is a primary alcohol. It is expected that the product obtained from 1-propanol oxidation should be propionaldehyde (C_3H_6O). As presented in figures 5.12 to 5.15, the main products observed are propionaldehyde and CO_2 . Small amounts of methane, ethane, propene, propane and formaldehyde are also produced. The conversion of 1-propanol increases with reaction temperature. It can be seen that an increase of concentration of water vapor causes higher conversion. From figures 5.12 and 5.13, when temperature increases the selectivity to propionaldehyde gradually decreases from nearly 100% at 200°C to a minimum value about 50% at 500°C. An increase of the selectivity to propylene is also observed. The same trend can be seen in figures 5.14 and 5.15 but the conversion in this case is higher and approaches to nearly 100% after 350°C.

To compare the ability of propionaldehyde production, yields to propionaldehyde from each figure are plotted in figure 5.16. For all cases, the aldehyde yields appear in rather same trend. At the beginning of the reaction (200-250°C), yields to propionaldehyde from the reaction with 40% water vapor are the highest value.

Like ethanol oxidation, it can be seen that the selectivity to propylene increases when the concentration of water increases. Moreover, in the case of 40% water vapor, at high reaction temperature the selectivity to CO_2 increases while the selectivity to propionaldehyde remains rather constant and the selectivity to propylene decreases. Consider the following combustion reactions.



From the above discussion, it can be concluded that the reaction (1) is preferred. Thus, the addition of water vapor promotes dehydration and combustion reactions.

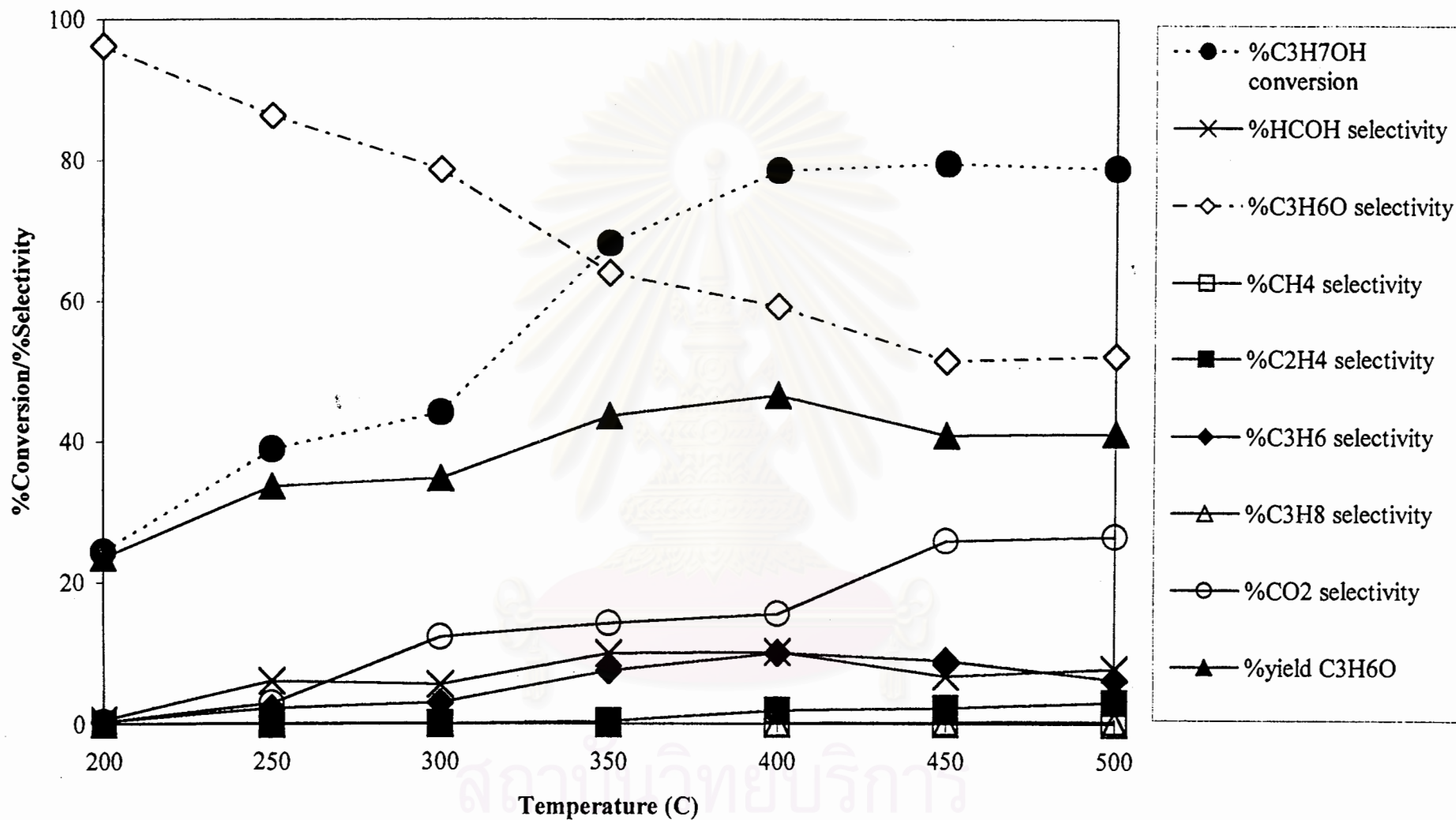


Figure 5.12 The result of 1-propanol oxidation (no water added)

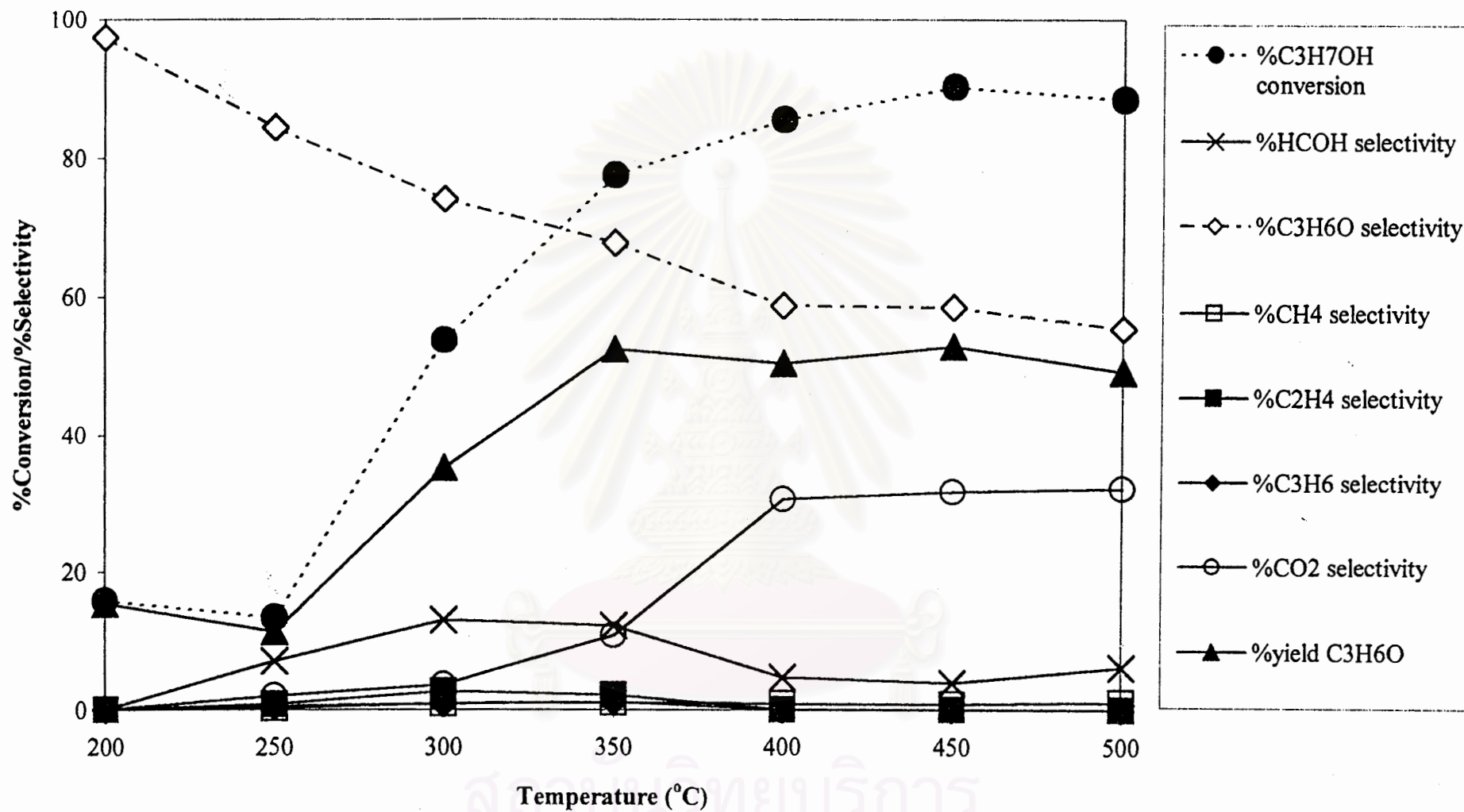


Figure 5.13 The result of 1-propanol oxidation in the presence of 7% water vapor

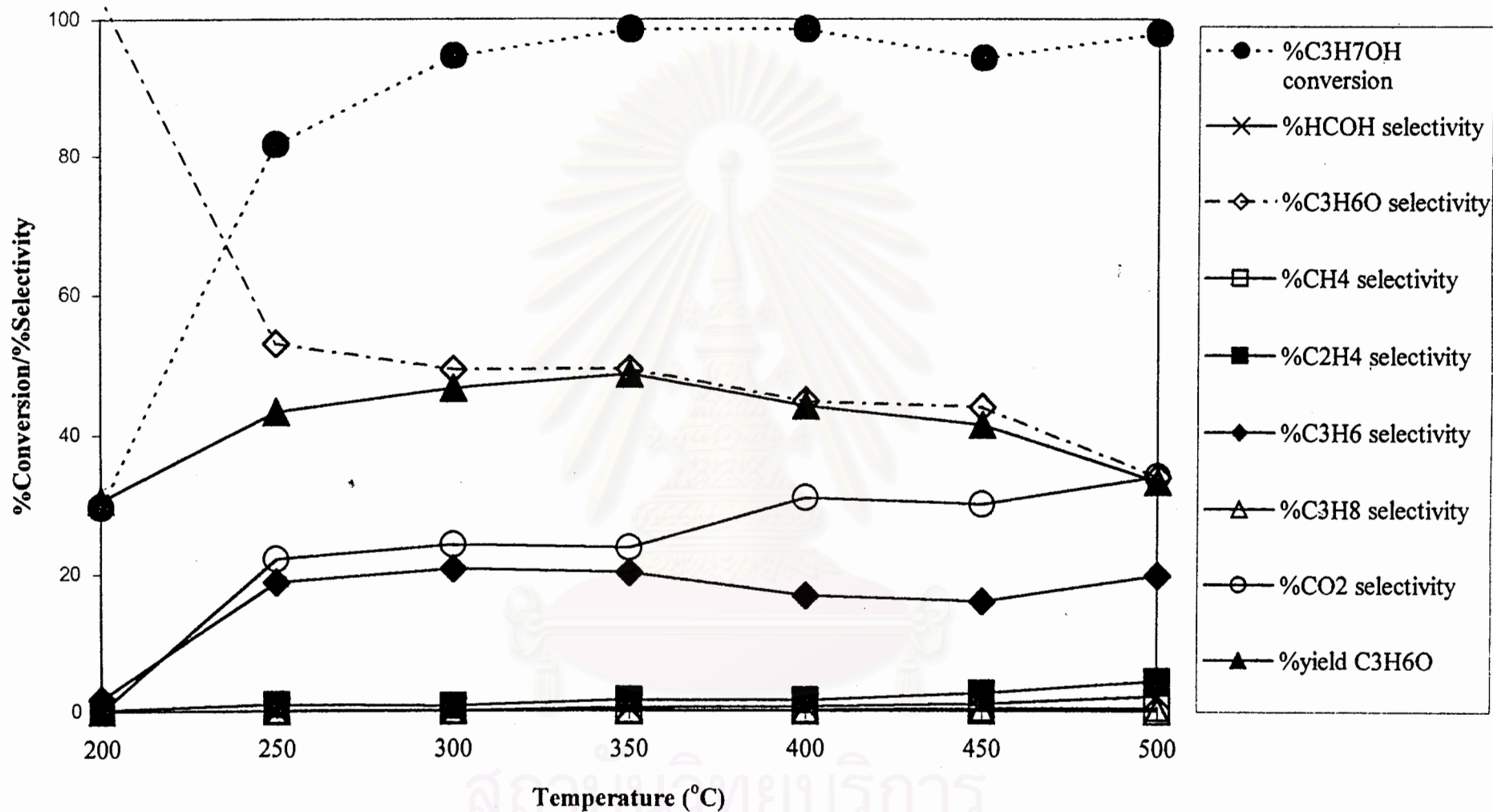


Figure 5.14 The result of 1-propanol oxidation in the presence of 20% water vapor

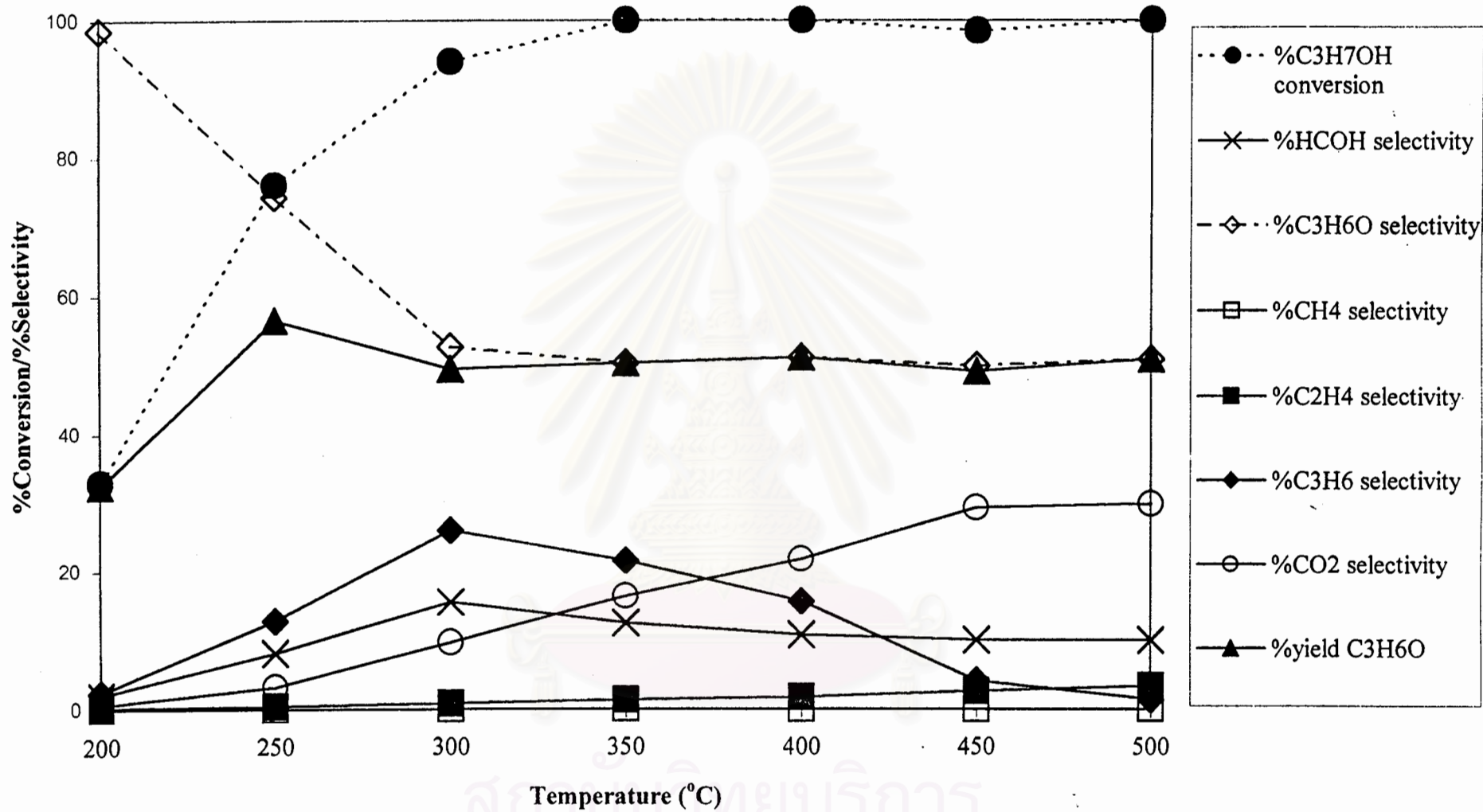


Figure 5.15 The result of 1-propanol oxidation in the presence of 40% water vapor

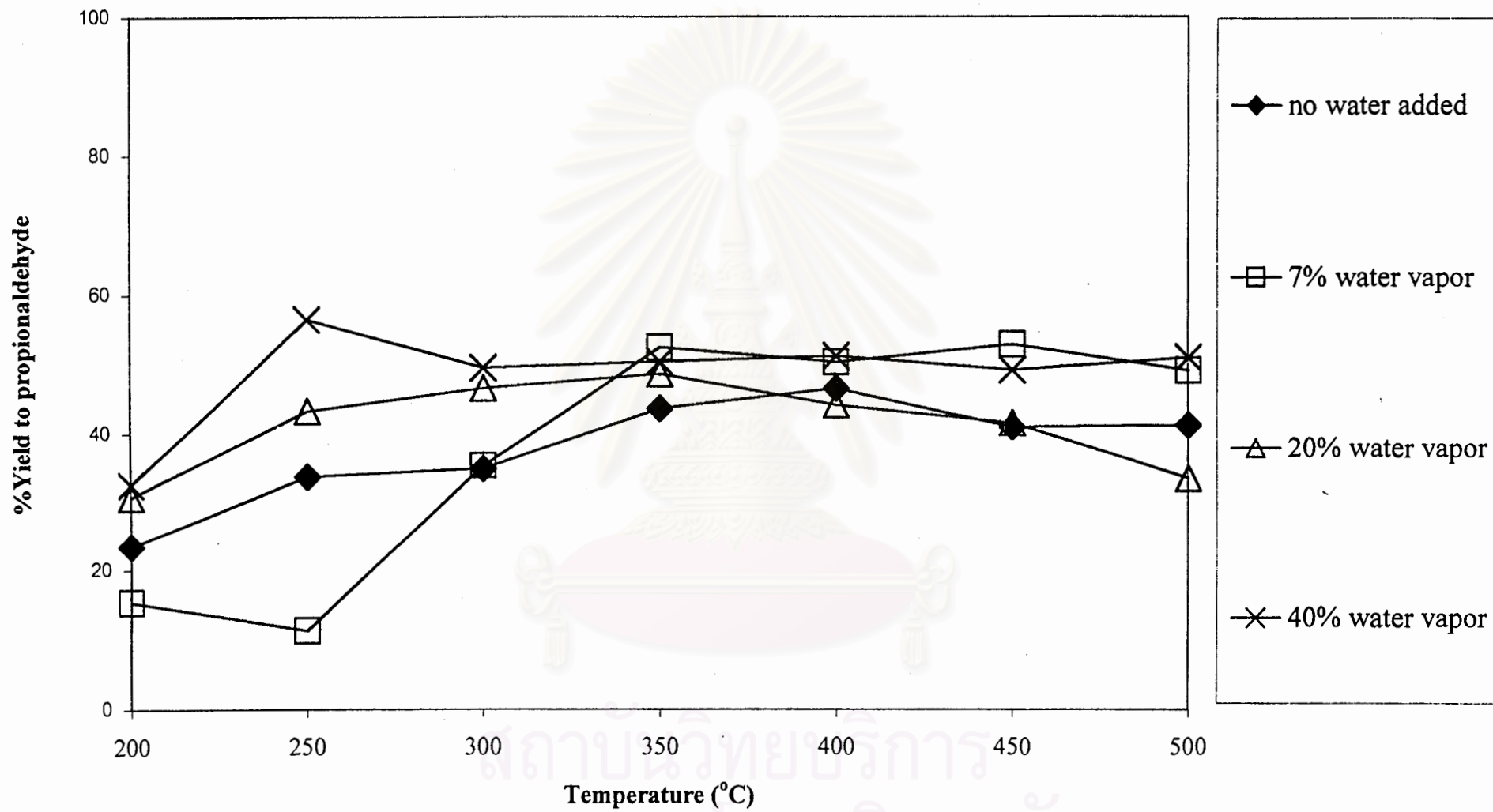


Figure 5.16 %yield to C₃H₆O

5.2.3 Methanol oxidation

The role of water vapor on methanol oxidation are described in figures 5.17 to 5.20. The main products in methanol oxidation consist of CO_2 and CO . Small amount of methane, ethylene and propylene are also formed. The conversion of methanol and the selectivity to CO increase with reaction temperature while the selectivity to CO_2 decrease. In figure 5.17, the conversion at 200°C is about 80% after that it slightly increases to nearly 100% at 300°C . For all water addition cases, the conversion at 200°C does not start at rather high value as the previous but water vapor causes low activity in the range of $200\text{-}300^\circ\text{C}$. The conversion increases from 20% at 200°C to 80% at 300°C for 7 and 20% water vapor cases and nearly 95% for 40% water vapor.

Figure 5.21 is plotted to compare the difference of conversion of methanol. 7 and 20% water vapor cases show the same trend in conversion. For 40% water vapor case, the conversion in the range of $200\text{-}350^\circ\text{C}$ is higher than the previous two cases but not still exceed blank test. The results show that addition of water to the reaction decreases the conversion of methanol. From the previous discussion, adsorption of water on catalyst surface plays an important role in ethanol and 1-propanol oxidation. Thus, in methanol oxidation the effect may due to the competitive adsorption between water and methanol.

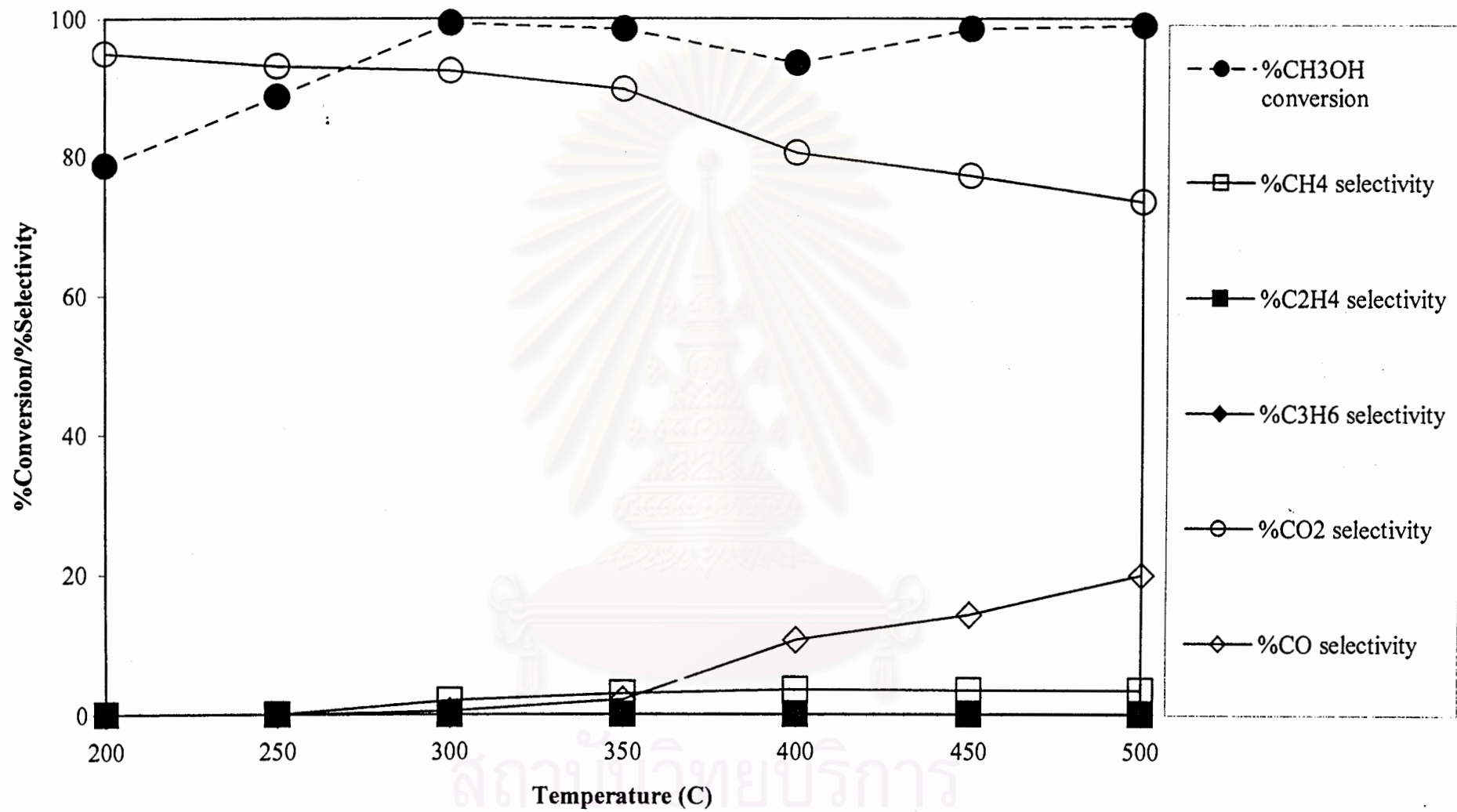


Figure 5.17 The result of methanol oxidation (no water added)

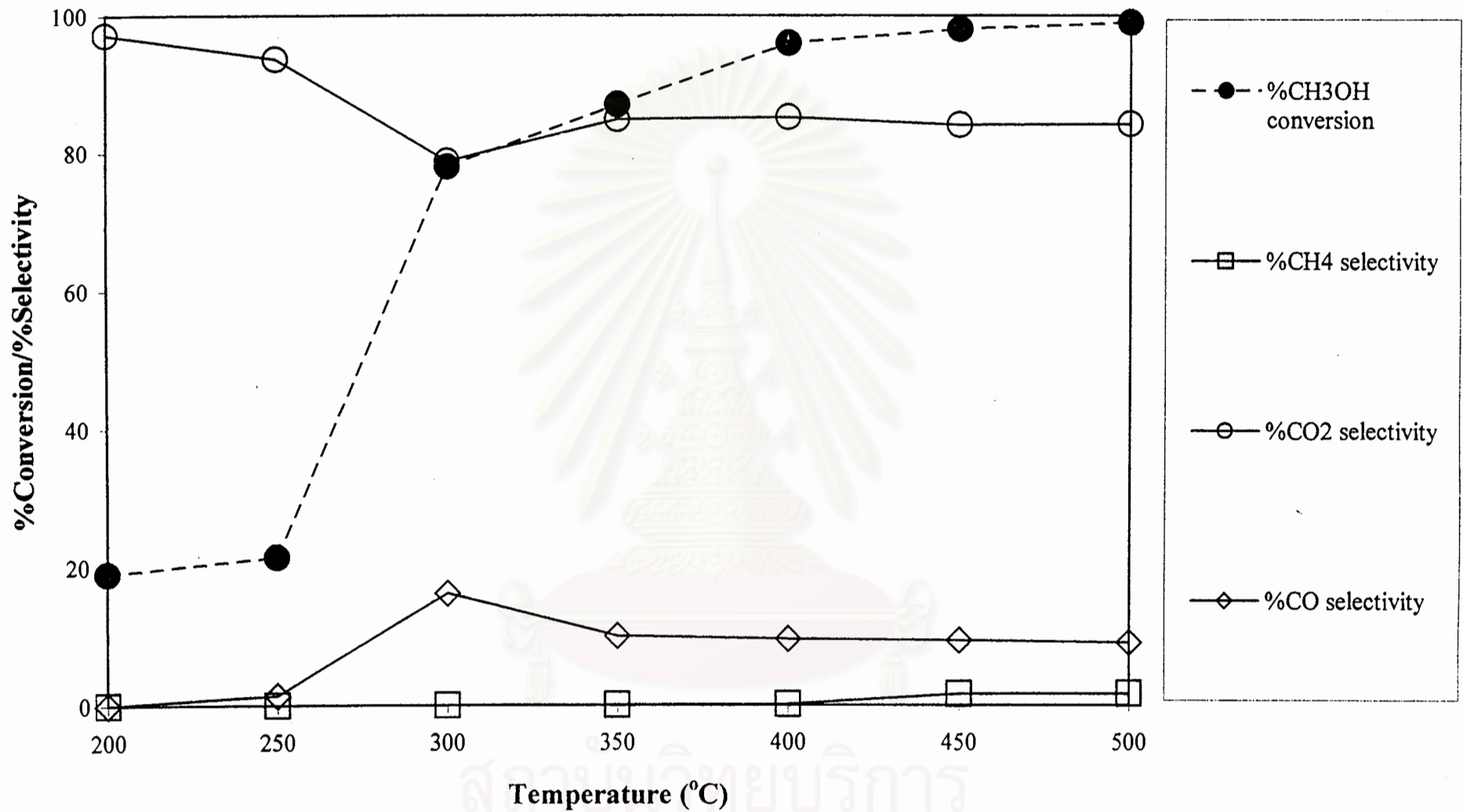


Figure 5.18 The result of methanol oxidation in the presence of 7% water vapor

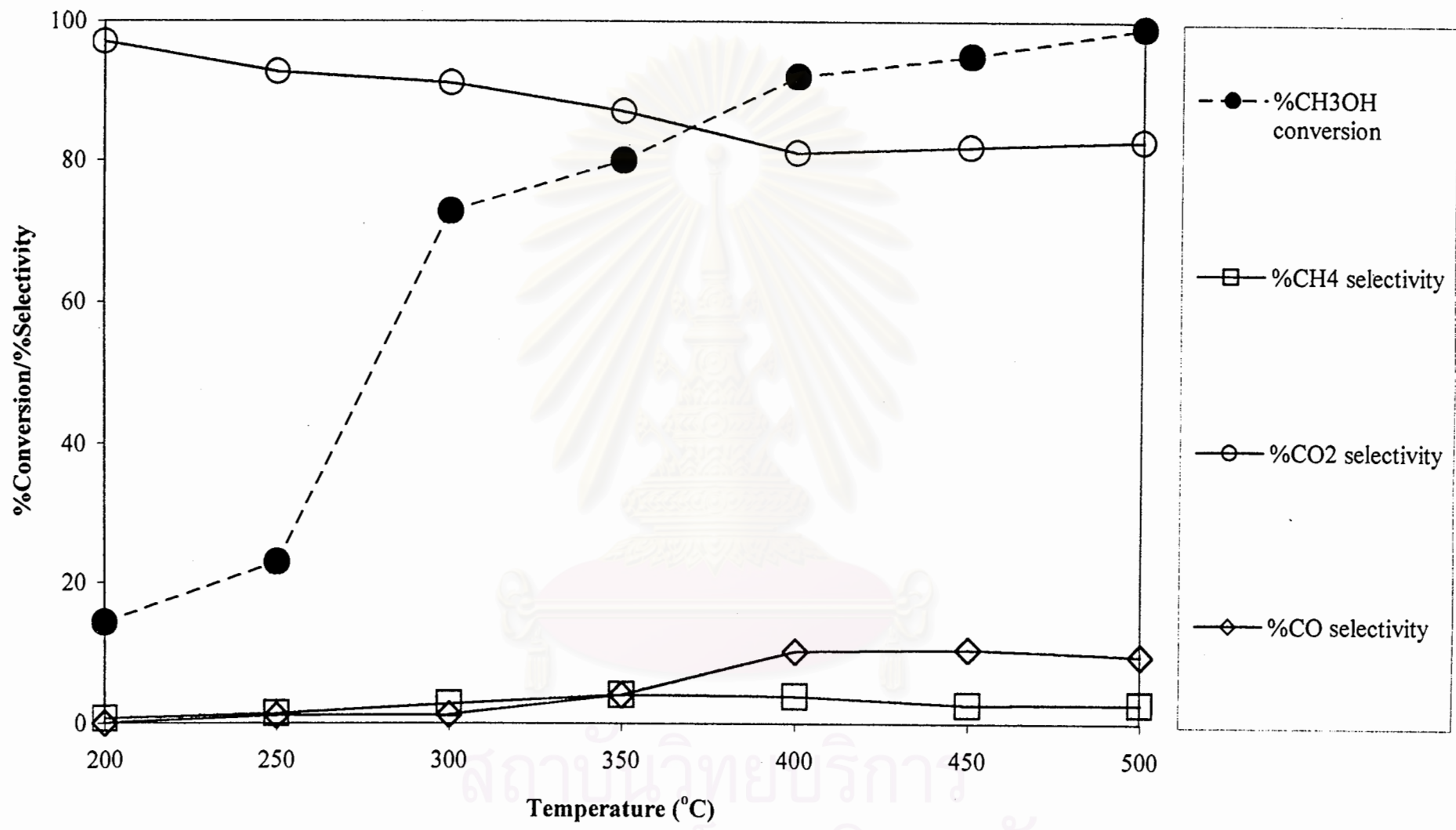


Figure 5.19 The result of methanol oxidation in the presence of 20% water vapor

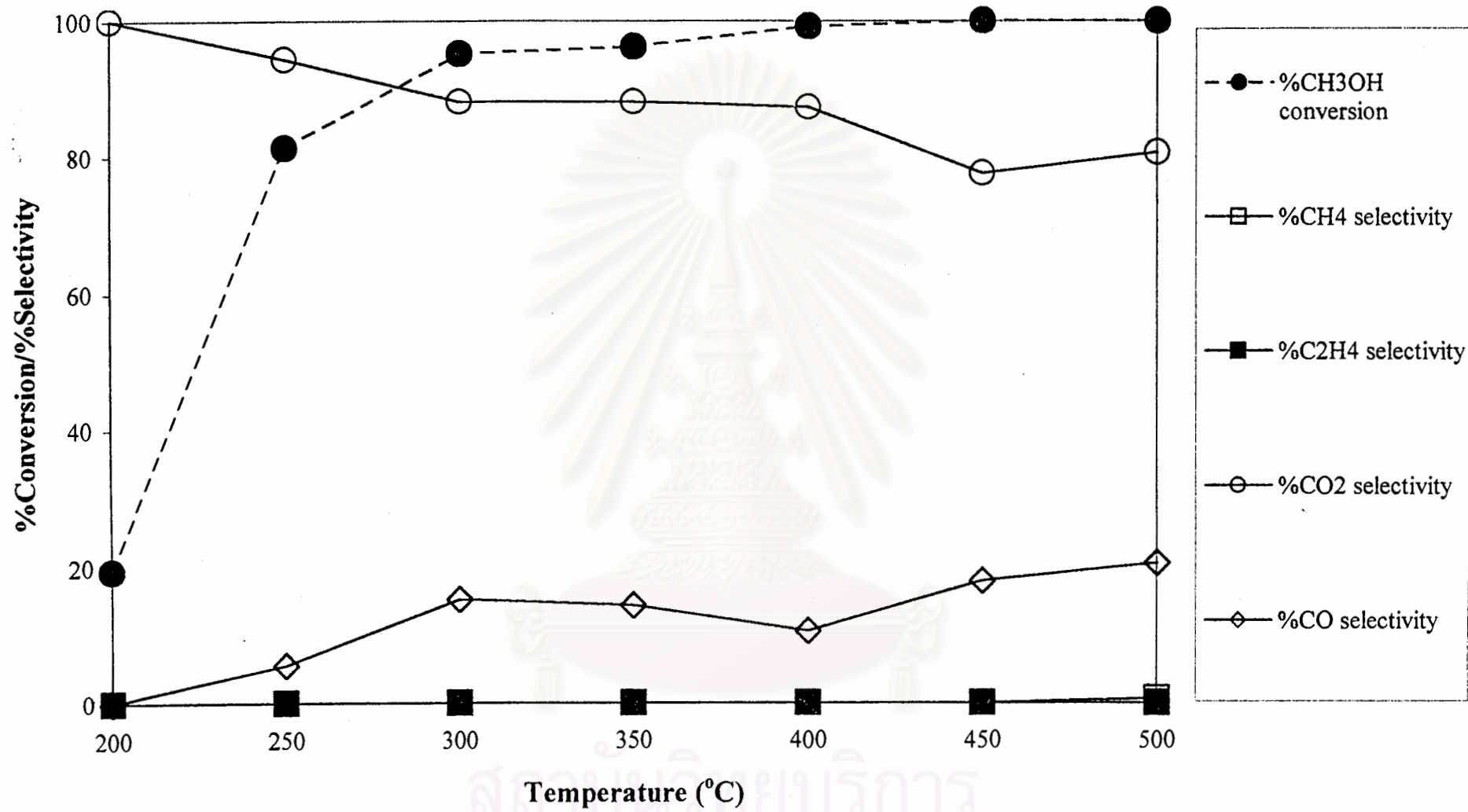


Figure 5.20 The result of methanol oxidation in the presence of 40% water vapor

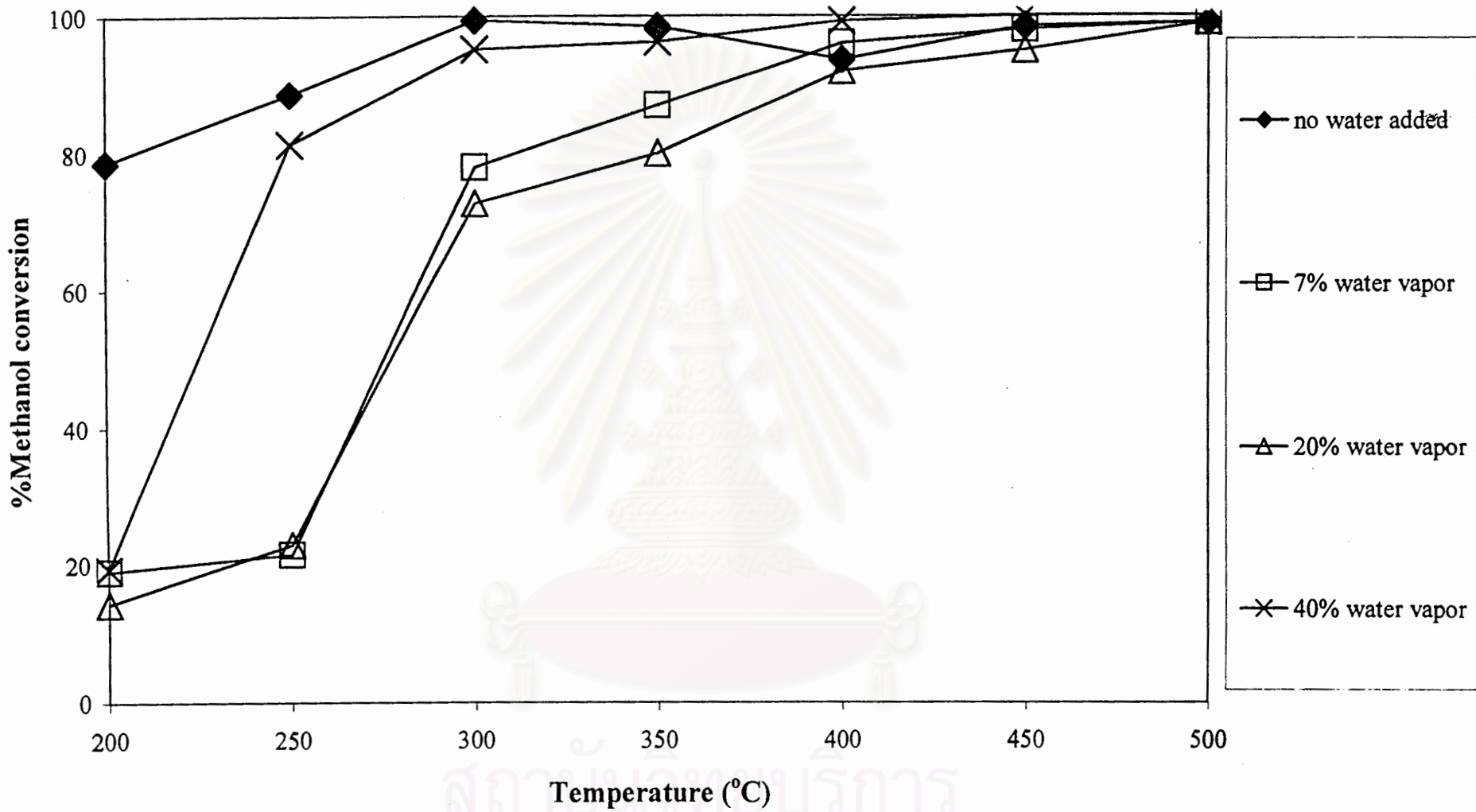


Figure 5.21 %methanol converted

5.2.4 2-Propanol oxidation

The role of water vapor for 2-propanol oxidation is presented in figures 5.22 to 5.25. From these figures, propene and CO₂ are the major products. Small amount of methane, ethene, propene and propane are also formed. The conversion increases continuously with reaction temperature. The selectivity to propene is very high at the beginning but drops gradually at 500°C. This trend can be seen obviously in figures 5.22, 5.23 and 5.25. In contrast, CO₂ selectivity rises to a maximum value between 40-60%. But in figure 5.24, 20% water vapor, the selectivity to propene and CO₂ still remain in the range of 80-90% and 15-20% respectively at all reaction temperature.

In this reaction, propene, the dehydration product, is produced as the main product, not acetone, the oxidation product, which contain the carbonyl group, C=O, as in 1-propanol oxidation reaction. Figure 5.26 is plotted to compare the difference of yield to propene. It can be seen that addition of water increases yield to propene.

It is known that 2-propanol is in the class of secondary alcohol, the reaction mechanism, thus, may be or may be not the same as in 1-propanol oxidation. One reason that can be attributed to the production of propene is the ease of the hydration which follows by this order; tertiary > secondary > primary.

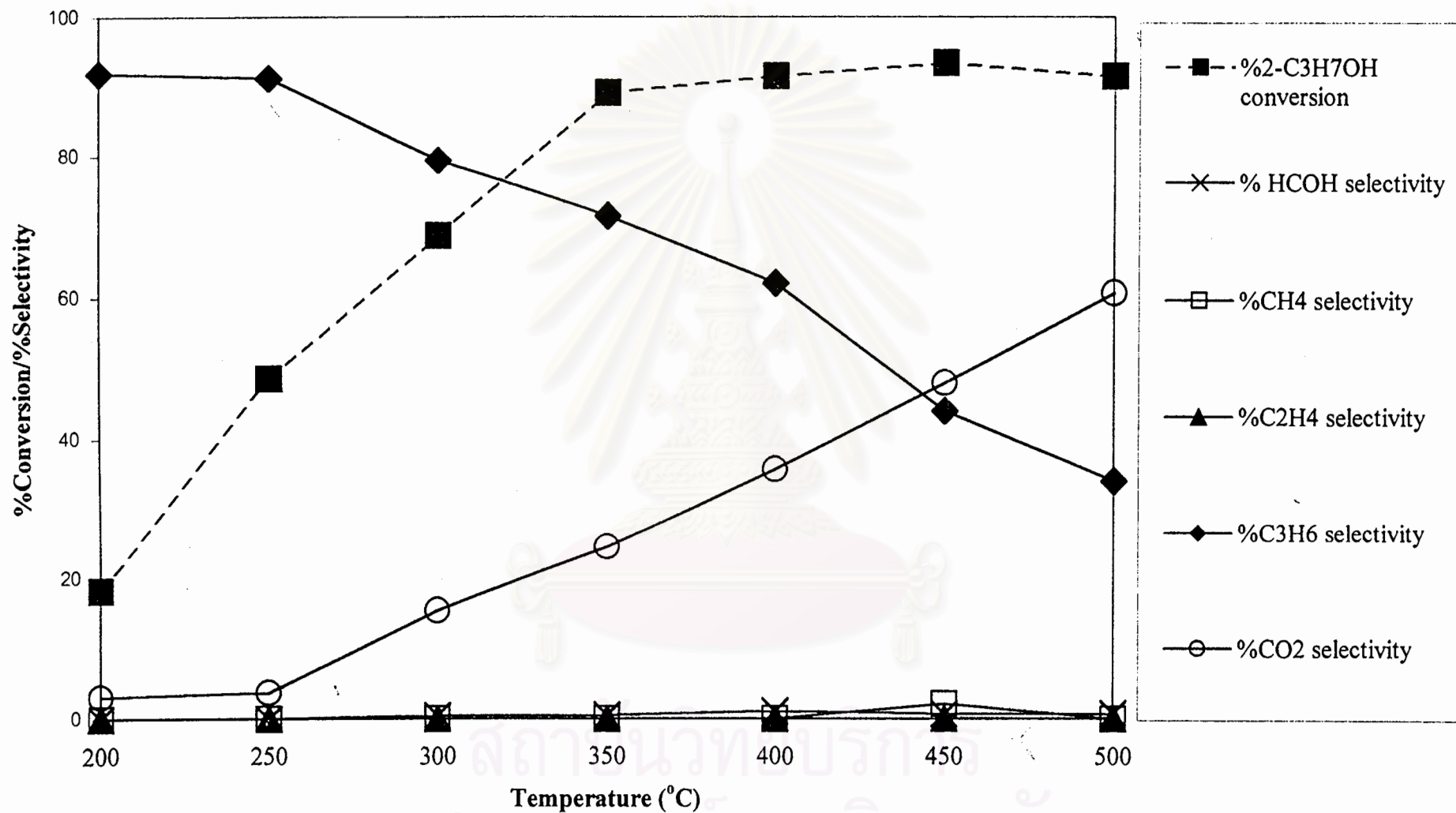


Figure 5.22 The result of 2-propanol oxidation (no water added)

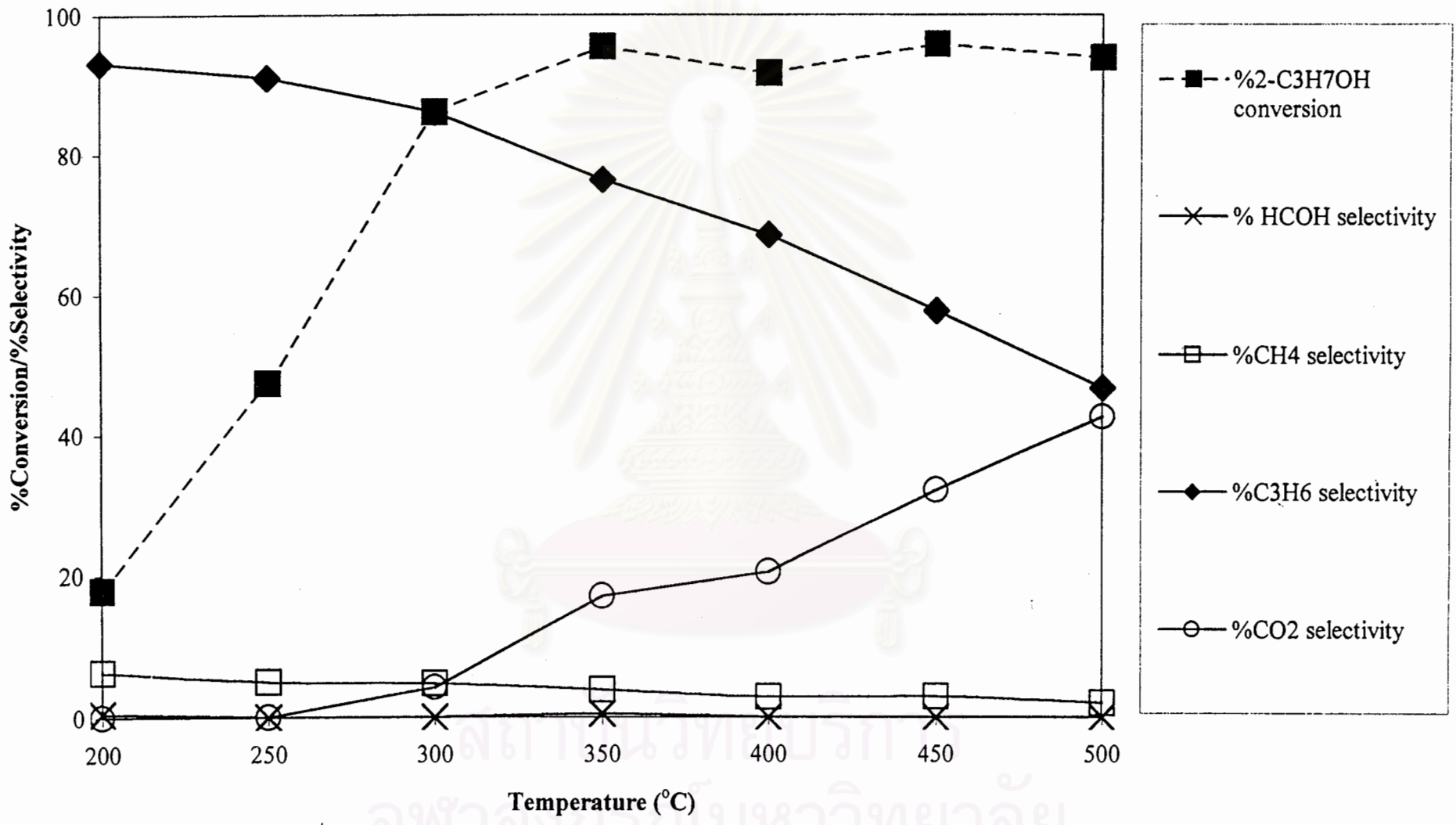


Figure 5.23 The result of 2-propanol oxidation (7% water vapor)

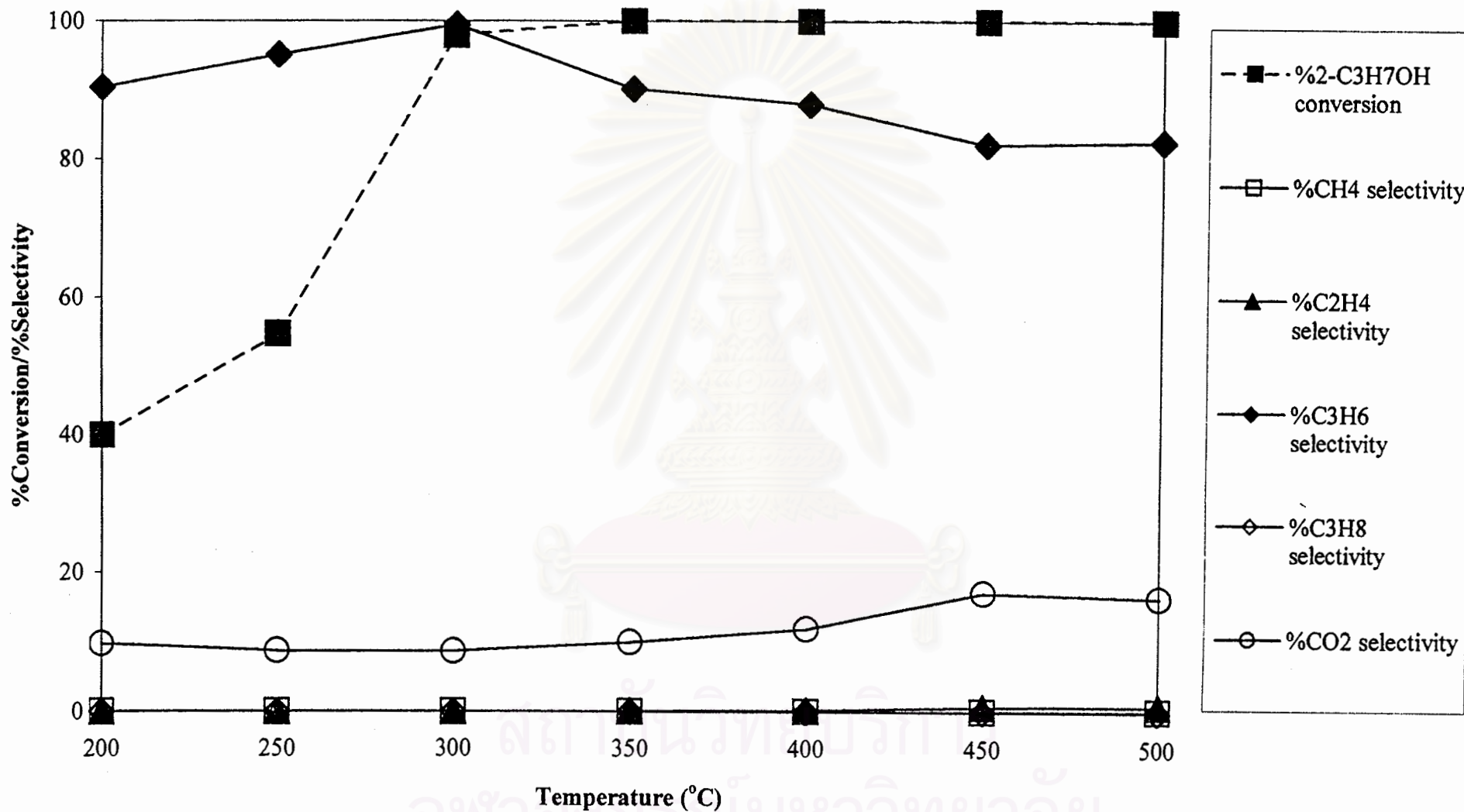


Figure 5.24 The result of 2-propanol oxidation (20% water vapor)

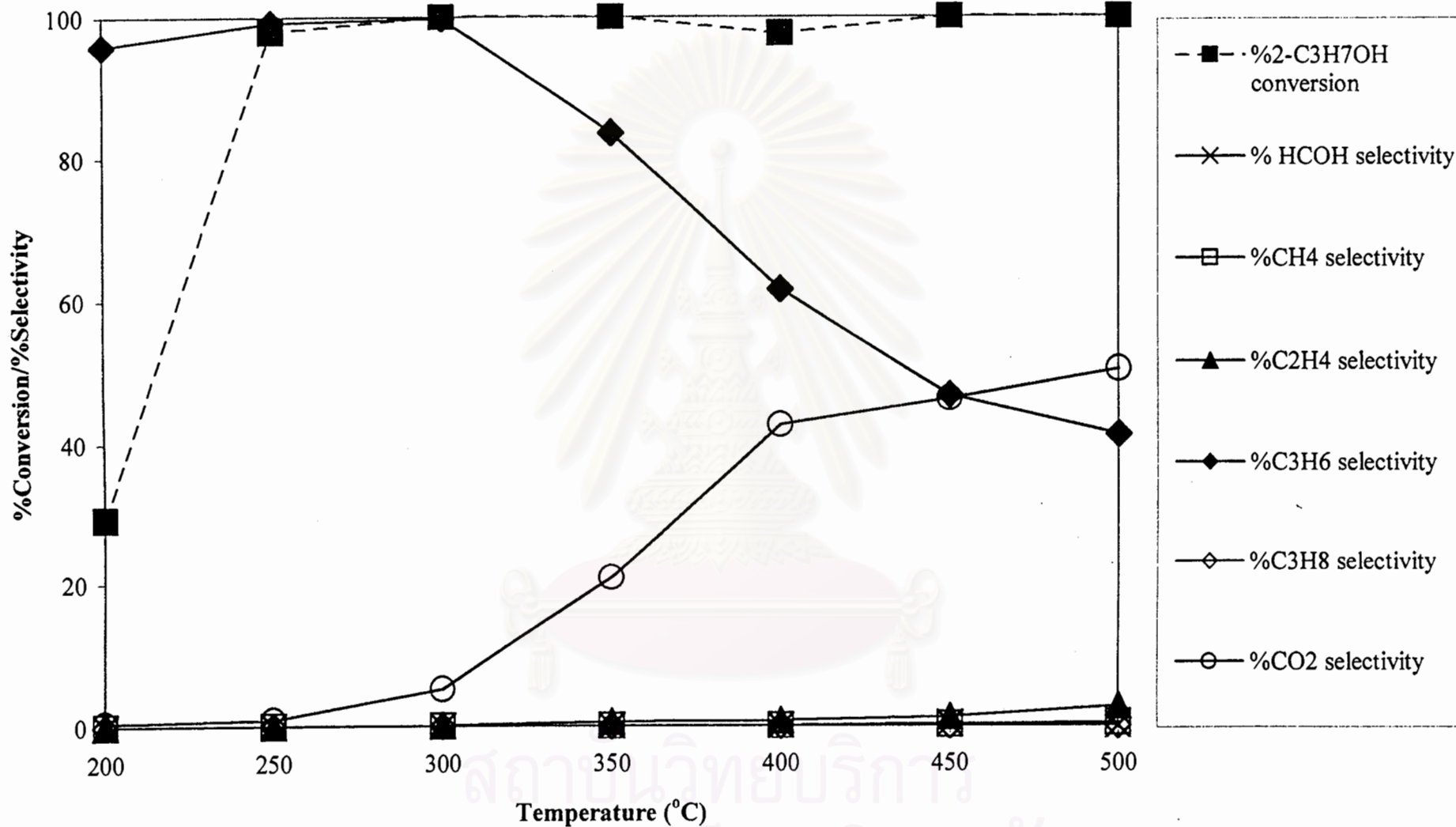


Figure 5.25 The result of 2-propanol oxidation in the presence of 40% water vapor

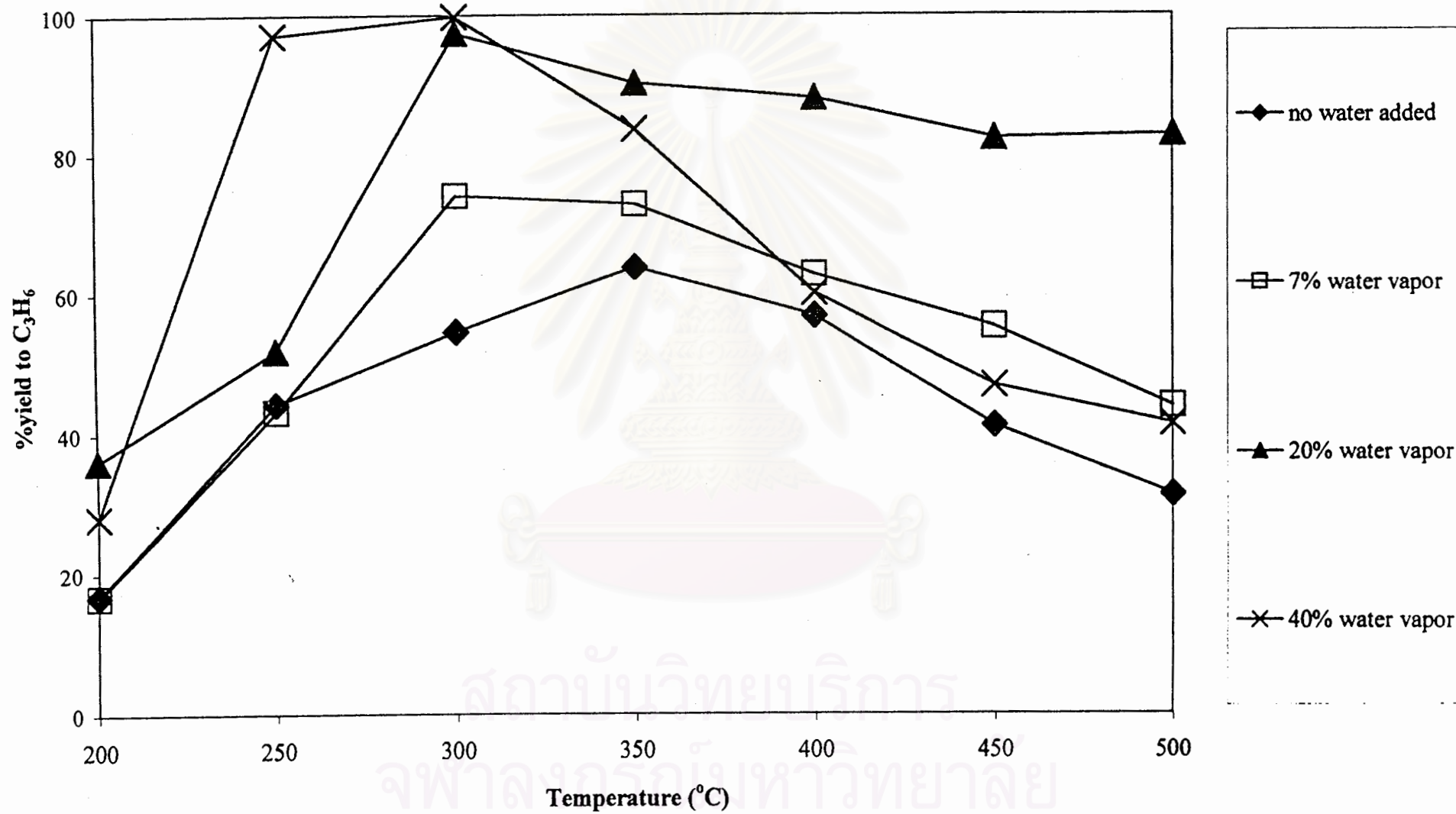
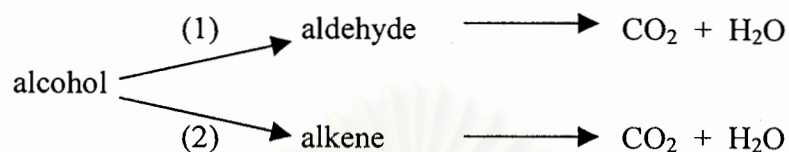


Figure 5.26 %yield to C_3H_6

5.3 Proposed reaction pathway

From the oxidation of methanol, ethanol, 1-propanol and 2-propanol, the following reaction pathway is proposed.



In the absence or low water contents, the pathway (1) is preferred. At high water contents, the catalyst surface becomes more acidic, hence, pathway (2) becomes more significant. This conclusion is supported by the results of 1-propanol and 2-propanol oxidation.

The oxidation of 1-propanol shows that at high temperature aldehyde selectivity still remains relatively constant while alkene selectivity drops. The oxidation of 2-propanol also confirms the above reaction. High water contents promote alkene formation but also decrease the selectivity by further combustion to combustion products. The oxidation of ethanol also exhibits the same behaviour. But ethylene is more resistant to oxidation than propylene. The drop of ethylene selectivity is more difficult to observe.

สถาบันวิทยบริการ
จุฬาลงกรณ์มหาวิทยาลัย

CHAPTER VI

CONCLUSIONS AND RECOMMENDATIONS

6.1 Conclusions

Addition of water increases acidity on catalyst surface which promotes the formation of alkenes. In the cases that main products consists of both an aldehyde and an alkene, water also decreases the combustion of aldehyde, obviously observed from 1-propanol oxidation.

For 2-propanol oxidation, the dehydration product, propene, is produced as the main product. Since 2-propanol is a secondary alcohol which prefer dehydration reaction more than 1-propanol. But the same result is the formation of propene increases with addition of water in both cases.



สถาบันวิทยบริการ
จุฬาลงกรณ์มหาวิทยาลัย

6.2 recommendations

1. From the above conclusions, water vapor tends to promote alkene formation in the selective oxidation of alcohols over V-Mg-O/TiO₂ catalyst. A more wide variation of the concentration of water vapor will be used to find the optimum content which give the best catalytic performance for each reaction.

2. The formation of carboxylic acid in the reaction is still in doubt. The assumptions may be the follows:

- There is no carboxylic acid formed or in a trace amount to detect. Sample analysis in detail or a decreasing of contact time may be needed.
- Carboxylic acid is formed but adsorbed by basic MgO and rapidly oxidized to CO₂ and water. To prove this, carboxylic acid will be used as a reactant. If it is rapidly oxidized, this assumption may be possible. However, it can not state that VMgO/TiO₂ can oxidize aldehyde to carboxylic acid but if it occure, carboxylic acid will be rapidly destroy.

REFERENCES

- Banares, M. A., Hu, H. C. and Wachs, I. E., "Molybdena on silica catalysts - role of preparation methods on the structure selectivity properties for the oxidation of methanol", J. Catal. 150 (1994) : 407-420.
- Burrows, A., Kiely, C. J., Perregaard, J., Højlund-Nielsen, P. E., Vorbeck, G., Calvino, J. J. and Lopez-Cartes, C., "Structural characterisation of a VMgO catalyst used in the oxidative dehydrogenation of propane", Catal. Lett. 57 (1999) : 121-128.
- del Val, S., Granados, M. L., Fierro, J. L. G., Santamaria-Gonzalez, J. and Jimenez-Lopez, A., "Oxidation of toluene and o-xylene on Ti phosphate-supported vanadium oxide catalysts", J. Catal. 188 (1999) : 203-214.
- Deo, G., Turek, A. M., Wachs, I. E., Machej, T., Haber, J., Das, N., Eckert, H. and Hirt, A. M., "Physical and chemical characterization of surface vanadium oxide supported on titania: influence of the titania phase (anatase, rutile, brookite)", Appl. Catal. A. General, 91 (1992) : 27-37.
- Deo, G. and Wachs, I. E., "Reactivity of supported vanadium-oxide catalysts - the partial oxidation of methanol", J. Catal. 146 (1994) : 323-334.
- Doornkamp, C., Clement, M., Gao, X., Deo, G., Wachs, I. E. and Ponec, V., "The oxygen isotopic exchange reaction on vanadium oxide catalysts", J. Catal., 185 (1999) : 415-422.
- Dunn, J. P., Koppula, P. R., Stenger, H. G. and Wachs, I. E., "Oxidation of sulfur dioxide to sulfur trioxide over supported vanadia catalysts", Appl. Catal. B. Environmental. 19 (1998) : 103-117.
- Dunn, J. P., Stenger, H. G. and Wachs, I. E., "Molecular structure-reactivity relationships for the oxidation of sulfur dioxide over supported metal oxide catalysts", Catal. Today. 53 (1999) : 543-556.

- Elguezabal, A. A. and Corberan, V. C., "Selective oxidation of toluene on $V_2O_5/TiO_2/SiO_2$ catalysts modified with Te, Al, Mg, and K_2SO_4 ", Catal.Today. 32 (1996) : 265-272.
- Faraldos, M., Banares, M. A. and Anderson, J. A., "Comparison of silica-supported MoO_3 and V_2O_5 catalysts in the selective partial oxidation of methane", J. Catal. 160 (1996) : 214-221.
- Leklertsunthorn, R., "Oxidation property of the V-Mg-O/ TiO_2 catalyst", Master of Engineering thesis, Chulalongkorn University, (1997).
- Lemonidou, A. A., Tjatjopoulos, G. J. and Vasalos, I. A., "Investigation on the oxidative dehydrogenation of n-butane over VMgO-type catalysts", Catal. Today. 45 (1998) : 65-71.
- Lemonidou, A. A. and Stambouli, A. E., "Catalytic and non-catalytic oxidative dehydrogenation of n-butane", Appl. Catal. A. General. 171 (1998) : 325-332.
- Lemonidou, A. A., Nalbandian, L. and Vasalos, I. A., "Oxidative dehydrogenation of propane over vanadium oxide based catalysts - Effect of support and alkali promoter", Catal. Today. 61 (2000) : 333-341.
- Liu, Y., Lu, Y., Liu, P., Gao, R. and Yin, Y., "Effects of microwaves on selective oxidation of toluene to benzoic acid over a V_2O_5/TiO_2 system", Appl. Catal. A. General. 170 (1998) : 207-214.
- Madeira, L. M., Martin Aranda, R. M. and Maldonado Hodar, F. J., "Oxidative dehydrogenation of n-butane over alkali and alkaline earth-promoted $\alpha-NiMoO_4$ catalysts", J. Catal. 169 (1997) : 469-479.
- Mars, P. and van Krevelen, D. W., "Oxidations carried out by means of vanadium oxide catalysts", Chem. Eng. Sc. (1954) : 41-59.
- Matralis, H. K., Papadopoulou, C., Elguezabal, A. A. and Corberan, V. C., "Selective oxidation of toluene over V_2O_5/TiO_2 catalysts - effect of vanadium loading and of molybdenum addition on the catalytic properties", Appl. Catal. A. General. 126 (1995) : 365-380.

- Medeiros, R. S., Eon, J. G. and Appel L. G., "The role of water in ethanol oxidation over SnO₂-supported molybdenum oxides", Catal. Lett. 69 (2000) : 79-82.
- Mongkhonsi, T., Pimanmas, P., Prasertdam, P., "Selective oxidation of ethanol and 1-propanol over V-Mg-O/TiO₂ catalyst", Chem. Lett. (2000) : 968-969.
- Morrison and Boyd, Organic Chemistry, Prentice Hall International Book Company, 6th ed., 1992.
- Nieto, J. M., Dejoz, A., Vazquez, M. I., O'leary, W. and Cunningham, J., "Oxidative dehydrogenation of *n*-butane on MgO-supported vanadium oxide catalysts", Catal. Today. 40 (1998) : 215-218.
- Owens, L. and Kung, H. H., "Effect of cesium modification of silica-supported vanadium-oxide catalysts in butane oxidation", J. Catal. 148 (1994) : 587-594.
- Pantazidis, A., Auroux, A., Herrmann and J.-M. and Mirodatos, C., "Role of acid-base, redox and structural properties of VMgO catalysts in the oxidative dehydrogenation of propane", Catal. Today. 32 (1996) : 81-88.
- Pantazidis, A., Bucholz, S. A., Zanthoff, H. W., Schurman, Y. and Mirodatos, C., "A TAP reactor investigation of the oxidative dehydrogenation of propane over a V-Mg-Ocatalyst", Catal. Today. 40 (1998a) : 207-214.
- Pantazidis, A., Burrows, A., Kiely, C. J. and Mirodatos, C., "Direct evidence of active surface reconstruction during oxidative dehydrogenation of propane over VMgO catalyst", J. Catal. 177 (1998b) : 325-334.
- Pimanmas, P., "Application of V-Mg-O/TiO₂ catalyst on the selective oxidation of alcohols", Master of Engineering thesis, Chulalongkorn university, (1998).
- Quaranta, N. E., Soria, J., Corberan, V. C. and Fierro, J. L. G., "Selective oxidation of ethanol to acetaldehyde on V₂O₅/TiO₂/SiO₂ catalysts - Effect of TiO₂-coating of the silica", J. Catal. 171 (1997) : 1-13.

- Ramis, G., Busca, G. and Bregani, F., "On the effect of dopants and additives on the state of surface vanadyl centers of vanadia-titania catalysts", Catal. Lett. 18 (1993) : 299-303.
- Reddy, B. M., Ganesh, I. and Chowdhury, B., "Design of stable and reactive vanadium oxide catalysts supported on binary oxides", Catal. Today. 49 (1999) : 115-121.
- Saleh-Alhamed, Y. A., Hudgins R. R. and Silveston, P. L., "Role of water vapor in the partial oxidation of propene", J. Catal. 161 (1996) : 430-440.
- Sun, Q., Jehng, J. M., Hu, H. C., Herman, R. G., Wachs, I. E. and Klier, K., "In situ Raman spectroscopy during the partial oxidation of methane to formaldehyde over supported vanadium oxide catalysts", J. Catal. 165 (1997) : 91-101.
- Tellez, C., Abon, M., Dalmon, J. A., Mirodatos, C. and Santamaria, J., "Oxidative dehydrogenation of butane over VMgO catalysts", J. Catal. 195 (2000) : 113-124.
- Wachs, I. E., "Raman and IR studies of surface metal oxide species on oxide supports: Supported metal oxide catalysts", Catal. Today. 27 (1996) : 437-455.
- Wachs, I. E., Deo, G. and Weckhuysen, B. M., "Selective catalytic reduction of NO with NH₃ over supported vanadia catalysts", J. Catal. 161 (1996) : 211-221.
- Wachs, I. E. and Weckhuysen, B. M., "Structure and reactivity of surface vanadium oxide species on oxide supports", Appl. Catal. A General 157 (1997) : 67-90.



APPENDICES

สถาบันวิทยบริการ
จุฬาลงกรณ์มหาวิทยาลัย

APPENDIX A

CALCULATION OF CATALYST PREPARATION

10V2MgTi catalyst preparation starts with 50 ml aqueous solution of NH_4VO_3 , consists of 0.2 g of NH_4VO_3 .

$$\text{The amount of V in 0.2 g of } \text{NH}_4\text{VO}_3 = \frac{0.2 \times 50.9414}{116.98}$$

$$\approx 0.0871 \text{ g}$$

$$\text{Therefore, mole of V} = \frac{0.0871}{50.9414}$$

$$\approx 0.0017 \text{ mole}$$

$$\text{The amount of V calculated as } \text{V}_2\text{O}_5 = \frac{0.0871 \times 181.8828}{101.8828}$$

If the weight of catalyst is 100 g, 10VTi would compose of 10 g of V_2O_5 and 90 g of TiO_2 . Thus, in this system,

$$\text{The amount of } \text{TiO}_2 = \frac{90 \times 0.1555}{10}$$

$$\approx 1.3995 \text{ g}$$

Then 2 wt% of Mg is added to the 10VTi catalyst (when the weight of V_2O_5 plus TiO_2 is calculated as 100%).

$$\text{The amount of Mg in 10V2MgTi} = 0.02 \times (0.1555 + 1.3995)$$
$$\approx 0.0311 \text{ g}$$

$$\text{The amount of } \text{Mg}(\text{NO}_3)_2 \text{ used} = \frac{0.0311 \times 256.41}{24.305}$$

$$\approx 0.3286 \text{ g}$$

APPENDIX B

CALCULATION OF DIFFUSIONAL LIMITATION EFFECT

In the present work there are doubt whether the external and internal diffusion limitations interfere with the propane reaction. Hence, the kinetic parameters were calculated based on the experimental data so as to prove the controlled system. The calculation is divided into two parts; one of which is the external diffusion limitation, and the other is the internal diffusion limitation.

1. External diffusion limitation

The 1-propanol oxidation reaction is considered to be an irreversible first order reaction occurred on the interior pore surface of catalyst particles in a fixed bed reactor. Assume isothermal operation for the reaction.

In the experiment, 8% 1-propanol, 5% O₂ balance with nitrogen was used as the unique reactant in the system. Molecular weight of 1-propanol and air (O₂ 5%) are 60 and 28.2, respectively. Thus, the average molecular weight of the gas mixture was calculated as follows:

$$\begin{aligned}M_{AB} &= 0.08 \times 60 + 0.92 \times 28.2 \\ &= 30.744 \text{ g/mol}\end{aligned}$$

Calculation of reactant gas density

Consider the 1-propanol oxidation is operated at low pressure and high temperature. We assume that the gases are respect to ideal gas law. The density of such gas mixture reactant at various temperatures is calculated in the following.

$$\rho = \frac{PM}{RT} = \frac{1.0 \times 10^5 \times 30.744 \times 10^{-3}}{8.314T}$$

We obtained :

$\rho = 0.782 \text{ kg/m}^3$	at T = 200°C
$\rho = 0.706 \text{ kg/m}^3$	at T = 250°C
$\rho = 0.645 \text{ kg/m}^3$	at T = 300°C
$\rho = 0.594 \text{ kg/m}^3$	at T = 350°C

Calculation of the gas mixture viscosity

The simplified methods for determining the viscosity of low pressure binary are described anywhere (Reid, 1988). The method of Wilke is chosen to estimate the gas mixture viscosity.

For a binary system of 1 and 2,

$$\mu_m = \frac{y_1 \mu_1}{y_1 + y_2 \Phi_{12}} + \frac{y_2 \mu_2}{y_2 + y_1 \Phi_{21}}$$

where μ_m = viscosity of the mixture
 μ_1, μ_2 = pure component viscosity
 y_1, y_2 = mole fractions

$$\phi_{12} = \frac{\left[1 + \left(\frac{\mu_1}{\mu_2} \right)^{1/2} \left(\frac{M_1}{M_2} \right)^{1/4} \right]^2}{\left[8 \left(1 + \frac{M_1}{M_2} \right) \right]^{1/2}}$$

$$\phi_{21} = \phi_{12} \left(\frac{\mu_2}{\mu_1} \right) \left(\frac{M_1}{M_2} \right)$$

M_1, M_2 = molecular weight

Let 1 refer to 1-propanol and 2 to air (O₂ 5%)

$$M_1 = 60 \text{ and } M_2 = 28.2$$

From Perry the viscosity of pure 1-propanol at 200°C, 250°C, 300°C, 350°C, 400°C, 450°C and 500°C are 0.0124, 0.0135, 0.015 and 0.0162 cP, respectively. The viscosity of pure air at 200°C, 250°C, 300°C and 350°C are 0.0248, 0.0265, 0.0285 and 0.030 cP, respectively.

$$\text{At } 200^\circ\text{C: } \phi_{12} = \frac{\left[1 + \left(\frac{0.0124}{0.0248} \right)^{1/2} \left(\frac{28.2}{60} \right)^{1/4} \right]^2}{\left[8 \left(1 + \frac{60}{28.2} \right) \right]^{1/2}} = 0.502$$

$$\phi_{21} = 0.502 \left(\frac{0.0248}{0.0124} \right) \left(\frac{60}{28.2} \right) = 2.14$$

$$\mu_m = \frac{0.08 \times 0.0124}{0.08 + 0.92 \times 0.502} + \frac{0.92 \times 0.0248}{0.92 + 0.08 \times 2.14} = 0.0227 \text{ cP} = 2.27 \times 10^{-5} \text{ kg / m - sec}$$

$$\text{At } 250^\circ\text{C: } \phi_{12} = \frac{\left[1 + \left(\frac{0.0135}{0.0265} \right)^{1/2} \left(\frac{28.2}{60} \right)^{1/4} \right]^2}{\left[8 \left(1 + \frac{60}{28.2} \right) \right]^{1/2}} = 0.506$$

$$\phi_{21} = 0.506 \left(\frac{0.0265}{0.0135} \right) \left(\frac{60}{28.2} \right) = 2.113$$

$$\mu_m = \frac{0.08 \times 0.0135}{0.08 + 0.92 \times 0.506} + \frac{0.92 \times 0.0265}{0.92 + 0.08 \times 2.113} = 0.0244 \text{ cP} = 2.44 \times 10^{-5} \text{ kg / m - sec}$$

$$\text{At } 300^{\circ}\text{C} : \quad \phi_{12} = \frac{\left[1 + \left(\frac{0.015}{0.0285} \right)^{1/2} \left(\frac{28.2}{60} \right)^{1/4} \right]^2}{\left[8 \left(1 + \frac{60}{28.2} \right) \right]^{1/2}} = 0.512$$

$$\phi_{21} = 0.512 \left(\frac{0.0285}{0.015} \right) \left(\frac{60}{28.2} \right) = 2.07$$

$$\mu_m = \frac{0.08 \times 0.015}{0.08 + 0.92 \times 0.512} + \frac{0.92 \times 0.0285}{0.92 + 0.08 \times 2.07} = 0.0263 \text{ cP} = 2.63 \times 10^{-5} \text{ kg / m - sec}$$

$$\text{At } 350^{\circ}\text{C} : \quad \phi_{12} = \frac{\left[1 + \left(\frac{0.0162}{0.030} \right)^{1/2} \left(\frac{28.2}{60} \right)^{1/4} \right]^2}{\left[8 \left(1 + \frac{60}{28.2} \right) \right]^{1/2}} = 0.517$$

$$\phi_{21} = 0.517 \left(\frac{0.030}{0.0162} \right) \left(\frac{60}{28.2} \right) = 2.037$$

$$\mu_m = \frac{0.08 \times 0.0162}{0.08 + 0.92 \times 0.517} + \frac{0.92 \times 0.030}{0.92 + 0.08 \times 2.037} = 0.0278 \text{ cP} = 2.78 \times 10^{-5} \text{ kg / m - sec}$$

Calculation of diffusion coefficients

Diffusion coefficients for binary gas system at low pressure calculated by empirical correlation are proposed by Reid (1988). Wilke and Lee method is chosen to estimate the value of D_{AB} due to the general and reliable method. The empirical correlation is

$$D_{AB} = \frac{\left(3.03 - \frac{0.98}{M_{AB}^{1/2}} \right) (10^{-3}) T^{3/2}}{PM_{AB}^{1/2} \sigma_{AB}^2 \Omega_D}$$

where D_{AB} = binary diffusion coefficient, cm^2/s

T = temperature, K

M_A, M_B = molecular weights of A and B ,g/mol

$$M_{AB} = 2 \left[\left(\frac{1}{M_A} \right) + \left(\frac{1}{M_B} \right) \right]^{-1}$$

P = pressure, bar

σ = characteristic length, $^{\circ}\text{A}$

Ω_D = diffusion collision integral, dimensionless

The characteristic Lennard-Jones energy and Length, ε and σ , of nitrogen and propane are as follows: (Reid,1988)

For $\text{C}_3\text{H}_7\text{OH}$: $\sigma(\text{C}_3\text{H}_7\text{OH}) = 4.549 \text{ }^{\circ}\text{A}$, $\varepsilon/k = 576.7$

For air : $\sigma(\text{air}) = 3.711 \text{ }^{\circ}\text{A}$, $\varepsilon/k = 78.6$

The sample rules are usually employed.

$$\sigma_{AB} = \frac{\sigma_A + \sigma_B}{2} = \frac{4.549 + 3.711}{2} = 4.13$$

$$\varepsilon_{AB}/k = \left(\frac{\varepsilon_A \varepsilon_B}{k^2} \right)^{1/2} = (576.7 \times 78.6)^{1/2} = 212.9$$

Ω_D is tabulated as a function of kT/ε for the Lennard-Jones potential. The accurate relation is

$$\Omega_D = \frac{A}{(T^*)^B} + \frac{C}{\exp(DT^*)} + \frac{E}{\exp(FT^*)} + \frac{G}{\exp(HT^*)}$$

where $T^* = \frac{kT}{\varepsilon_{AB}}$, $A = 1.06036$, $B = 0.15610$, $C = 0.19300$, $D = 0.47635$, $E =$

1.03587 , $F = 1.52996$, $G = 1.76474$, $H = 3.89411$

$$\text{Then } T^* = \frac{473}{212.9} = 2.222 \text{ at } 200^\circ\text{C}$$

$$T^* = \frac{523}{212.9} = 2.456 \text{ at } 250^\circ\text{C}$$

$$T^* = \frac{573}{212.9} = 2.691 \text{ at } 300^\circ\text{C}$$

$$T^* = \frac{623}{212.9} = 2.926 \text{ at } 350^\circ\text{C}$$

$$\Omega_D = \frac{1.06036}{(T^*)^{0.15610}} + \frac{0.19300}{\exp(0.47635T^*)} + \frac{1.03587}{\exp(1.52996T^*)} + \frac{1.76474}{\exp(3.89411T^*)}$$

$$\Omega_D = 1.038 ; 200^\circ\text{C}$$

$$\Omega_D = 1.006 ; 250^\circ\text{C}$$

$$\Omega_D = 0.979 ; 300^\circ\text{C}$$

$$\Omega_D = 0.956 ; 350^\circ\text{C}$$

With Equation of D_{AB} ,

$$\begin{aligned} \text{At } 200^\circ\text{C} : D(\text{C}_3\text{H}_7\text{OH-air}) &= \frac{\left(3.03 - \frac{0.98}{30.24^{0.5}}\right)(10^{-3})473^{3/2}}{1 \times 30.24^{0.5} \times 4.13^2 \times 1.038} \\ &= 3.01 \times 10^{-5} \text{ m}^2/\text{s} \end{aligned}$$

$$\begin{aligned} \text{At } 250^\circ\text{C} : D(\text{C}_3\text{H}_7\text{OH-air}) &= \frac{\left(3.03 - \frac{0.98}{30.24^{0.5}}\right)(10^{-3})523^{3/2}}{1 \times 30.24^{0.5} \times 4.13^2 \times 1.006} \\ &= 3.62 \times 10^{-5} \text{ m}^2/\text{s} \end{aligned}$$

$$\begin{aligned} \text{At } 300^\circ\text{C} : D(\text{C}_3\text{H}_7\text{OH-air}) &= \frac{\left(3.03 - \frac{0.98}{30.24^{0.5}}\right)(10^{-3})573^{3/2}}{1 \times 30.24^{0.5} \times 4.13^2 \times 0.979} \\ &= 4.26 \times 10^{-5} \text{ m}^2/\text{s} \end{aligned}$$

$$\begin{aligned} \text{At } 350^{\circ}\text{C} : D(\text{C}_3\text{H}_7\text{OH-air}) &= \frac{\left(3.03 - \frac{0.98}{30.24^{0.5}}\right)(10^{-3})623^{3/2}}{1 \times 30.24^{0.5} \times 4.13^2 \times 0.956} \\ &= 5.04 \times 10^{-5} \quad \text{m}^2/\text{s} \end{aligned}$$

Reactant gas mixture was supplied at 100 ml/min. in tubular microreactor used in the 1-propanol oxidation system at 30°C

1-propanol flow rate through reactor = 100 ml/min. at 30°C

$$\text{The density of 1-propanol, } \rho = \frac{1.0 \times 10^5 \times 30.744 \times 10^{-3}}{8.314(273 + 30)} = 1.236 \text{ kg/s}$$

$$\text{Mass flow rate} = 1.236 \left(\frac{100 \times 10^{-6}}{60} \right) = 2.06 \times 10^{-6} \text{ kg/s}$$

Diameter of quartz tube reactor = 8 mm

$$\text{Cross-sectional area of tube reactor} = \frac{\pi(8 \times 10^{-3})^2}{4} = 5.03 \times 10^{-5} \text{ m}^2$$

$$\text{Mass Velocity, } G = \frac{2.06 \times 10^{-6}}{5.03 \times 10^{-5}} = 0.04 \text{ kg/m}^2\text{-s}$$

Catalysis size = 40-60 mesh = 0.178-0.126 mm

Average catalysis = (0.126+0.178)/2 = 0.152 mm

Find Reynolds number, Re_p , which is well known as follows:

$$Re_p = \frac{d_p G}{\mu}$$

We obtained

$$\text{At } 200^{\circ}\text{C} : Re_p = \frac{(0.152 \times 10^{-3} \times 0.04)}{2.27 \times 10^{-5}} = 0.268$$

$$\text{At } 250^{\circ}\text{C} : \text{Re}_p = \frac{(0.152 \times 10^{-3} \times 0.04)}{2.44 \times 10^{-5}} = 0.249$$

$$\text{At } 300^{\circ}\text{C} : \text{Re}_p = \frac{(0.152 \times 10^{-3} \times 0.04)}{2.63 \times 10^{-5}} = 0.231$$

$$\text{At } 350^{\circ}\text{C} : \text{Re}_p = \frac{(0.152 \times 10^{-3} \times 0.04)}{2.78 \times 10^{-5}} = 0.219$$

Average transport coefficient between the bulk stream and particles surface could be correlated in terms of dimensionless groups, which characterize the flow conditions. For mass transfer the Sherwood number, $k_m \rho / G$, is an empirical function of the Reynolds number, $d_p G / \mu$, and the Schmit number, $\mu / \rho D$. The j -factors are defined as the following functions of the Schmidt number and Sherwood numbers:

$$j_D = \frac{k_m \rho}{G} \left(\frac{a_m}{a_t} \right) (\mu / \rho D)^{2/3}$$

The ratio (a_m/a_t) allows for the possibility that the effective mass-transfer area a_m , may be less than the total external area, a_t , of the particles. For Reynolds number greater than 10, the following relationship between j_D and the Reynolds number well represents available data.

$$j_D = \frac{0.458}{\varepsilon_B} \left(\frac{d_p G}{\mu} \right)^{-0.407}$$

where G = mass velocity(superficial) based upon cross-sectional area of empty reactor

$$(G = u\rho)$$

d_p = diameter of catalyst particle for spheres

μ = viscosity of fluid

ρ = density of fluid

ε_B = void fraction of the interparticle space (void fraction of the bed)

D = molecular diffusivity of component being transferred

Assume $\varepsilon_B = 0.5$

$$\text{At } 200^\circ\text{C} ; j_D = \frac{0.458}{0.5} (0.268)^{-0.407} = 1.565$$

$$\text{At } 250^\circ\text{C} ; j_D = \frac{0.458}{0.5} (0.249)^{-0.407} = 1.613$$

$$\text{At } 300^\circ\text{C} ; j_D = \frac{0.458}{0.5} (0.231)^{-0.407} = 1.663$$

$$\text{At } 350^\circ\text{C} ; j_D = \frac{0.458}{0.5} (0.219)^{-0.407} = 1.699$$

A variation of the fixed bed reactor is an assembly of screens or gauze of catalytic solid over which the reacting fluid flows. Data on mass transfer from single screens has been reported by Gay and Maughan. Their correlation is of the form

$$j_D = \frac{\varepsilon k_m \rho}{G} (\mu / \rho D)^{2/3}$$

Where ε is the porosity of the single screen.

$$\text{Hence, } k_m = \left(\frac{j_D G}{\mu} \right) (\mu / \rho D)^{2/3}$$

$$k_m = \left(\frac{0.458 G}{\varepsilon_B \rho} \right) \text{Re}^{-0.407} \text{Sc}^{-2/3}$$

Find Schmidt number, Sc : $Sc = \frac{\mu}{\rho D}$

$$\text{At } 200^{\circ}\text{C} : Sc = \frac{2.27 * 10^{-5}}{0.782 * 3.01 * 10^{-5}} = 0.964$$

$$\text{At } 250^{\circ}\text{C} : Sc = \frac{2.44 * 10^{-5}}{0.706 * 3.62 * 10^{-5}} = 0.955$$

$$\text{At } 300^{\circ}\text{C} : Sc = \frac{2.63 * 10^{-5}}{0.645 * 4.26 * 10^{-5}} = 0.957$$

$$\text{At } 350^{\circ}\text{C} : Sc = \frac{2.78 * 10^{-5}}{0.594 * 5.04 * 10^{-5}} = 0.928$$

Find k_m : $\text{At } 200^{\circ}\text{C}, k_m = \left(\frac{1.565 \times 0.04}{0.782} \right) (0.964)^{-2/3} = 0.082 \text{ m/s}$

$$\text{At } 250^{\circ}\text{C}, k_m = \left(\frac{1.613 \times 0.04}{0.706} \right) (0.955)^{-2/3} = 0.094 \text{ m/s}$$

$$\text{At } 300^{\circ}\text{C}, k_m = \left(\frac{1.663 \times 0.04}{0.645} \right) (0.957)^{-2/3} = 0.106 \text{ m/s}$$

$$\text{At } 350^{\circ}\text{C}, k_m = \left(\frac{1.699 \times 0.04}{0.594} \right) (0.928)^{-2/3} = 0.12 \text{ m/s}$$

Properties of catalyst

Density = 0.375 g/ml catalyst

Diameter of 40-60 mesh catalyst particle = 0.152 mm

$$\text{Weight per catalyst particle} = \frac{\pi(0.152 \times 10^{-1})^3 \times 0.375}{6} = 6.895 \times 10^{-7} \text{ g/particle}$$

$$\text{External surface area per particle} = \pi(0.152 \times 10^{-3})^2 = 7.26 \times 10^{-7} \text{ m}^2/\text{particle}$$

$$a_m = \frac{7.26 \times 10^{-7}}{6.895 \times 10^{-7}} = 1.052 \times 10^{-2} \text{ m}^2/\text{gram catalyst}$$

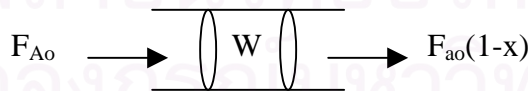
$$\text{Volumetric flow rate of gaseous feed stream} = 100 \text{ ml/min}$$

$$\text{Molar flow rate of gaseous feed stream} = \frac{(1 \times 10^5) \left(\frac{100 \times 10^{-6}}{60} \right)}{8.314(273 + 30)} = 6.62 \times 10^{-5} \text{ mol/s}$$

$$\text{1-propanol molar feed rate} = 0.08 \times 6.62 \times 10^{-5} = 5.29 \times 10^{-6} \text{ mol/s}$$

$$\begin{aligned} \text{1-propanol conversion (experimental data):} & \quad 1.78 \text{ \% at } 200^\circ\text{C} \\ & \quad 5.73 \text{ \% at } 250^\circ\text{C} \\ & \quad 28.07 \text{ \% at } 300^\circ\text{C} \\ & \quad 59.93 \text{ \% at } 350^\circ\text{C} \end{aligned}$$

The estimated rate of 1-propanol oxidation reaction is based on the ideal plug flow reactor which there is no mixing in the direction of flow and complete mixing perpendicular to the direction of flow (i.e., in the radial direction). The rate of reaction will vary with reaction length. Plug flow reactors are normally operated at steady state so that properties at any position are constant with respect to time. The mass balance around plug flow reactor becomes



$$\begin{aligned} & \{ \text{rate of } i \text{ into volume element} \} - \{ \text{rate of } i \text{ out of volume element} \} \\ & + \{ \text{rate of production of } i \text{ within the volume element} \} \\ & = \{ \text{rate of accumulation of } i \text{ within the volume element} \} \end{aligned}$$

$$F_{A0} = F_{A0}(1-x) + (r_w W)$$

$$(r_w W) = F_{A_0} - F_{A_0}(1-x) = F_{A_0} = F_{A_0}x$$

$$r_w = \frac{F_{A_0}x}{W} = \frac{5.29 \times 10^{-6} \times 0.0178}{0.1} = 4.717 \times 10^{-7} \text{ mol/s-gram catalyst at } 200^\circ\text{C}$$

$$r_w = \frac{F_{A_0}x}{W} = \frac{5.29 \times 10^{-6} \times 0.0573}{0.1} = 1.518 \times 10^{-6} \text{ mol/s-gram catalyst at } 250^\circ\text{C}$$

$$r_w = \frac{F_{A_0}x}{W} = \frac{5.29 \times 10^{-6} \times 0.28}{0.1} = 7.42 \times 10^{-6} \text{ mol/s-gram catalyst at } 300^\circ\text{C}$$

$$r_w = \frac{F_{A_0}x}{W} = \frac{5.29 \times 10^{-6} \times 0.599}{0.1} = 1.587 \times 10^{-5} \text{ mol/s-gram catalyst at } 350^\circ\text{C}$$

At steady state the external transport rate may be written in terms of the diffusion rate from the bulk gas to the surface. The expression is:

$$\begin{aligned} R_{\text{obs}} &= k_m a_m (C_b - C_s) \\ &= \frac{1 - \text{propanol converted (mole)}}{(\text{time})(\text{gram of catalyst})} \end{aligned}$$

where C_b and C_s are the concentrations in the bulk gas and at the surface, respectively.

$$\text{At } 200^\circ\text{C, } (C_b - C_s) = \frac{r_{\text{obs}}}{k_m a_m} = \frac{4.717 \times 10^{-7}}{0.082 \times 1.052 \times 10^{-1}} = 5.47 \times 10^{-4} \text{ mol/m}^3$$

$$\text{At } 250^\circ\text{C, } (C_b - C_s) = \frac{r_{\text{obs}}}{k_m a_m} = \frac{1.518 \times 10^{-6}}{0.094 \times 1.052 \times 10^{-1}} = 1.53 \times 10^{-4} \text{ mol/m}^3$$

$$\text{At } 300^\circ\text{C, } (C_b - C_s) = \frac{r_{\text{obs}}}{k_m a_m} = \frac{7.42 \times 10^{-6}}{0.106 \times 1.052 \times 10^{-1}} = 6.65 \times 10^{-3} \text{ mol/m}^3$$

$$\text{At } 350^\circ\text{C, } (C_b - C_s) = \frac{r_{\text{obs}}}{k_m a_m} = \frac{1.587 \times 10^{-5}}{0.12 \times 1.052 \times 10^{-1}} = 1.26 \times 10^{-3} \text{ mol/m}^3$$

From C_b (1-propanol) = 1.59 mol/m³

Consider the difference of the bulk and surface concentration is small. It means that the external mass transport has no effect on the 1-propanol oxidation reaction rate.

2. Internal diffusion limitation

Next, consider the internal diffusion limitation of the 1-propanol reaction. An effectiveness factor, η , was defined in order to express the rate of reaction for the whole catalyst pellet, r_p , in terms of the temperature and concentrations existing at the outer surface as follows:

$$\eta = \frac{\text{actual rate of whole pellet}}{\text{rate evaluated at outer surface conditions}} = \frac{r_p}{r_s}$$

The equation for the local rate (per unit mass of catalyst) may be expected functionally as $r = f(C, T)$.

Where C represents, symbolically, the concentrations of all the involved components

Then, $r_p = \eta r_s = \eta f(C_s, T_s)$

Suppose that the 1-propanol oxidation is an irreversible reaction $A \rightarrow B$ and first order reaction, so that for isothermal conditions $r = f(C_A) = k_1 C_A$. Then $r_p = \eta k_1 (C_A)_s$.

For a spherical pellet, a mass balance over the spherical-shell volume of thickness Δr . At steady state the rate of diffusion into the element less the rate of diffusion out will equal the rate of disappearance of reactant with in the element. This

rate will be $\rho_p k_1 C_A$ per unit volume, where ρ_p is the density of the pellet. Hence, the balance may be written, omitting subscript A on C,

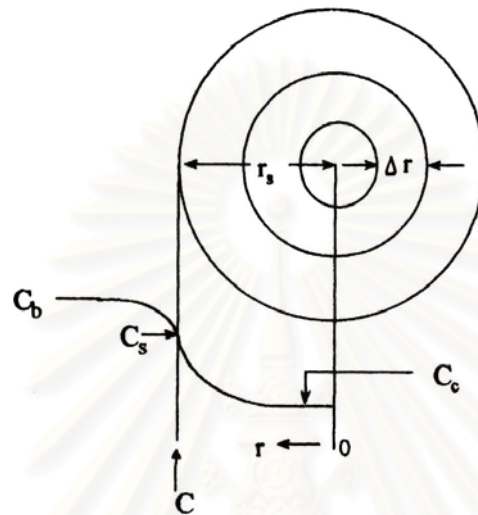


Figure B1. Reactant (A) concentration vs. position for first-order reaction on a spherical catalyst pellet.

$$\left(-4\pi r^2 D_e \frac{dC}{dr} \right)_r - \left(-4\pi r^2 D_e \frac{dC}{dr} \right)_{r+\Delta r} = -4\pi r^2 \Delta r \rho_p k_1 C$$

Take the limit as $\Delta r \rightarrow 0$ and assume that the effective diffusivity is independent of the concentration of reactant, this difference equation becomes

$$\frac{d^2 C}{dr^2} + 2 \frac{dC}{dr} - \frac{k_1 \rho_p C}{D_e} = 0$$

At the center of the pellet symmetry requires

$$\frac{dC}{dr} = 0 \text{ at } r = 0$$

and at outer surface

$$C = C_s \text{ at } r = r_s$$

Solve linear differential equation by conventional methods to yield

$$\frac{C}{C_s} = \frac{r_s \sinh\left(3\phi_s \frac{r}{r_s}\right)}{r \sinh 3\phi_s}$$

where ϕ_s is Thiele modulus for a spherical pellet defined by $\phi_s = \frac{r_s}{3} \sqrt{\frac{k_1 \rho_p}{D_e}}$

Both D_e and k_1 are necessary to use $r_p = \eta k_1 (C_A)_s$. D_e could be obtained from the reduced pore volume equation in case of no tortuosity factor.

$$D_e = (\epsilon_s^2 D_{AB})$$

$$\text{At } 200^\circ\text{C}, D_e = (0.5)^2 (3.01 \times 10^{-5}) = 7.53 \times 10^{-6}$$

$$\text{At } 250^\circ\text{C}, D_e = (0.5)^2 (3.62 \times 10^{-5}) = 9.04 \times 10^{-6}$$

$$\text{At } 300^\circ\text{C}, D_e = (0.5)^2 (4.26 \times 10^{-5}) = 1.06 \times 10^{-5}$$

Substitute radius of catalyst pellet, $r_s = 0.107 \times 10^{-3}$ m with ϕ_s equation

$$\phi_s = \frac{0.076 \times 10^{-3} \text{ m}}{3} \sqrt{\frac{k(\text{m}^3/\text{s} - \text{kg cat.}) \times 1000(\text{kg}/\text{m}^3)}{7.53 \times 10^{-6} (\text{m}^2/\text{s})}}, \text{ at } 200^\circ\text{C}$$

$$\phi_s = 0.292 \sqrt{k} \text{ (dimensionless) at } 200^\circ\text{C}$$

$$\phi_s = 0.266 \sqrt{k} \text{ (dimensionless) at } 250^\circ\text{C}$$

$$\phi_s = 0.246 \sqrt{k} \text{ (dimensionless) at } 300^\circ\text{C}$$

Find k (at 200°C) from the mass balance equation around plug-flow reactor.

$$r_w = \frac{F_{A_0} dx}{dW}$$

where $r_w = kC_A$

Thus,
$$kC_A = \frac{F_{A_0} dx}{dW}$$

$$kC_{A_0}(1-x) = \frac{F_{A_0} dx}{dW}$$

$$W = \frac{F_{A_0}}{kC_{A_0}} \int_0^{0.1} \frac{1}{1-x} dx$$

$$W = \frac{F_{A_0}}{kC_{A_0}} [-\ln(1-x)]_0^{0.1} = \frac{F_{A_0}}{kC_{A_0}} (-\ln(0.9))$$

$$k = \frac{F_{A_0}}{WC_{A_0}} (-\ln(0.9822))$$

$$k = \frac{5.29 \times 10^{-6} \text{ (mol/s)}}{0.1 \times 10^{-3} \text{ (kg)} \times 1.03 \text{ (mol/m}^3\text{)}} (-\ln(0.9822))$$

$$= 0.92 \times 10^{-4} \text{ m}^3/\text{s-kg catalyst}$$

Calculate ϕ_s : $\phi_s = 0.292 \sqrt{0.92 \times 10^{-4}} = 0.0028$ at 200°C

$$\phi_s = 0.266 \sqrt{3.03 \times 10^{-3}} = 0.015 \text{ at } 250^\circ\text{C}$$

$$\phi_s = 0.246 \sqrt{1.68 \times 10^{-2}} = 0.032 \text{ at } 300^\circ\text{C}$$

For such small values of ϕ_s it was concluded that the internal mass transport has no effect on the rate of 1-propanol oxidation reaction.

APPENDIX C

GAS CHROMATOGRAPH

C1 Operating condition

Flame ionization detector gas chromatographs, model 14A and 14B, were used to analyze the concentration of oxygenated compounds and light hydrocarbons, respectively. Methanol, ethanol, 1-propanol, 2-propanol, formaldehyde, acetaldehyde and propionaldehyde were analyzed by GC model 14A while methane, ethane, propane and propene were analyzed by GC model 14B.

Gas chromatograph with the thermal conductivity detector, model 8A was used to analyze the concentrations of CO₂ and CO by using Porapak QS and Molecular Sieve 5A column, respectively.

The operation conditions for gas chromatograph are described below:

GC model	Shimadzu GC-14B	Shimadzu GC-14A	Shimadzu GC-8A
Detector	FID	FID	TCD
Column	VZ-10	Capillary	Porapak QS and Molecular sieve 5A
Nitrogen flow rate	60 ml/min	25 ml/min	-
Helium flow rate	-	-	25 ml/min
Column temperature			
- Initial	55°C	40°C	100°C
- Final	65°C	140°C	100°C
Injection temperature	100°C	150°C	130°C
Detector temperature	150°C	150°C	130°C

C2 Calibration curve

The calibration curves of methane, ethane, propene, propane, formaldehyde, acetaldehyde, propionaldehyde, methanol, ethanol, 1-propanol, 2-propanol, CO and CO₂ are presented in the following figures.

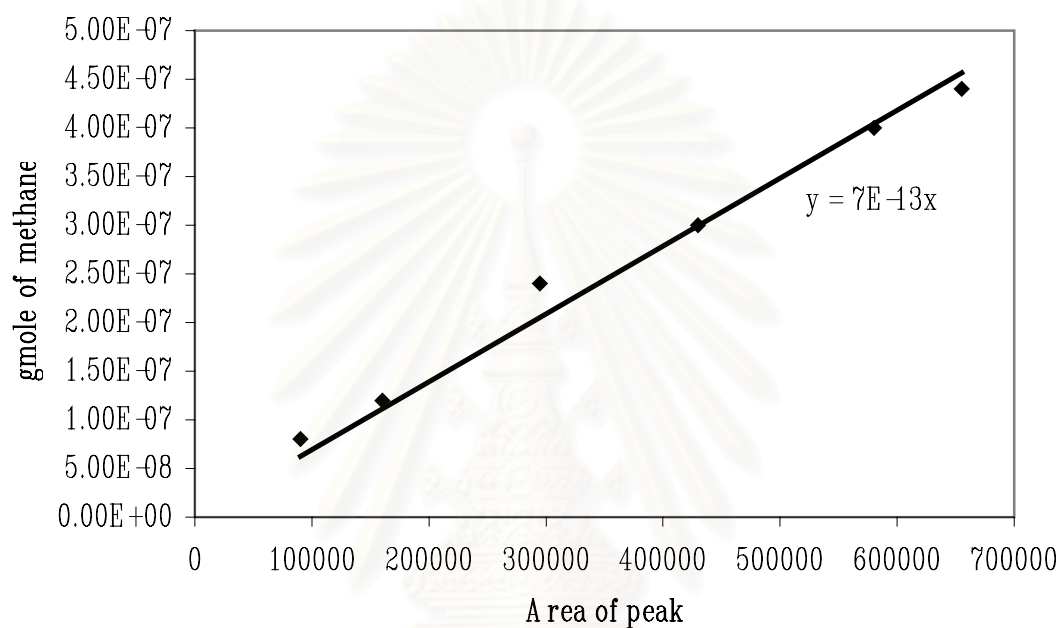


Figure C1 The calibration curve of methane

สถาบันวิทยบริการ
จุฬาลงกรณ์มหาวิทยาลัย

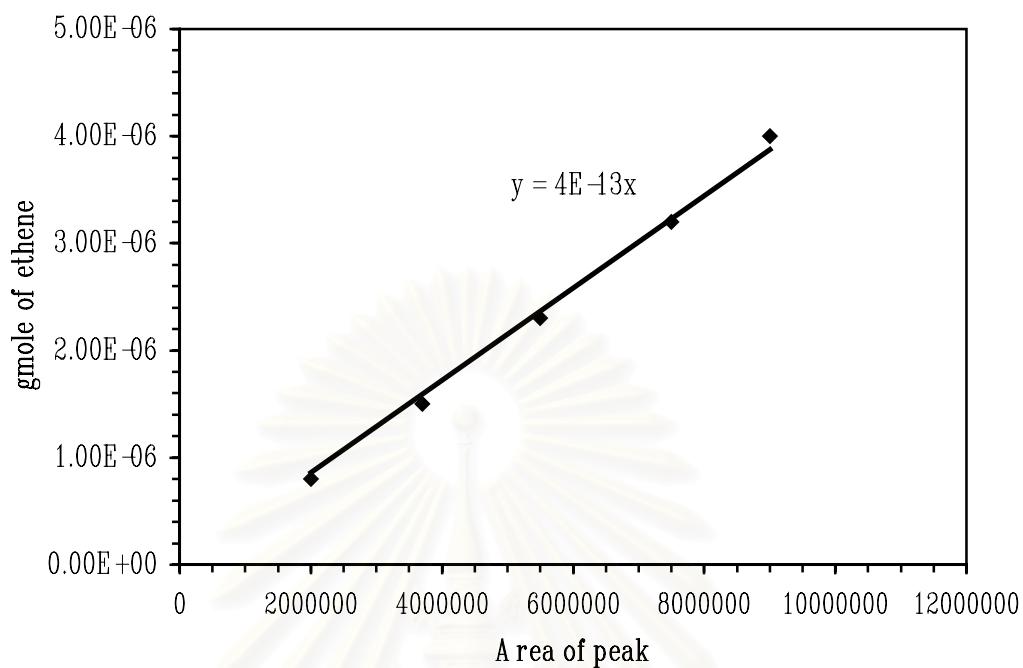


Figure C2 The calibration curve of ethene

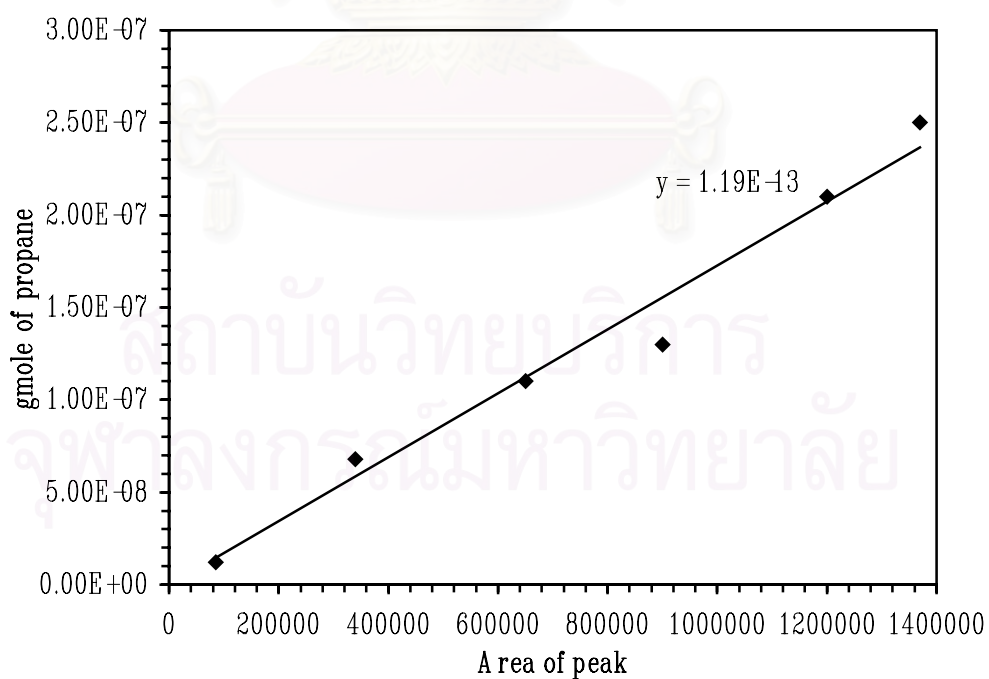


Figure C3 The calibration curve of propane

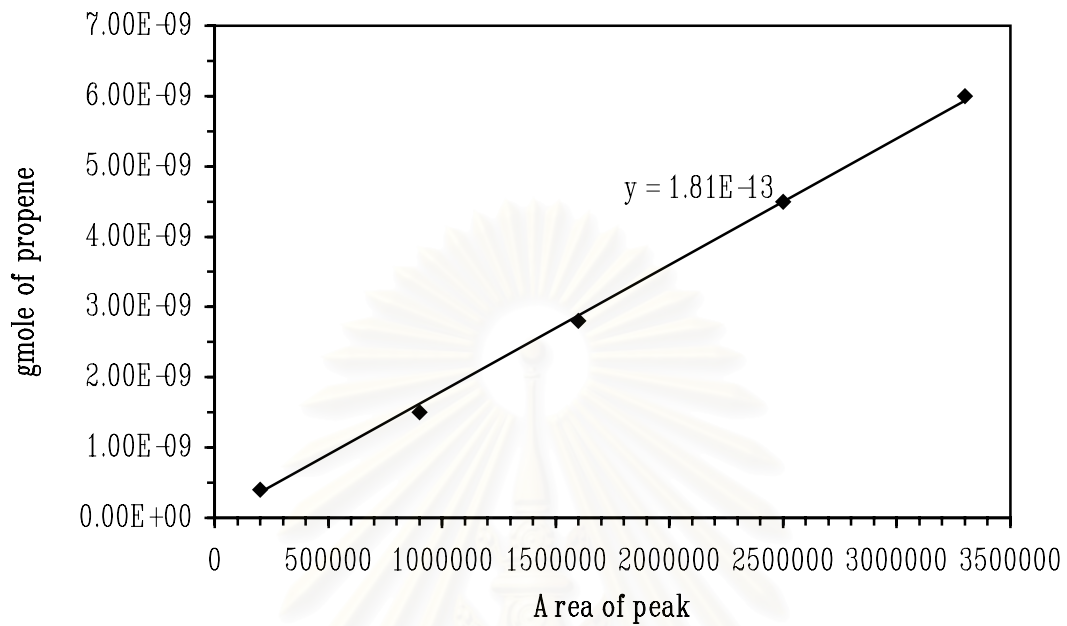


Figure C4 The calibration curve of propene

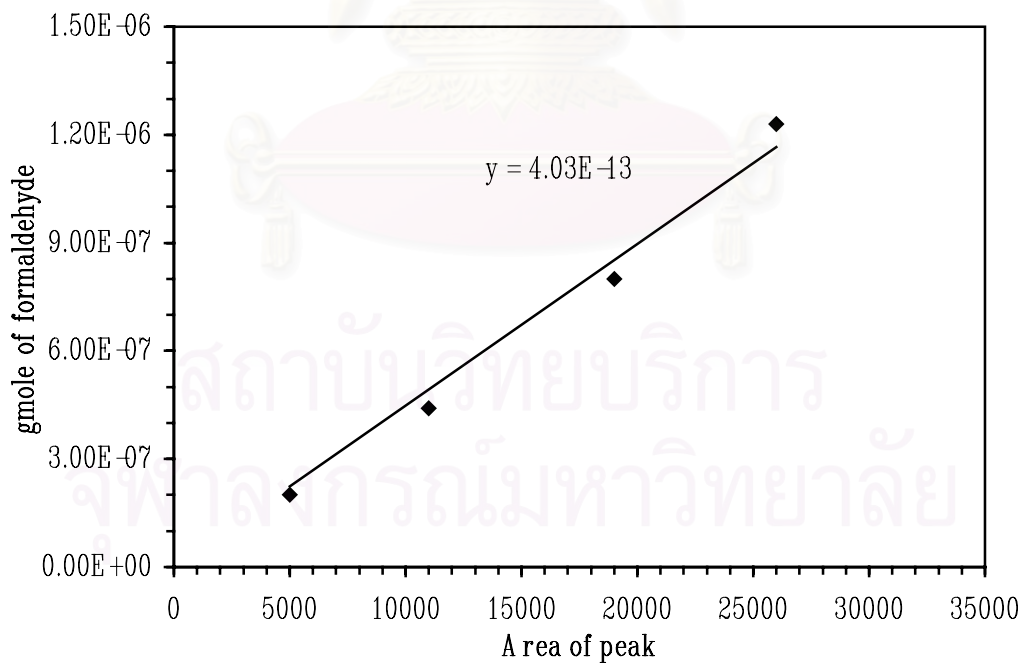


Figure C5 The calibration curve of formaldehyde

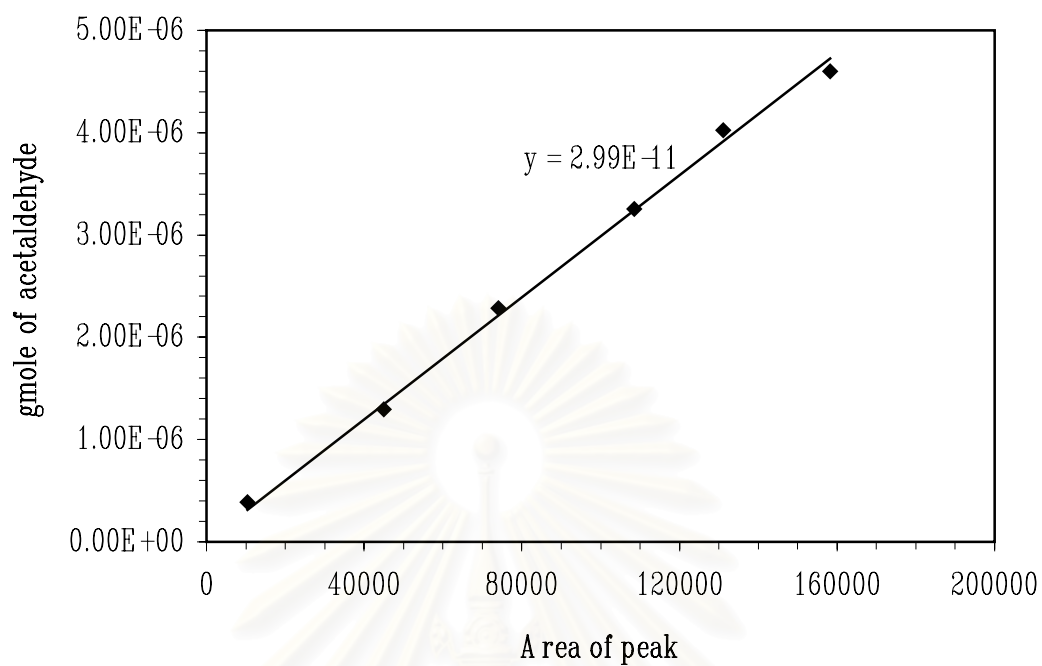


Figure C6 The calibration curve of acetaldehyde

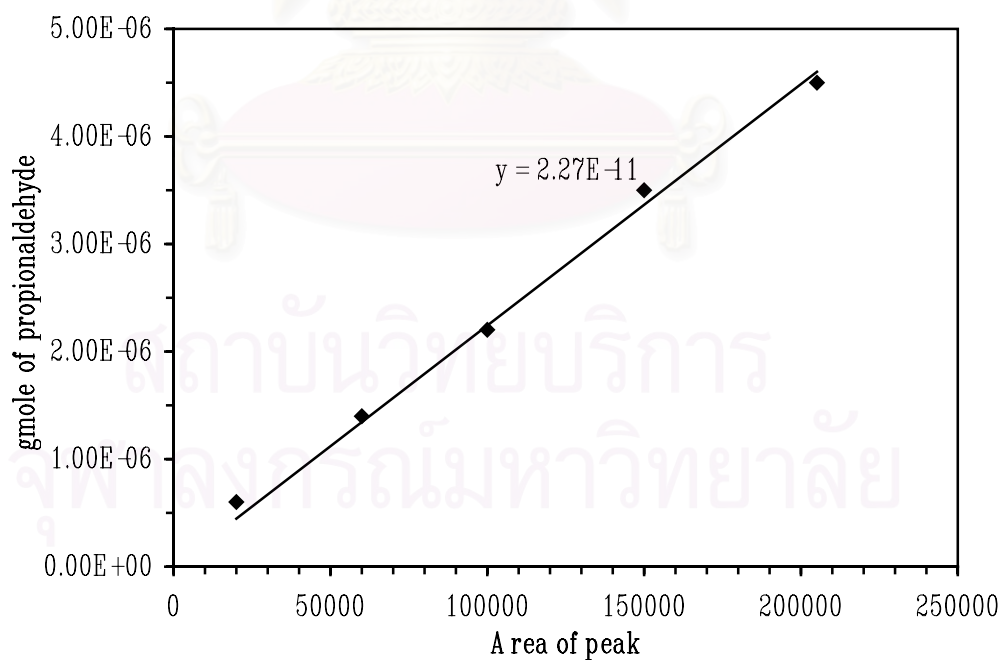


Figure C7 The calibration curve of propionaldehyde

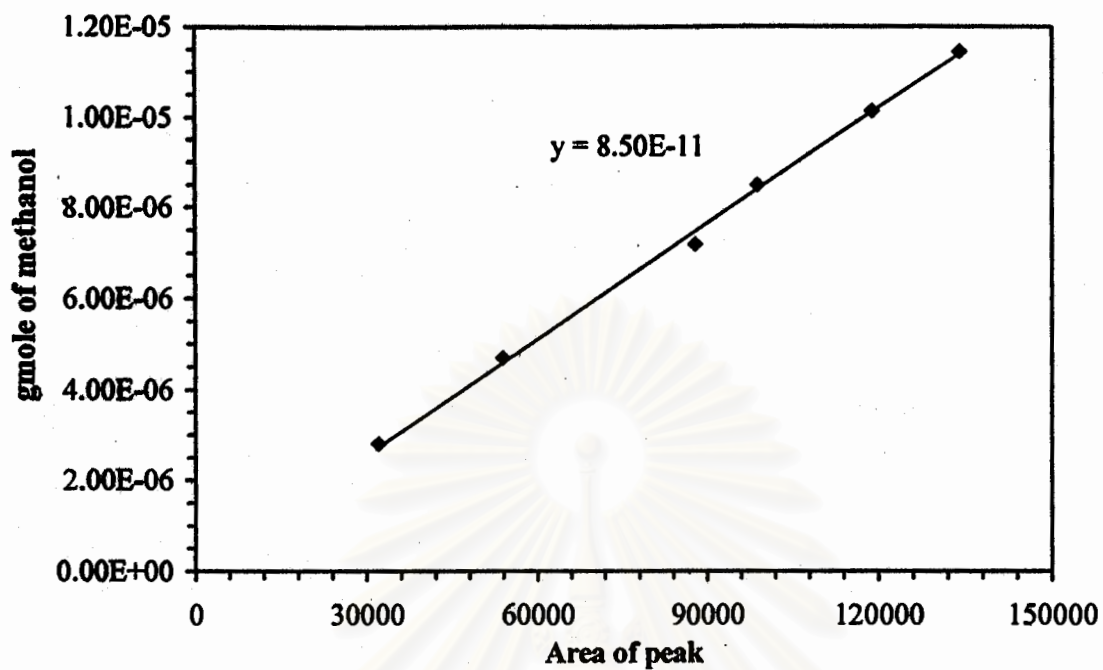


Figure C8 The calibration curve of methanol

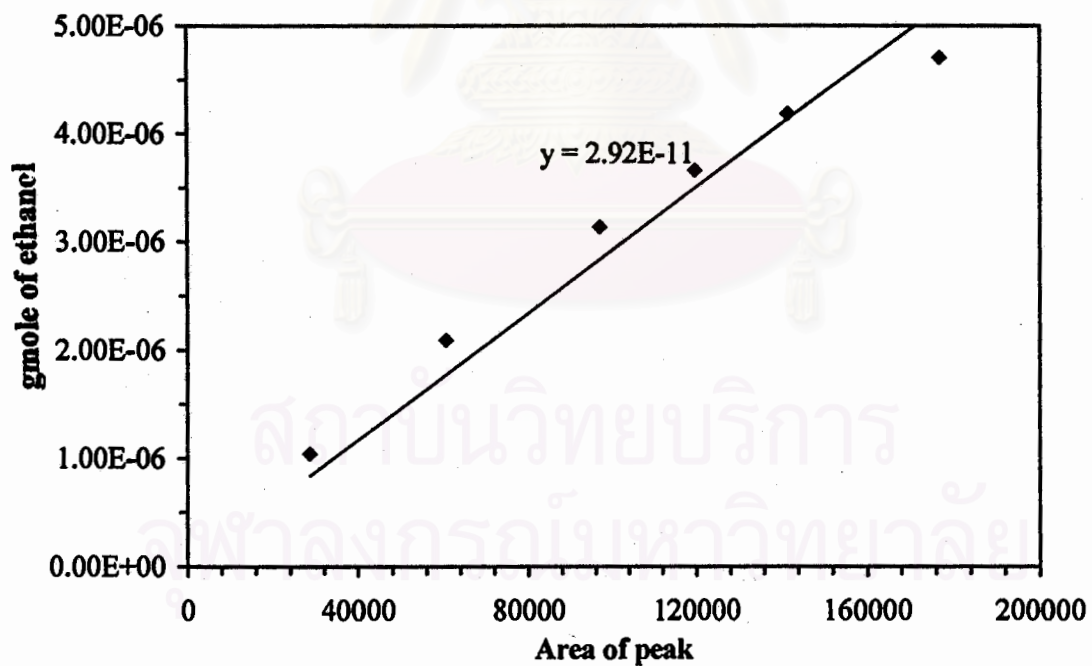


Figure C9 The calibration curve of ethanol

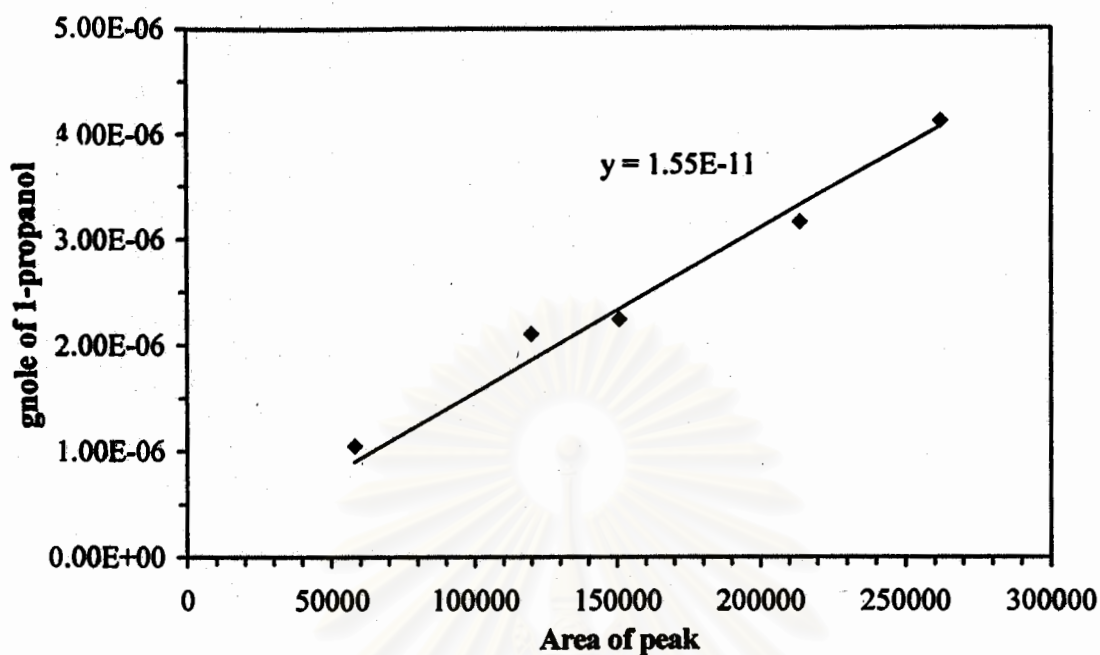


Figure C10 The calibration curve of 1-propanol

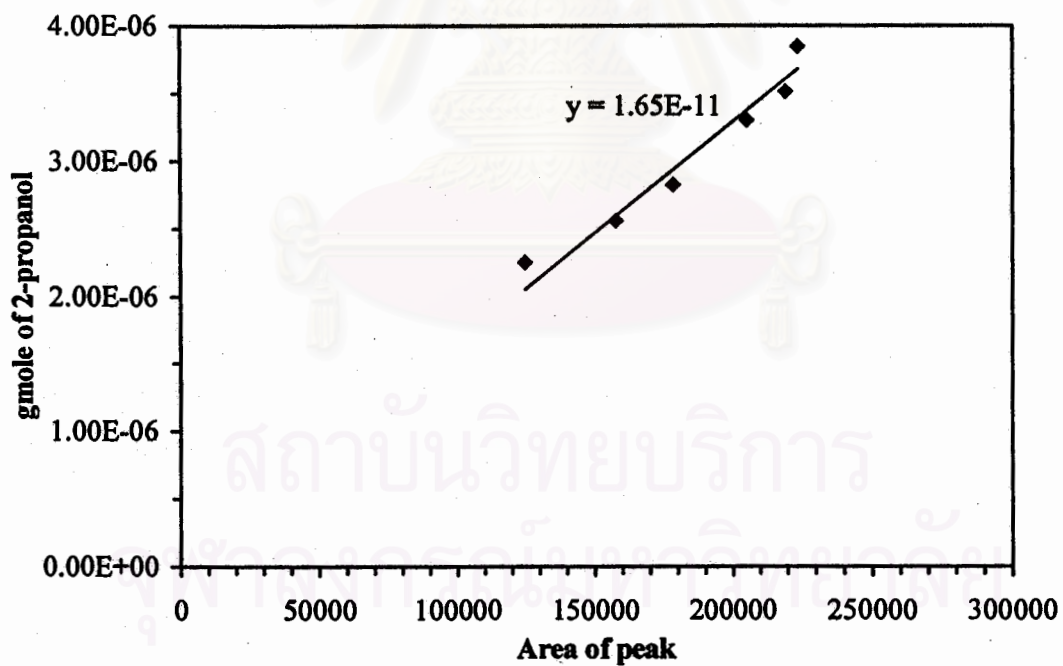


Figure C11 The calibration curve 2-propanol

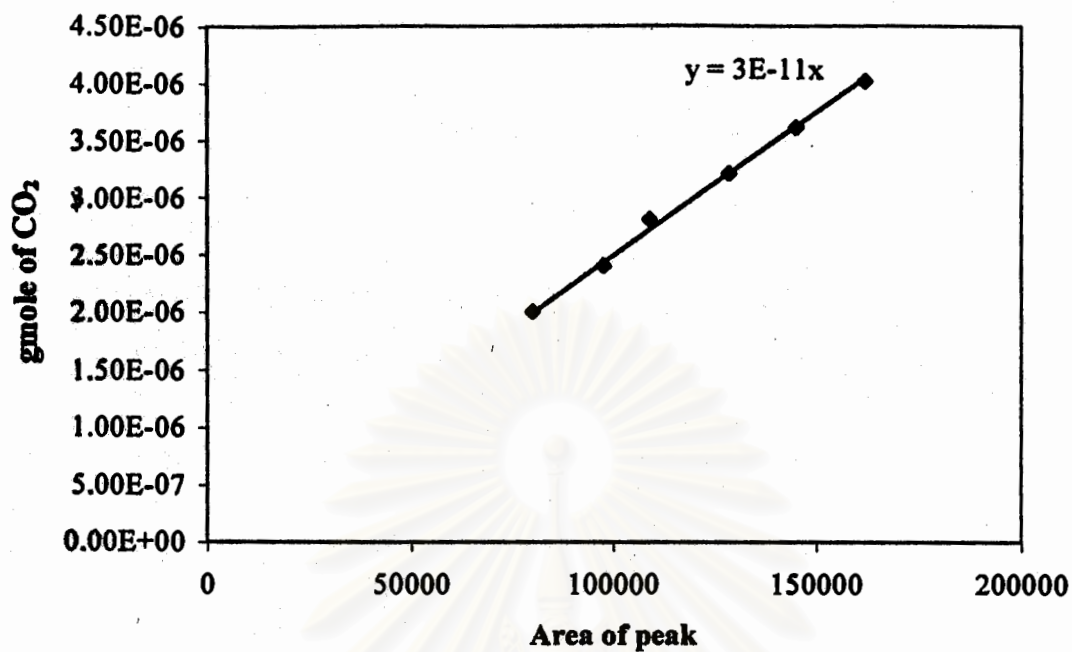


Figure C12 The calibration curve of CO₂

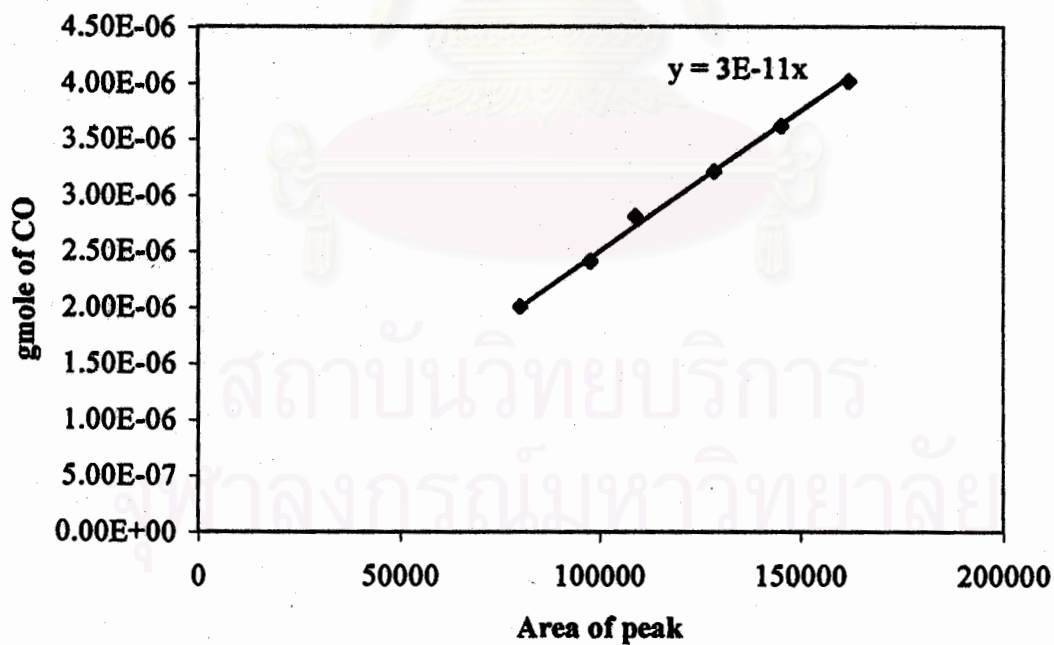


Figure C13 The calibration curve of CO

APPENDIX D

DATA OF EXPERIMENT

Table D1 Data of figure 5.7

Temperature (°C)	%C ₂ H ₅ OH conversion	%C ₂ H ₄ O selectivity	%CH ₄ selectivity	%C ₂ H ₄ selectivity	%C ₃ H ₆ selectivity	%CO ₂ selectivity
200	22.2	91.74	1.08	1.13	0	1.05
250	78.62	89.5	1.1	2.87	0.01	1.52
300	93.52	86.57	1.17	2.97	0.01	4.27
350	98.68	76.06	1.04	3.05	0.01	17.82
400	99.02	70.17	4.11	6.18	0.05	22.33
450	94.27	65.47	4.32	6.79	0.08	25.27
500	89.27	60.68	4.57	8.61	0.06	29.54

Table D2 Data of figure 5.8

Temperature (°C)	%C ₂ H ₅ OH conversion	%C ₂ H ₄ O selectivity	%CH ₄ selectivity	%C ₂ H ₄ selectivity	%C ₃ H ₆ selectivity	%C ₃ H ₈ selectivity	%CO ₂ selectivity
200	9.87	93.4	0.05	0.24	0.17	0	1.39
250	48.13	91.76	0.19	1.27	0.06	0	2.17
300	79.66	90.79	0.41	2.87	0.15	0	2.22
350	93.01	78.45	1.4	4.34	0.08	0	10.43
400	88.88	69.75	2.36	4.78	0.15	0.01	17.91
450	88.03	61.94	3.19	5.11	0.18	0.02	24.56
500	82.61	56.14	3.51	6.15	0.22	0.01	28.96

Table D3 Data of figure 5.9

Temperature (°C)	%C ₂ H ₅ OH conversion	%C ₂ H ₄ O selectivity	%CH ₄ selectivity	%C ₂ H ₄ selectivity	%C ₃ H ₆ selectivity	%CO ₂ selectivity
200	34.75	98.59	0.02	0.31	0.15	0.94
250	55.97	96.36	0.04	1.27	0.12	2.21
300	88.57	78.42	0.15	5.19	0.12	15.32
350	93.82	69.55	2.57	11.09	0.27	16.23
400	95.96	56.4	6.27	18.42	0.41	17.53
450	96.07	59.13	2.48	14.93	0.41	22.74
500	94.09	51.21	2.25	15.32	0.47	30.87

Tble D4 Data of figure 5.10

Temperature (°C)	%C ₂ H ₅ OH conversion	%C ₂ H ₄ O selectivity	%CH ₄ selectivity	%C ₂ H ₄ selectivity	%C ₃ H ₆ selectivity	%CO ₂ selectivity
200	46.5	94.04	0.1	0.43	0.36	0.47
250	83.62	90.48	0.29	2.56	0.5	1.6
300	87.82	58.38	1.62	7.51	0.57	27.87
350	88.89	46.04	2.98	13.5	0.42	22.55
400	93.03	47	2.64	19.79	0.19	26.2
450	92.13	47	0.96	22.59	0.15	25.67
500	93.37	46.1	0.73	21.98	0.05	26.13

สถาบันวิทยบริการ
จุฬาลงกรณ์มหาวิทยาลัย

Table D5 Data of figure 5.12

Temperature (°C)	%C ₃ H ₇ OH conversion	selectivity	%C ₃ H ₆ O selectivity	%CH ₄ selectivity	%C ₂ H ₄ selectivity	%C ₃ H ₆ selectivity	%C ₃ H ₈ selectivity	%CO ₂ selectivity
200	24.4	0.54	96.25	0.1	0.02	0.26	0	0.27
250	38.96	6.09	86.33	0.04	0.04	2.24	0	2.97
300	44.18	5.62	78.7	0.04	0	3.04	0	12.23
350	68.15	9.99	64.04	0.03	0.34	7.55	0	14.19
400	78.54	10.17	59.3	0.1	1.89	10.02	0.01	15.56
450	79.56	6.72	51.48	0.25	2.22	8.99	0.02	25.98
500	78.96	7.8	52.18	0.39	3.03	6.26	0.02	26.62

Table D6 Data of figure 5.13

Temperature (°C)	%C ₃ H ₇ OH conversion	selectivity	%C ₃ H ₆ O selectivity	%CH ₄ selectivity	%C ₂ H ₄ selectivity	%C ₃ H ₆ selectivity	%CO ₂ selectivity
200	15.81	0	97.34	0	0	0	0
250	13.43	7.06	84.38	0.19	0.84	0.51	2.02
300	53.74	13.04	74.02	0.89	2.63	0.81	3.61
350	77.52	12.26	67.66	1	2.16	1.08	10.84
400	85.59	4.68	58.83	0.9	0	0	30.6
450	90.27	3.9	58.59	0.79	0	0	31.74
500	88.54	6.2	55.55	1.08	0	0	32.22

Table D7 Data of figure 5.14

Temperature (°C)	%C ₃ H ₇ OH conversion	%HCOH selectivity	%C ₃ H ₆ O selectivity	%CH ₄ selectivity	%C ₂ H ₄ selectivity	%C ₃ H ₆ selectivity	%C ₃ H ₈ selectivity	%CO ₂ selectivity
200	29.68	0	102.98	0	0.16	1.82	0	0
250	81.65	0.01	53.03	0.09	0.98	18.8	0.01	22.13
300	94.53	0.01	49.32	0.06	0.71	20.73	0.01	24.21
350	98.48	0.52	49.43	0.09	1.61	20.17	0.01	23.8
400	98.48	0.64	44.86	0.17	1.53	16.81	0.02	31
450	94.26	1.07	44.02	0.34	2.63	16.03	0.05	30.09
500	97.94	2.18	34.07	0.47	4.36	19.81	0.02	34.12

Table D8 Data of figure 5.15

Temperature (°C)	%C ₃ H ₇ OH conversion	selectivity	%C ₃ H ₆ O selectivity	%CH ₄ selectivity	%C ₂ H ₄ selectivity	%C ₃ H ₆ selectivity	%CO ₂ selectivity
200	32.94	2	98.49	0	0.2	2.38	0.61
250	76.04	8.05	74.27	0.03	0.41	12.75	3.17
300	94	15.48	52.68	0.06	0.87	26.03	9.62
350	100	12.44	50.42	0.12	1.38	21.58	16.36
400	100	10.73	51.22	0.08	1.77	15.62	21.86
450	98.43	0.01	50.01	0.1	2.63	4.13	29.37
500	100	0.01	51	0.12	3.37	1.48	30

Table D9 Data of figure 5.17

Temperature (°C)	%CH ₃ OH conversion	%CH ₄ selectivity	%C ₂ H ₄ selectivity	%C ₃ H ₆ selectivity	%CO ₂ selectivity	selectivity
200	78.62	0.02	0	0.03	94.97	0
250	88.62	0.02	0	0.03	93.07	0
300	99.33	2.03	0	0.03	92.41	0.54
350	98.45	3.04	0	0.05	89.76	2.17
400	93.58	3.61	0.03	0.1	80.55	10.74
450	98.47	3.48	0.05	0.05	77.24	14.22
500	99	3.44	0.08	0.05	73.46	19.95

Table D10 Data of figure 5.18

Temperature (°C)	%CH ₃ OH conversion	%CH ₄ selectivity	%CO ₂ selectivity	selectivity
200	19	0	97.14	0
250	21.5	0	93.62	1.39
300	78	0.02	78.8	16.2
350	87	0.05	84.91	10.06
400	96	0.17	85.2	9.63
450	98	1.58	84.09	9.35
500	99	1.68	84.26	9.08

Table D11 Data of figure 5.19

Temperature (°C)	%CH ₃ OH conversion	%CH ₄ selectivity	%CO ₂ selectivity	selectivity
200	14.24	0.66	97	0
250	22.92	1.34	92.61	1.07
300	72.68	2.73	91.04	1.25
350	80	4.02	86.98	4.02
400	92	3.81	81.07	10.14
450	95	2.61	81.99	10.42
500	99	2.72	82.79	9.51

Table D12 Data of figure 5.20

Temperature (°C)	%CH ₃ OH conversion	%CH ₄ selectivity	%C ₂ H ₄ selectivity	%CO ₂ selectivity	selectivity
200	19.35	0.01	0.01	100	0.01
250	81.36	0.01	0.01	94.37	5.61
300	95.18	0.01	0.01	88.11	15.26
350	96.21	0.02	0.01	88.12	14.34
400	99.16	0.03	0.01	87.35	10.64
450	100	0.01	0.01	77.69	17.97
500	100	0.64	0.01	80.74	20.66

Table D13 Data of figure 5.22

Temperature (°C)	%2-C ₃ H ₇ OH conversion	selectivity	%CH ₄ selectivity	%C ₂ H ₄ selectivity	%C ₃ H ₆ selectivity	%CO ₂ selectivity
200	18.26	0	0.02	0	91.85	3.14
250	48.56	0	0.02	0	91.2	3.8
300	68.69	0.42	0.02	0	79.47	15.39
350	89.05	0.51	0.01	0.02	71.55	24.54
400	91.45	1.06	0	0.01	62.1	35.71
450	93.33	0.73	2.14	0.1	44.04	48.01
500	91.45	0.78	0	0.06	34.09	60.73

Table D14 Data of figure 5.23

Temperature (°C)	% 2-C ₃ H ₇ OH conversion	selectivity	%CH ₄ selectivity	%C ₃ H ₆ selectivity	%CO ₂ selectivity
200	17.84	0.51	6.36	93.07	0
250	47.45	0	5.01	90.9	0
300	86.04	0	4.79	86	4.25
350	95.36	0.51	3.86	76.26	17.09
400	91.57	0	2.9	68.47	20.43
450	95.7	0	2.92	57.73	32.19
500	93.78	0	2	46.8	42.65

Table D15 Data of figure 5.24

Temperature (°C)	% 2-C ₃ H ₇ OH conversion	%CH ₄ selectivity	%C ₂ H ₄ selectivity	%C ₃ H ₆ selectivity	%C ₃ H ₈ selectivity	%CO ₂ selectivity
200	39.93	0	0	90.36	0	9.64
250	54.66	0.01	0	95.06	0	8.66
300	97.89	0.01	0.01	99.44	0	8.55
350	100	0.02	0.08	90.09	0	9.88
400	100	0.03	0.2	87.93	0	11.83
450	100	0.07	0.7	82.2	0	17.03
500	100	0.11	0.89	82.7	0.01	16.29

Table D16 Data of figure 5.25

Temperature (°C)	% 2-C ₃ H ₇ OH conversion	%HCOH selectivity	%CH ₄ selectivity	%C ₂ H ₄ selectivity	%C ₃ H ₆ selectivity	%C ₃ H ₈ selectivity	%CO ₂ selectivity
200	29.23	0	0.02	0.02	95.76	0	0.43
250	97.86	0	0	0	99.17	0	0.83
300	100	0	0	0.08	99.73	0	5.14
350	100	0	0.02	0.59	83.5	0	20.83
400	97.56	0	0.03	0.73	61.52	0	42.67
450	100	0.32	0.12	1.25	46.91	0.01	46.42
500	100	0.01	0.42	2.72	41.33	0.02	50.54

APPENDIX E

X-RAY DIFFRACTION (XRD)

In X-ray Diffraction (XRD) a collimated beam of X rays, with wavelength $\lambda \sim 0.5\text{-}2 \text{ \AA}$, is incident on a specimen and is diffracted by the crystalline phases in the specimen according to Bragg's law ($\lambda = 2d\sin \theta$, where d is the spacing between atomic planes in the crystalline phase). The intensity of the diffracted X rays is measured as a function of the diffraction angle 2θ and the specimen's orientation. This diffraction pattern is used to identify the specimen's crystalline phases and to measure its structural properties, including strain (which is measured with great accuracy), epitaxy, and the size and orientation of crystallites (small crystalline regions). XRD can also determine concentration profiles, film thickness, and atomic arrangements in amorphous materials and multilayers. It also can characterize defects. To obtain this structural and physical information from thin films, XRD instruments and techniques are designed to maximize the diffracted X-ray intensities, since the diffracting power of thin films is small.

Range of elements	All, but not element specific. Low -Z elements may be difficult to detect
Probing depth	Typically a few μm but material dependent; monolayers sensitivity with synchrotron radiation
Detection limits	Material dependent, but $\sim 3\%$ in a two phase mixture; with synchrotron radiation can be $\sim 0.1\%$
Destructive	No, for most materials
Depth profiling	Normally no; but this can be achieved
Sample requirements	Any material, greater than $\sim 0.5 \text{ cm}$, although smaller with microfocus
Lateral resolution	Normally none; although $\sim 10 \mu\text{m}$ with microfocus
Main use	Identification of crystalline phases; determination of strain, and crystallite orientation and size; accurate determination of atomic arrangements
Specialized uses	Defect imaging and characterization

APPENDIX F

FOURIER TRANSFORM INFRARED SPECTROSCOPY (FTIR)

The vibrational motions of the chemically bound constituents of matter have frequencies in the infrared regime. The oscillations induced by certain vibrational modes provide a means for matter to couple with an impinging beam of infrared electromagnetic radiation and to exchange energy with it when the frequencies are in resonance. In the infrared experiment, the intensity of a beam of infrared radiation is measured before (I_0) and after (I) it interacts with the sample as a function of light frequency, $\{\omega_i\}$. A plot of I / I_0 versus frequency is the “infrared spectrum”. The identities, surrounding environments, and concentrations of the chemical bonds that are present can be determined.

Information	Vibrational frequencies of chemical bonds
Element Range	All, but not element specific
Destructive	No
Chemical bonding	Yes, identification of functional groups
Information	
Depth profiling	No, not under standard conditions
Depth probed	Sample dependent, from μm 's to 10 nm
Detection limits	Ranges from undetectable to $< 10^{13}$ bonds/cc. Submonolayer sometimes
Quantification	Standards usually needed
Reproducibility	0.1% variation over months
Lateral resolution	0.5 cm to 20 μm
Imaging/mapping	Available, but not routinely used
Sample requirements	Solid, liquid, or gas in all forms; vacuum not required
Main use	Qualitative and quantitative determination of chemical species, both trace and bulk, for solids and thin films. Stress, structural inhomogeneity

Vita

Miss Jaichanok Panyawong was born in Lampang on April 7, 1978. She graduated high school from Bunyawatwittayalai school, Lampang in 1994 and received her Bachelor degree of Chemical Engineering from the faculty of Engineering, Chulalongkorn University in 1998.



สถาบันวิทยบริการ
จุฬาลงกรณ์มหาวิทยาลัย